2020

Characterising the role of pharyngeal cell surface glycans in Group A Streptococcus biofilm formation

Heema Kumari Nilesh Vyas
University of Wollongong

UNIVERSITY OF WOLLONGONG AUSTRALIA

Characterising the role of pharyngeal cell surface glycans in Group A *Streptococcus* biofilm formation

Heema Kumari Nilesh Vyas

Supervisors:
A/Prof Martina Sanderson-Smith
Dr Jason McArthur
Prof Marie Ranson

This thesis is presented as part of the requirement for the conferral of the degree:
Doctor of Philosophy (PhD)

This research has been conducted with the support of the
Australian Government Research Training Program Scholarship

University of Wollongong
School of Chemistry and Molecular Biosciences

December 2020

Abstract

Group A *Streptococcus* (GAS) is a major bacterial causative agent of a wide variety of human diseases that range from mild superficial infections such as impetigo, and pharyngitis, to more serious invasive infections, and numerous autoimmune sequelae. Globally, GAS is estimated to cause 700 million infections, and accounts for half a million deaths per year, and consequently poses a considerable burden financially and on healthcare systems. Of the GAS disease etiologies, GAS pharyngitis is the most common disease manifestation, with an annual estimate of 616 million cases globally. Penicillin is the standard antibiotic treatment of GAS infections. Whilst GAS remains sensitive to penicillin, an alarming antibiotic treatment failure rate of 20-40% has been reported. It has been proposed that GAS may exist as biofilms in the pharynx contributing to persistent and recurrent pharyngitis that is non-responsive to antibiotic treatment. *In vitro*, plate-based models have shown that several GAS M-types form biofilms, and multiple GAS virulence factors have been linked to biofilm formation. Although the contributions of these plate-based studies have been valuable, most have failed to mimic the host environment, with many studies utilising abiotic surfaces. Moreover, GAS is a human specific pathogen, and colonisation and subsequent biofilm formation is likely facilitated by distinct interactions with host tissue surfaces. Thus, the overarching aim of chapter 2 was to optimise a GAS biofilm-host pharyngeal cell model to support and grow GAS biofilms of a variety of GAS M-types. Improvements and adjustments to the crystal violet biofilm biomass assay were also tailored to reproducibly detect delicate GAS biofilms. 72 h was deemed as an optimal growth period for yielding detectable biofilm biomass. The GAS biofilms formed were robust and durable, and can be reproducibly assessed via staining/washing intensive assays such as crystal violet with the aid of methanol fixation prior to staining. SEM imaging of GAS biofilms formed by this model resembled those previously found on excised tonsils of patients suffering chronic pharyngo-tonsillitis. Taken together, an efficacious GAS

biofilm host-cell model has been developed that can support long-term GAS biofilm formation, with biofilms formed closely resembling those seen *in vivo*.

The host cell surface is integral in early host-pathogen interactions, thus there is a need to better understand the role of host cell surface receptors in GAS biofilm formation. Whilst this process is complex, dynamic, and multifaceted, glycans which are abundantly present on all host epithelial surfaces have recently gained attention as an important component mediating GAS pathogenesis. However, much remains to be understood of the glyco-interactions occurring at the host-GAS interface, with much of the prior research having only been conducted in the context of planktonic GAS. Utilising the previously optimised GAS-pharyngeal cell biofilm model, chapters 3 and 4 describe, for the first time, the biofilm forming abilities of a variety of GAS M-types on modified pharyngeal monolayers. The targeted removal of terminal mannose and sialic acid, which predominate the surface of Detroit 562 pharyngeal cells, increased biofilm biomass with EPS production implicated for some M-types. These increases in biofilm biomass occurred in a glycan- and strain-dependent manner, suggesting that the influence of the host glycome on the biofilm phenotype is not limited to a single strain or M-type. M12 GAS biofilms formed on pre-modulated glycomic pharyngeal cell surface monolayers were further interrogated for their penicillin susceptibility, with findings indicating significantly increased penicillin tolerance for biofilms grown on pharyngeal cell surfaces that were exoglycosidase pre-treated. Taken together, this study describes the effect of host glycosylation on GAS biofilm formation, and GAS biofilm formation as an important proponent in penicillin tolerance. Given the increasingly appreciated importance of glycans in the host-pathogen relationship and the abundance of glycosylated structures in the oropharynx, this work contributes to an improved understanding of the role of host glycans in the pathogenesis of GAS pharyngitis and antibiotic treatment failure, and may contribute towards the development of novel therapeutics and antimicrobial treatment strategies.

Acknowledgments

I would like to thank A/Prof Martina Sanderson-Smith who has been a valuable source of support, knowledge, and guidance. To my co-supervisor Dr Jason McArthur who started me on this journey of biofilms when I was a baby scientist in Honors – I really thank you for introducing me to this small, but big microbial world!!! Additional thanks to my co-supervisor Prof Marie Ranson for assisting in keeping me on track.

Shout out to lab members past and present of the McArthur/MSS lab that have contributed to this experience. Specifically, Emma, Mitch, Anuk, Di, and Jono who have been a notable source of support and strength! To my pals across IHMRI and MH (namely Chelle, Ili, Bella, and Megan C) – you have all been an endless source of support, care, love, and laughs. To the Biofilm Baddies Hannah, Bhavs, Nathan, and Callum, thank you for being my friends at my first BIOFILM conference and beyond #MonthlyPandemicZoomChats. And to the countless academics who have voluntarily taken the various roles of mentors, shoulders to cry on, friends, coffee catch ups, technical support, and so forth - I appreciate you all so much! To Dr Emma Mabin (my counsellor) and Miss Tabitha Hudson aka Ma'am (my PT), you have both helped and supported me in my mental and physical health/wellbeing tremendously throughout this mammoth of a task -Thank you!!!!!!!!!!!!!

Importantly, to my family (special shout out to Numsy and my baby Dhanu) and non-uni friends (Asha and Ben, Emma R and Chris, Christina, Divya, Reni and Amanda, and Keelan)…Without your love, laughs, good wishes, support…Moreover… understanding/patience through these full on four+ years where my lack of presence in your lives is literally due to the lab life (nothing more, nothing less)….THANK YOU and big love to you all!

To my ancestors, my religious/spiritual Guru, and Gods… I also thank you for being present in my life. Showering me with countless blessings, sending me strength when I felt weak and weary, showing me light when I thought there was only darkness, and guiding me through thick and thin.

Certification

I, Heema Kumari Nilesh Vyas, declare that this thesis submitted in fulfilment of the requirements for the conferral of the degree Doctor of Philosophy, from the University of Wollongong, is wholly my own work unless otherwise referenced or acknowledged. This document has not been submitted for qualifications at any other academic institution.

_____

Heema Kumari Nilesh Vyas

December, 2020

Publications arising from this thesis

Heema K. N. Vyas, Jason D. McArthur, Martina L. Sanderson-Smith, "An optimised host cell-GAS biofilm model", Scientific Reports (2021), 11 (1), 8200.

Incorporated in part as chapter 2

Contributor	Extent of contribution
Heema K. N. Vyas	Wrote the paper (100%) Experimental (100%)
Jason D. McArthur	Supervised (20%) Edited the paper (20%)
Martina L. Sanderson-Smith	Supervised (80%) Edited the paper (80%)

Heema K. N. Vyas, Anuk D. Indraratna, Arun Everest-Dass, Nicolle H. Packer, David M. P. De Oliveira, Marie Ranson, Jason D. McArthur, Martina L. Sanderson-Smith. "Assessing the role of pharyngeal cell surface glycans in Group A *Streptococcus* biofilm formation", Antibiotics (2020), 9 (11), 775.

Impact Factor: 3.893

Incorporated in part as chapter 3 and chapter 4

Contributor	Extent of contribution
Heema K. N. Vyas	Human Detroit 562 pharyngeal cell culturing, monolayer formation, and glycosidase pre-treating (100%) Characterisation of Detroit 562 pharyngeal cell surface *N*-linked glycans (5%) GAS culturing and biofilm formation (100%) GAS biofilm assays (100%) GAS planktonic assays (100%) GAS penicillin susceptibility testing (100%) Scanning electron microscopy (100%) Statistical analysis (95%) Preparation of figures (95%) Wrote the paper (95%)
Anuk D. Indraratna	Characterisation of Detroit 562 pharyngeal cell surface *N*-linked glycans (75%) Statistical analysis (5%) Preparation of figures (10%) Wrote the paper (5%)
Arun Everest-Dass	Characterisation of Detroit 562 pharyngeal cell surface *N*-linked glycans (10%) Edited the paper (10%)
Nicolle H. Packer	Characterisation of Detroit 562 pharyngeal cell surface *N*-linked glycans (10%) Edited the paper (10%)
David M. P. De Oliveira	Edited the paper (10%)
Marie Ranson	Supervised (5%) Edited the paper (10%)
Jason D. McArthur	Supervised (10%) Edited the paper (10%)
Martina L. Sanderson-Smith	Supervised (85%) Edited the paper (50%)

Heema K. N. Vyas, Emma J. Proctor, Jason D. McArthur, Jody Gorman and Martina L. Sanderson-Smith, "Current understanding of Group A *Streptococcal* biofilms", Current Drug Targets (2019) 20 (9), 982.

Impact Factor: 2.632

Incorporated in part as chapter 1

Contributor	Extent of contribution
Heema K. N. Vyas	Preparation of figures (5%) Wrote the paper (66%)
Emma J. Proctor	Preparation of figures (95%) Wrote the paper (33%)
Jason D. McArthur	Supervised (20%) Edited the paper (10%)
Jody Gorman	Edited the paper (10%)
Martina L. Sanderson-Smith	Supervised (80%) Edited the paper (80%)

Other publications

Jonathan G. Williams, Diane Ly, Nicholas J. Geraghty, Jason D. McArthur, **Heema K. N. Vyas**, Jody Gorman, James A. Tsatsaronis, Ronald Sluyter, Martina L. Sanderson-Smith, "*Streptococcus pyogenes* M1T1 variants activate caspase-1 and induce an inflammatory neutrophil phenotype", Frontiers in Cellular and Infection Microbiology, Microbes and Innate Immunity (2020), 10, 872.

Impact Factor: 4.300

Dina M. Silva, **Heema K. N. Vyas**, Martina L. Sanderson-Smith, Vitor Sencadas, "Development and optimisation of ciprofloxacin-loaded gelatin microparticles by single-step spray-drying technique", Powder Technology (2018), 330, 201.

Impact Factor: 4.142

Conference proceedings

Heema K N Vyas, ‘Assessing the role of pharyngeal cell surface glycans in Group A *Streptococcus* biofilm formation’, JAMS, Virtual Seminar Series, September 2020.
Invited Speaker

Heema K N Vyas, ‘Assessing the role of pharyngeal cell surface glycans in Group A *Streptococcus* biofilm formation’, Sydney Micro Meeting, Sydney, NSW, Australia, January 2020.
Invited Speaker

Heema K N Vyas, Jason McArthur, David De Oliveira, Jody Gorman, and Martina Sanderson-Smith, ‘Assessing the role of pharyngeal cell surface glycans in Group A *Streptococcus* biofilm formation’, Eurobiofilms, Glasgow, Scotland, United Kingdom, September 2019.
Poster presentation

Heema K N Vyas, Jason McArthur, David De Oliveira, Jody Gorman, and Martina Sanderson-Smith, ‘Assessing the role of pharyngeal cell surface glycans in Group A *Streptococcus* biofilm formation’, Bugs by the Beach, Newcastle, NSW, Australia, November 2018.
Poster presentation

General conference attendance

UOW Annual Higher Degree Research Conference, 2015-2020, Presenter/Attendee

Australian Society for Microbiology (ASM) 'Sydney Micro Meeting', Sydney (Australia), 2016 – 2020, Attendee

ASM 'Bugs by the beach Meeting', Wollongong/Newcastle (Australia), 2017-2020, Attendee

ASM 'Molecular Microbiology Meeting', Sydney (Australia), 2018, Attendee

Australian Chapter of the Controlled Release Society, 'Drug Delivery Australia Conference', Wollongong (Australia), 2017, Attendee and Conference Volunteer.

European Molecular Biology Laboratory, 'Australia PhD Symposium', Melbourne (Australia), 2015, Attendee

List of names or abbreviations

α	Alpha
ACN	Acetonitrile
BSA	Bovine serum albumin
˚C	Degrees Celsius
CFU	Colony forming units
CO_2	Carbon dioxide
dHex	Fucose
DMMB	1,9-dimethyl methylene blue
DNA	Deoxyribonucleic acid
eDNA	Extracellular Deoxyribonucleic acid
EPS	Extracellular polymeric substances
ESI	Electrospray ionisation
EtOH	Ethanol
FBS	Fetal bovine serum
g	Gram
g	Gravitational force
GAGs	Glycosaminoglycans
GAS	Group A *Streptococcus*
h	Hours
HCl	Hydrochloric acid
HEPES	Hydroxyethyl piperazineethanesulfonic acid
KOH	Potassium hydroxide
L	Litre
LB media	Luria-Bertani media
LC	Liquid chromatography
M	Molar
m (prefix)	Milli
m (suffix)	Meters
Man	Mannose
MeOH	Methanol
MIC	Minimum inhibitory concentration
MBC	Minimum bactericidal concentration
MBEC	Minimum biofilm eradication concentration

MFI	Mean fluorescence intensity
min	Minutes
MS	Mass spectrometry
m/v	Mass per volume
m/z	Mass to charge ratio
n	Nano
NaCl	Sodium Chloride
NeuAc	Sialic acid
NH_4HCO_3	Ammonium bicarbonate
OD	Optical density
O_2	Oxygen
PBS	Phosphate buffer saline
PFA	Paraformaldehyde
PGC	Porous graphitic carbon
PNGase F	Peptide-*N*-glycosidase F
PVDF	Polyvinylidene fluoride
RPM	Revolutions per minute
s	Seconds
Scl-1	Streptococcal collagen-like protein-1
SDS	Sodium dodecyl sulphate
SEM	Standard error of the mean
SEM	Scanning electron microscopy
Sialidase A	α2-3,6,8,9 Neuraminidase A, broad specificity sialidase
SilC	Streptococcal invasion locus C
SpeB	Streptococcal pyrogenic exotoxin B
STSS	Streptococcal toxic shock syndrome
THY	Todd-Hewitt broth with yeast
THYA	Todd-Hewitt broth with yeast agar
THY-G	Todd-Hewitt broth with yeast and glucose
TFA	Trifluoroacetic acid
U	Units
µ	Micro
V	Volts
v/v	Volume per volume
w/v	Weight per volume

Table of contents

List of tables and figures

Chapter 1: Introduction

A part of this work has been published in Current Drug Targets, Bentham Science.

Overview: *Streptococcus pyogenes* (Group A *Streptococcus*; Group A *streptococci*; GAS) is a Gram-positive pathogen, known to cause an array of diseases ranging from mild, superficial infections such as impetigo, and pharyngitis, to more serious invasive infections, and numerous autoimmune sequelae. Despite GAS remaining sensitive to penicillin, antibiotic treatment failure rates of 20-40% have been reported. It has been proposed that GAS may exist as biofilms. Biofilms are microbial communities that can aggregate upon a surface and exist within a self-produced matrix of extracellular polymeric substances. Biofilms offer bacteria an increased survival advantage, in which bacteria persist and tolerate host immunity and antimicrobial treatment. The biofilm phenotype has long been recognised as a virulence mechanism for many Gram-positive and Gram-negative bacteria, however, very little is known about the role of GAS biofilms in pathogenesis.

Several virulence factors have been implicated in GAS biofilm formation. However, most models use abiotic surfaces for biofilm growth and poorly represent the *in vivo* environment of the host. The host cell surface is integral in initial host-pathogen interactions, bacterial cell adherence, and subsequent biofilm formation. Thus, there is a need to better understand the role of host cell surface receptors in GAS biofilm formation. Glycans decorate most epithelial cell surfaces and are the initial point of contact for many pathogens, including GAS. There is a growing body of evidence that implicates glycans in planktonic GAS adherence, however, their role in GAS biofilm formation has not been previously investigated. Herein, GAS biofilm formation has been thoroughly reviewed in

the context of virulence factors, biofilm models, and the role of human pharyngeal glycans in bacterial adherence and biofilm formation.

1.1. Biofilms in GAS pathogenesis

Biofilm formation is recognised as a virulence mechanism for a variety of Gram-positive and Gram-negative bacterial species (Zalewska-Piatek et al., 2009, Abee et al., 2011, Al-Wrafy et al., 2017). The presence of GAS biofilms in a variety of clinical infections suggests this phenotype may play a role in GAS pathogenesis (Roberts et al., 2012, Siemens et al., 2016). While multiple studies have characterised the role of various GAS virulence factors in biofilm formation, studies assessing the role of biofilm formation in GAS pathogenesis have been limited. To understand GAS as a biofilm it is important to understand the biofilm phenotype.

1.1.1. Bacterial biofilms

Bacteria can exist either in planktonic or biofilm states. Planktonic cells are singular 'free floating' entities existing in a liquid environment (Percival et al., 2012), whereas biofilm bacteria exist as sessile aggregates encased in a self-produced matrix of extracellular polymeric substances (EPS) and may attach to a biological or non-biological surface (Bjarnsholt et al., 2008). Biofilm cells vary drastically in their physiology, growth rate, and gene expression when compared to planktonic cells. Furthermore, it has become clear that bacteria frequently transition between planktonic and biofilm states, which is central to biofilm formation and development (Rollet et al., 2009, McDougald et al., 2012).

1.1.2. Biofilm formation and development

Biofilm formation is a dynamic, multifaceted process triggered by environmental cues that prompt changes in gene expression. This results in a re-organisation of the spatial and

temporal arrangement of bacterial cells leading to a transition from the planktonic phenotype, to a biofilm (Kostakioti et al., 2013). Overall, biofilm formation and development has been well-defined, and can be simplified into 4 steps: i) reversible bacterial attachment, ii) irreversible bacterial attachment, iii) biofilm maturation, and iv) biofilm dispersal (Kostakioti et al., 2013). In brief, initial reversible attachment of free floating planktonic cells to a host tissue surface is a random process, driven by environmental cues (e.g. pH, temperature, ions, nutrients and gas/O_2 availability), forces of gravity, Brownian motion, and local environmental hydrodynamics (Donlan, 2002, Shunmugaperumal, 2010). Some motile bacteria may use appendages (e.g. pili and flagella) for migration (O'Toole and Kolter, 1998, Caiazza et al., 2007). Upon irreversible attachment, EPS, consisting of polysaccharides, proteins, nucleic acids, and lipids is produced and this meshwork provides the scaffold for complex, three-dimensional biofilm architecture (Abee et al., 2011, Gloag et al., 2013). At this stage, initial micro-colonies begin to form (Rutherford and Bassler, 2012). Biofilm maturation is induced by quorum sensing signals, which prompt phenotypic changes and genetic diversification. This process results in enhanced structural defense against biological, physical, and chemical stress, assisting nutrient acquisition by forming complex water/nutrient channels, and facilitating enhanced reproductive ability (Wolcott et al., 2008). Dispersal of bacterial cells into the host environment is the final stage of the biofilm cycle which can occur passively through physical forces such as fluid shear or abrasion, or be induced in response to various environmental conditions (e.g. pH, nutrient levels, gas concentrations), highly regulated signal transduction pathways, and effectors. Dispersal is key for biofilm re-colonisation and biofilm re-establishment at other sites (Gjermansen et al., 2005, McDougald et al., 2012).

1.1.3. Biofilm tolerance to immune clearance and antimicrobial agents

It has been suggested that 99% of the world's bacteria exist in a biofilm state, highlighting an adaptive advantage of this phenotype (Vickery et al., 2013). Biofilms are highly tolerant to both antimicrobial treatment and immune action (Davies, 2003). Biofilm communities are ~10-1000 fold more tolerant to antimicrobials when compared to their planktonic bacterial cell counterparts (Nickel et al., 1985, Prosser et al., 1987). Tolerance displayed by biofilm communities is attributed to, but not limited to; i) changes in gene expression, ii) sharing of resistance genes via horizontal gene transfer or adaptive mutations, iii) active release of antibiotic degrading enzymes, iv) three-dimensional structure, v) the physical EPS barrier (to both antibiotics/antimicrobials and immune cells), and vi) reduced metabolic activity among some bacterial cells found deep within the biofilm (Brown et al., 1995, Cowan, 2010, de la Fuente-Núñez et al., 2013).

1.2. Evidence of GAS biofilm formation

GAS is a Gram-positive human bacterium causing several diseases ranging from mild, superficial infections such as impetigo, and pharyngitis, to more serious invasive infections (necrotising fasciitis, cellulitis, toxic shock syndrome etc), and numerous autoimmune sequelae (rheumatic heart disease, rheumatic fever, glomerulonephritis etc) (Walker et al., 2014). GAS impetigo and pharyngitis are the most common disease manifestations contributing significantly to the global incidence and disease burden, estimated at 111 million and 600 million cases per year respectively (Carapetis et al., 2005, Walker et al., 2014).

GAS typically infects the skin and mucosal surface of the oropharynx. The earliest evidence for the presence of GAS biofilms *in vivo* was found in impetigo lesions, where glycocalyx encapsulated micro-colonies, resembling early stage biofilm formation, were

detected via FITC-ConA staining and visualised under confocal laser scanning microscopy (CLSM) (Akiyama et al., 2003). A more recent clinical case study investigated a previously healthy male presenting with a necrotising soft tissue infection (NSTI) persisting over 24 days. The surgeon noted a presence of "thick layer biofilm" in the patient's fascia (Siemens et al., 2016). This observation prompted the team to further investigate biofilm as a constituent of GAS NSTI. A multicenter study revealed that 32% of patient tissue biopsies (N=31) contained GAS biofilm. The biofilms found in these NSTIs exacerbated inflammation and led to severe tissue damage at the site of the NSTI infection, moreover, presence of bacterial loads far exceeded those of wound biopsies lacking the biofilm. Taken together, these studies highlight the need for further consideration of GAS biofilms as a complicating factor in NSTIs.

GAS enters the throat via the oral cavity and typically colonises the oro-nasopharynx. Asymptomatic and persistent oropharyngeal GAS carriage has been in part attributed to biofilm formation, complicating and contributing to oropharyngeal disease (Fiedler et al., 2013). Although penicillin resistant GAS has not been reported, it has been hypothesised that GAS biofilms may broadly be a contributing factor to the antibiotic treatment failure rate of 20-40% (Lembke et al., 2006, Pichichero and Casey, 2007). A number of clinically relevant GAS serotypes (M2, M6, M14, and M18) have been found to form biofilms *in vitro* on both uncoated surfaces, and surfaces coated with human fibronectin, human fibrinogen, human collagen types I and IV, and human laminin (Lembke et al., 2006). In a study observing GAS pharyngitis and antibiotic treatment failure, all 99 GAS isolates collected from patients suffering GAS pharyngitis displayed biofilm forming abilities with varying capacities (Conley et al., 2003). The minimum biofilm eradication concentrations (MBECs) were overall higher than the minimum inhibitory concentration (MIC) values for

all GAS isolates, with penicillin tolerance demonstrated by 60% of the GAS isolates when in the biofilm phenotype. This study conducted by Conley et al. (2003) is one of the earliest to demonstrate a link between *in vitro* GAS biofilm formation and penicillin insensitivity, highlighting the protective advantages offered by the biofilm phenotype against antibiotics like penicillin (Conley et al., 2003).

Another study investigated 289 differing clinical GAS isolates from carriers, pharyngitis cases, and invasive/non-invasive infections in an attempt to understand the link between clinical source, biofilm forming ability, and antibiotic insensitivity (Baldassarri et al., 2006). Although 90% of isolates were found to be biofilm forming *in vitro*, some *emm* types displayed a greater propensity towards biofilm formation than others, this was especially apparent among *emm* 6 strains when assessed for biofilm biomass. However, intra-strain variability within an M-type suggested biofilm formation was strain specific rather than an overall characteristic offered by the serotype. Moreover, this study found that GAS strains that are less capable of host cell internalisation may utilise the biofilm phenotype to survive β-lactam treatment (Baldassarri et al., 2006). A more recent study explored biofilm formation by 15 differing GAS *emm* types frequently isolated from patients suffering recurrent GAS pharyngitis (Ogawa et al., 2011). Findings indicated that *emm* types 1, 12, and 28 were most abundant; however the *emm6* strains produced significantly more biofilm (Ogawa et al., 2011). These GAS biofilms were 10 times more tolerant to penicillin, erythromycin, and clindamycin, used individually or in combination, when MICs were used for comparison with their planktonic cell counterpart (Ogawa et al., 2011).

An *in vivo* study by Roberts et al. (2012) revealed GAS residing within tonsillar crypts of sufferers of recurrent GAS tonsillo-pharyngitis using fluorescence microscopy and

scanning electron microscopy. The group also observed cocci chains typical of GAS arranged in three-dimensional communities resemblant of biofilms in an *ex vivo* pig epithelium model (Roberts et al., 2012).

Overall, it is apparent that both the skin and the throat are able to cultivate GAS biofilms from the earlier stages of micro-colony formation, to the more mature biofilm communities. Moreover, these findings highlight the clinical relevance of GAS biofilms and their potential role in antibiotic treatment failure in recurrent GAS infections. Taken together, these observations reinforce the need for further investigation into GAS biofilm formation *in vitro*, *in vivo,* and *ex vivo*.

1.2.1. Virulence factors involved in GAS biofilm formation

GAS expresses multiple virulence factors involved in adherence to host tissue surfaces. GAS virulence factor expression is variable among individual strains, and differs among GAS serotypes, with expression and regulation impacted by both host and environmental stimuli (Walker et al., 2014, Fiedler et al., 2015). Several GAS virulence factors have been implicated in various stages of biofilm development (summarised in Table 1.1, and schematically depicted in Fig 1.1).

1.2.1.1. M protein family and lipoteichoic acid

The M protein is abundantly expressed on the surface of GAS, and numerous studies have demonstrated a role for M protein in adherence, as it facilitates attachment of GAS to host epithelial cells (Ellen and Gibbons, 1972, Tylewska et al., 1988, Caparon et al., 1991). Adherence is both M type and epithelial cell type specific (Smeesters et al., 2010, Walker et al., 2014). It has also been proposed that the M protein mediates initial cell-surface interactions during biofilm formation. Cho and Caparon (2005) demonstrated this using an

isogenic M protein deficient GAS HSC5 (*emm*14) mutant grown on abiotic polystyrene surfaces under static conditions. The mutant displayed a decrease in biofilm biomass relative to wild-type through safranin staining. Courtney et al. (2009) also observed significantly reduced biofilm biomass, relative to wild-type, for isogenic M protein mutants of *emm*1, 5, 6, and 24 isolates under similar growth conditions. In *emm* types 1, 5, 6, and 24, isogenic M protein deficient mutants displayed diminished bacterial hydrophobicity, decreased membrane bound LTA, and biofilm biomass relative to wild-type strains. These findings demonstrated a correlation between M protein, bound lipoteichoic acid (LTA), surface hydrophobicity, and the overall ability to form biofilms. It was suggested that complex interactions between M protein and LTA expose the ester fatty acids of LTA, increasing bacterial hydrophobicity, ultimately favouring LTA-host cell interactions (Courtney et al., 2009). Conversely, no significant reduction in biofilm biomass, hydrophobicity and membrane bound LTA was observed for isogenic M protein deficient GAS strains for *emm*2, 4, and 49 expressing strains. Notably, a key difference between the strains displaying the M-protein-LTA mediated adherence and those that did not is their *emm* pattern classification. The *emm*1, 5, 6, and 24 strains all belong to the *emm* pattern A classification, which display a single M protein family member on their surface whilst the *emm*2, 4, and 49 belong to the pattern D and E classification, which express other surface proteins of the M protein family, such as the M-related protein (*mrp*) and M-like protein (*enn*) on their surface (Courtney et al., 2009). Therefore, it appears that the M-protein and LTA interaction is specific to strains expressing only one M protein family member.

Courtney et al. (2009) also investigated if other *emm*-family proteins, M-related protein (Mrp) and M-like proteins (Enn) which also contribute to GAS adherence (Brouwer et al., 2016), participated in LTA complex mediated biofilm formation. They found a significant

decrease in hydrophobicity, membrane-bound LTA, and biofilm formation relative to wild-type using an isogenic mrp4 deficient GAS mutant of the *emm*4 expressing strain. However, an isogenic *enn*4 deficient GAS mutant was also examined and there was no difference in hydrophobicity, membrane-bound LTA, or biofilm formation compared to the wild-type. The M protein has previously been shown to be expressed at significantly higher levels than Mrp and Enn in a CS101 GAS (*emm*49) strain (Podbielski et al., 1995). Expression levels may play a part in the role of these proteins in LTA complex initiation and biofilm formation; however, this has yet to be determined. Collectively, this research highlights the need to study GAS biofilm formation using strains with diverse genetic backgrounds to understand the complex interplay between differing GAS virulence factors in the formation of GAS biofilms.

Table 1.1. Summary of GAS biofilm studies assessing effect of different virulence factor and growth conditions on biofilm formation. The following molecules have been shown to contribute to GAS biofilm formation (BF): Lipoteichoic acid (LTA) and M protein (emm), M-related protein (Mrp), and M-like protein (Enn) complexes, pili, Streptococcal collagen like protein 1 (Scl-1), short hydrophobic peptides (SHP 1 and 2), the hyaluronic acid (HA) capsule, Group A Streptococcal protein A (AspA), Streptococcal regulator of virulence (Srv) and cysteine protease (SpeB), and Streptococcal invasion locus peptide (SilC).

Virulence factor	Mutation	Genetic background		Biofilm model	Growth substratum	Ref
		Role in BF	No role in BF			
M protein-LTA complex	Δe*mm*	*emm*14	-	Flow model (34 µm s-1) Static model	Glass coverslips Uncoated polystyrene	Cho and Caparon (2005)
	Δe*mm*	*emm*1 *emm*5 *emm*6 *emm*24	*emm*2 *emm*4	Static model	Uncoated polystyrene	Courtney et al. (2009)
MRP-LTA complex	Δ*mrp*	*emm*4 *emm*49	*emm*2	Static model	Uncoated polystyrene	Courtney et al. (2009)
ENN-LTA complex	Δ*enn*	-	*emm*2 *emm*4	Static model	Uncoated polystyrene	Courtney et al. (2009)
Pili	Δ*spy0128* (pili backbone) Δ*spy0129* (C1 sortase)	*emm*1	-	Static model	Polylysine-coated glass coverslips	(Manetti et al., 2007)
	Δ*tee6* (pilus backbone) Δ*fctX* (ancillary protein) Δ*srtA* (sortase) Δ*srtB* (sortase)	*emm*6	- -	Static model	Glass coverslips Uncoated polystyrene	Kimura et al. (2012)
	Δ*ALP-1*(ancillary protein 1)	*emm*6	-	Static model	Uncoated polystyrene	Becherelli et al. (2012)
Scl-1	ΔScl-1	*emm*1 *emm*28 *emm*41	-	Static model	Glass cover slips	Oliver-Kozup et al. (2011)
	ΔScl-1	*emm*3	-	Static model	Polystyrene coated with fibronectin and laminin	Bachert et al. (2016)
HA capsule	Δ*HasA (*Hyaluronan synthase)	*emm*14	-	Static model	Uncoated polystyrene	Cho and Caparon (2005)
	Δ*CovS* (sensor kinase)	*emm*18	-	Static model	Uncoated + fibronectin/collagen coated polystyrene	Sugareva et al. (2010)
AspA	Δ*AspA*	*emm*28	-	Static model	Saliva-coated coverslips	Maddocks et al. (2011)
Srv and SpeB	Δ*Srv*	*emm*1	-	Flow model (0.7 ml/min)	Polystyrene chamber	Doern et al. (2008)
SilC	Δ*silC*	*emm*14 *emm*18	- -	Flow model (1.2 ml/min) Static model	Fibronectin/ collagen IV coated plastic coverslips Uncoated, fibronectin, fibrinogen, laminin, collagen I and IV coated polystyrene	Lembke et al. (2006)

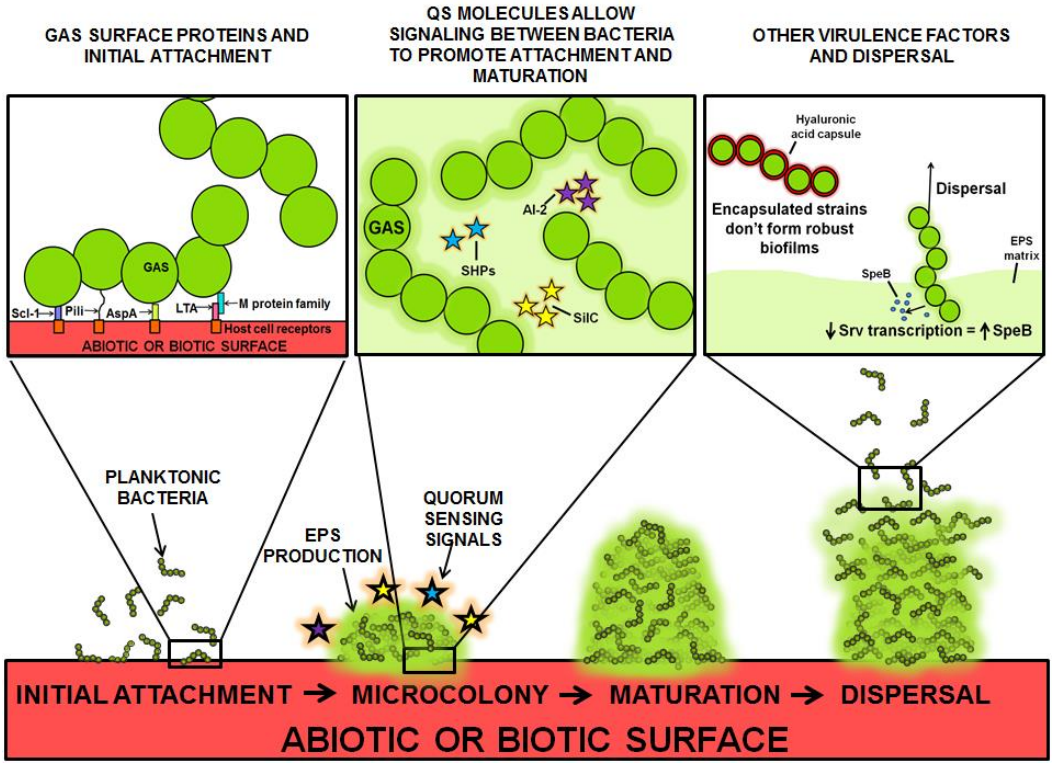

Figure 1.1. Role of GAS virulence factors in biofilm formation. Many bacterial surface molecules aid in the initial attachment of planktonic GAS to abiotic/biotic surfaces. This includes streptococcal collagen-like protein (Scl-1), pili, Group A *Streptococcus* protein A (AspA), as well as members of the M protein family such as the M protein and M-related protein, which form complexes with LTA to facilitate adherence (Cho and Caparon, 2005, Manetti et al., 2007, Courtney et al., 2009, Maddocks et al., 2011, Becherelli et al., 2012, Kimura et al., 2012, Oliver-Kozup et al., 2013, Bachert et al., 2016). Communication between bacteria utilises quorum sensing (QS) systems, secreting QS molecules such as streptococcal invasion locus protein (SilC), Short Hydrophobic Peptides (SHP) and Autoinducer-2 (Al-2) of the streptococcal invasion locus (Sil), Regulatory gene of glucosyltransferase (Rgg), and LuxS/autoinducer-2 QS systems, respectively to facilitate adherence and maturation of biofilms which includes the production of the extracellular polymeric matrix (EPS) (Lembke et al., 2006, Thenmozhi et al., 2011, Aggarwal et al., 2014, Jimenez and Federle, 2014). Studies have also demonstrated strains that are encapsulated by hyaluronic acid do not form biofilm as readily as un-encapsulated strains, and it has been suggested that the hyaluronic acid capsule decreases biofilm forming capacity (Cho and Caparon, 2005, Sugareva et al., 2010, Marks et al., 2014). Decreased transcription of the Streptococcal regulator of virulence has also been shown to increase production of SpeB, a cysteine protease which may play a role in biofilm dispersal (Doern et al., 2008).

1.2.1.2. Pili

Pili are long filamentous structures that exist on the surface of GAS, and numerous other bacterial species (Nakata et al., 2011, Young et al., 2016). Pili are encoded by the FCT (fibronectin-binding protein, collagen-binding protein, and trypsin-resistant antigen) genomic region of GAS. This is a highly variable 11kb pathogenicity island which contains genes for a pilus backbone protein, at least one matrix protein binding ancillary protein, sortases (SrtB/SrtC2), and a signal peptidase (Manetti et al., 2007, Köller et al., 2010, Fiedler et al., 2015). GAS can be classified into nine FCT subtypes based on the diversity of gene content and nucleotide sequence (Kratovac et al., 2007, Falugi et al., 2008, Kimura et al., 2012). Pili are identified as a major adhesin of GAS, and their involvement in the adherence of GAS to human tonsillar tissue, keratinocytes, lungs and throat epithelial cells has been characterised (Abbot et al., 2007, Crotty Alexander et al., 2010, Smith et al., 2010). Numerous studies have demonstrated that pili play an integral part in GAS biofilm formation and have shown associations between several different FCT types and the capacity of GAS to form bacterial biofilms *in vitro* (Manetti et al., 2007, Köller et al., 2010, Nakata et al., 2011, Ogawa et al., 2011, Kimura et al., 2012). Manetti et al. (2007) confirmed GAS FCT-2 pili are essential for efficient attachment of the GAS M1 strain SF370 to human epithelial cells as GAS pilus negative mutants, constructed by either deletion of the pilus backbone structural protein (*Δspy0128*) or the sortase C1 (*Δspy0129*) gene which are essential for pili assembly, were unable to attach

to epithelial cells. The same mutants did not efficiently aggregate in liquid culture and did not form the same amount of biofilm relative to the wild-type strain on polystyrene as determined by crystal violet biomass staining, or epithelial cells as observed by confocal microscopy (Manetti et al., 2007). The visualisation of the wild-type, Δspy0128 and Δspy0129 strains demonstrated that the EPS was virtually absent for the mutant strains. This dramatically contrasted to the wild-type GAS SF370 strain and the complementation mutant for which the biofilm phenotype was restored. Together these results demonstrate that FCT-2 pili are important in transition to the biofilm phenotype for this SF370, and M1 serotype GAS strain. Following on from these findings, Köller et al. (2010) assayed biofilm formation, under an array of different growth conditions, for 183 isolates that were *emm* and FCT-typed in an effort to demonstrate novel correlations between FCT-type and biofilm formation. Whilst novel associations between FCT-type and biofilm formation by multiple isolates was demonstrated, the data alone was inadequate to support a direct link between biofilm formation and FCT-type. This is most likely because there are many other virulence factors that play a role in biofilm formation by GAS.

There are also data to suggest that the role of individual FCT-types in biofilm formation may be dependent on environmental conditions during infection. In a study of clinical isolates obtained from University Hospital in Rostock, Germany, between 2001 and 2006, an association between environmental conditions (acidity) and biofilm formation for different FCT-types was observed (Manetti et al., 2010). Biofilm formation on abiotic

surfaces and micro-colony formation on epithelial cells for FCT-types 2, 3, 5, and 6 and a subset of FCT-4 strains increased as a result of acidification caused by fermentative sugar metabolism. The subsequent decrease in environmental pH was associated with an enhanced expression of the pilus components and transcriptional regulators including the RofA-like protein (RALP) regulator family proteins RofA and Nra and the AraC/XylS type transcriptional regulator family protein, MsmR. Manetti et al. (2010) speculated that a decreased pH during colonisation at the cell surface due to sugar metabolism may favour biofilm formation; however, this requires further investigation, particularly to determine if this plays a role in the context of biofilm formation in the oropharynx.

As an extension to the Köller et al. (2010) study that demonstrated *emm* type 6 strains with the FCT-1 type pili form high levels of biofilm *in vitro,* Kimura et al. (2012) characterised the role of FCT-1 pili in the GAS TW3558 (*emm* 6) strain. In-frame deletions of the pilus backbone (*tee6*), ancillary protein (*fctX),* and sortases *(srtB and srtA)* were used to produce isogenic pili deficient GAS mutants. Use of the mutants in biofilm growth assays demonstrated that deletion of the *tee6* gene compromised the ability of the strain to form a biofilm on an abiotic surface, with deletion of *fctX* and *srtB* genes (pilus ancillary protein and class C pilus-associated sortase, respectively) further decreasing the capacity for biofilm formation. It was also noted that assembly of the pili, rather than individual pili components, are required for biofilm formation. The FCT-1 pilus region (*fctX* operon) was then ectopically expressed in M1 strain SF370, and an increase in biofilm formation was observed, substantiating the role of FCT-1 pili in

biofilm formation. A similar study was conducted by Becherelli et al. (2012), whereby isogenic mutants of ancillary protein 1 (ALP-1) of FCT-1 type GAS were examined for biofilm formation. Wild-type bacteria produced substantial biofilms, whilst the mutant strain exhibited impaired biofilm forming capacity. Taken together, the data from Becherelli et al. (2012) and Kimura et al. (2012) suggests both structural, and assembly components of pili are important in adherence and biofilm formation of FCT-1 type GAS. However, the authors highlight that the role of pili should not be considered in isolation, as GAS biofilm formation is likely to be dependent on multiple factors (Kimura et al., 2012).

1.2.1.3. *Streptococcal* collagen-like protein

Streptococcal collagen-like protein-1 (Scl-1) is expressed on the surface of GAS as a homotrimeric protein consisting of an N-terminal variable region, a collagen-like region containing Gly-X-Y repeats, and a cell-wall-anchored C-terminal region which contains a linker region connecting the collagen-like region to the cell wall and membrane associated portions of the protein (Lukomski et al., 2000, Xu et al., 2002, Oliver-Kozup et al., 2013). Transcription of Scl-1 is positively regulated by multiple gene activator regulons, suggesting it may be co-expressed with many other GAS virulence factors such as the M protein family (Oliver-Kozup et al., 2011). Scl-1 is present within all strains of GAS and regarded as a major cell surface adhesin (Lukomski et al., 2000, Xu et al., 2002). It is also recognised as a contributor to the biofilm forming capacity of GAS on abiotic surfaces. Isogenic *scl1*-silenced mutants have been shown to have a significantly reduced

capacity for adhesion and biofilm development, as well as variation in surface morphology and EPS production (Oliver-Kozup et al., 2011). In this study by Oliver-Kozup et al. (2011), the expression of the Scl-1 protein in a heterologous *Lactococcus lactis* (*L. lactis*) system facilitated biofilm formation, further implicating this protein in biofilm production. Results from a study by Bachert et al. (2016) assayed biofilm formation in M3 GAS, supported these earlier findings. They introduced a nonsense mutation into the *scl1* coding sequence, which reduced the transcription of the gene in the M3 GAS. Biofilms grown using this mutant on abiotic surfaces coated with fibronectin and laminin exhibited a significantly reduced capacity to form a biofilm. Moreover, the M3 GAS mutant was not able to form micro-colonies when introduced into a skin infection model. When the nonsense mutation was repaired, restoration of expression increased biofilm formation upon fibronectin and laminin surfaces (Bachert et al., 2016).

1.2.1.4. Hyaluronic acid capsule

The hyaluronic acid (HA) capsule, a major virulence factor of GAS, is highly conserved and surface-exposed, and made from a polymer of repeating units of glucuronic and *N*-acetylglucosamine (Stoolmiller and Dorfman, 1969). Some studies suggest that HA is an adhesin that aids in the attachment of GAS strains to host cells (Schrager et al., 1998, Cywes et al., 2000). Conversely, it has been reported that HA capsule can decrease streptococcal adherence by preventing the surface-exposed adhesins from attaching to host cell receptors (Bartelt and Duncan, 1978). The capsule is also central to immune evasion upon colonisation of host tissues, and generally, encapsulated strains display a

greater propensity for virulence than those with a reduced/absent capsule (Henningham et al., 2014). Investigations into the role of capsule in GAS biofilm formation have implicated HA in biofilm maturation. When Cho and Caparon (2005) assessed the biofilm forming capacity of a wild-type HSC5 GAS (M5) strain and an isogenic capsule deficient mutant whereby the hyaluronate synthase (HasA) gene was abolished, they found the biofilm forming ability of the mutant was not affected under static conditions. This suggests HA does not affect the initial bacterial attachment that is required for subsequent biofilm formation. To illustrate the role of HA in later stages of biofilm maturation, flow chambers were utilised, and although the mutant was able to adhere to the surface of the chamber it was unable to propagate the biofilm phenotype and cells seemed to appear dispersed across the substratum evenly, suggesting that HA has a role in biofilm maturation (Cho and Caparon, 2005). A more recent study observed a decrease in HasA transcription in biofilms of MGAS315 (*emm* 3) grown on live keratinocytes (SCC13) in comparison to planktonic bacteria. Marks et al. (2014) suggested other factors (e.g. the host environment) must affect the role of HA in biofilm formation. Indirect evidence that the amount of capsule inhibits GAS biofilm formation was reported by Sugareva et al. (2010). CovS is a sensor kinase involved in regulation of hyaluronic acid synthesis. Deletion of CovS was shown to lead to increased capsule production but lower biofilm biomass for *emm* 2, 6, 18, and 49. Furthermore, Sugareva et al. (2010) suggested strains with less HA seem to form biofilm more readily. It could therefore be suggested that the reduction in capsule production upon change from planktonic to biofilm phenotypes may

facilitate biofilm maturation. Overall, the role of HA in GAS biofilms has yet to be fully elucidated.

1.2.1.5. Streptococcal antigen I/II

Most oral streptococci express streptococcal antigen I/II (Agl I/II) family polypeptides, which have demonstrated roles in adhesion to human salivary glycoproteins, other microbial cells, and calcium to facilitate colonisation in the oral cavity (Jenkinson and Demuth, 1997, Maddocks et al., 2011). An Agl I/II polypeptide produced by M28 GAS called Group A *Streptococcus* protein A (AspA) has been shown to have a role in biofilm formation in two independently isolated M28 serotypes (Maddocks et al., 2011). Deletion of the *aspA* gene in these strains abolished their ability to propagate the biofilm phenotype on saliva-coated surfaces. The biofilm developing capacity of the strain was reinstated upon trans-complementation of the *aspA* deletion. Additionally, expression of the AspA protein in *L. lactis* allowed for biofilm development in this species, relative to wild-type *L. lactis*. Whilst AspA is a relatively understudied GAS virulence factor, these results indicate AspA plays a role in adhesion and biofilm propagation in GAS.

1.2.1.6. Regulators of gene expression in GAS biofilms

The Streptococcal regulator of virulence (*srv*) is a transcriptional regulator required for GAS virulence, as it controls the transcription of many extracellular proteins (Reid et al., 2006, Doern et al., 2008). There is also some evidence indicating participation of this virulence factor in biofilm formation. An isogenic *srv* deficient GAS strain (MGAS5005)

and its complementation mutant were used to demonstrate that *srv*-mediated transcription is an important contributor to biofilm formation (Doern et al., 2009). A decreased capacity to form a biofilm was observed for the Srv deficient strain which was restored to levels comparable to the wild-type strain following complementation. It was suggested that *srv* may control transcription of genes necessary for adherence and micro-colony formation. One of the extracellular proteases controlled by *srv* is the cysteine protease SpeB (Doern et al., 2009). In the absence of Srv, over-production of SpeB is associated with decreased biofilm formation (Doern et al., 2009). Complementation decreased SpeB production and restored biofilm formation comparably to the wild-type. This suggests that SpeB may degrade the components required for biofilm formation and could play a role in dispersion, however, further investigation is required.

1.2.2. Quorum sensing

Quorum sensing (QS), a hallmark feature of many bacterial biofilms, has also been noted for GAS biofilms. Three GAS QS systems have been described: streptococcal invasion locus (Sil), regulatory gene of glucosyltransferase (Rgg), and LuxS/autoinducer-2.

Sil has been linked to regulating genes involved in invasive disease (Jimenez and Federle, 2014). SilC is a signaling peptide of Sil, and has been linked to the ability of GAS to spread in soft tissues (Belotserkovsky et al., 2009). Importantly, SilC has been shown to have a role in QS for GAS biofilm formation (Lembke et al., 2006, Thenmozhi et al., 2011). Using safranin-staining, an isogenic *emm*14 *silC* mutant showed reduced adherence to surfaces coated with fibronectin, fibrinogen, and polystyrene surfaces,

relative to the wild-type strain, but this was not statistically significant (Lembke et al., 2006). An isogenic *emm*18 *silC* mutant exhibited reduced adherence to collagen type I and IV substrates, relative to the wild-type strain, but this was also not statistically significant. SEM analysis of the *emm*14 and *emm*18 *silC* mutants revealed phenotypic changes in the strain relative to the wild-type. The *emm*14, *silC* mutant biofilm surface displayed more clefts than the wild-type analogue whilst the *emm*18 *silC* mutant displayed a thinner biofilm with a patchy appearance, whilst its wild-type comparator presented a solid and thick biofilm (Lembke et al., 2006).

Conversely, in a study by Thenmozhi et al. (2011), it was suggested that strains from different serotypes form biofilms regardless of the presence of the *sil*C gene. Crystal violet staining of biofilms grown from strains of 11 different serotypes distinguished M56, M65, M74, M89, M100, and st38 as biofilm formers and M49, M63, M88.3, M122, and st2147 as non-biofilm formers. These biofilms were grown under static conditions on uncoated polystyrene. These strains were screened for the presence of *sil*C which was found present in only M100, M74, and st38 from the biofilm formers and the non-biofilm former M122. Serotypes lacking *silC* were the most proficient biofilm producers under these conditions suggesting that the involvement of SilC in quorum sensing is not required for biofilm formation in all strains.

The Rgg QS system is one of the most conserved systems among Firmicutes, universally existing among all species of *Streptococcus*. Within this large family of regulatory proteins, many paralogs exist. For GAS, biofilm formation, biofilm development and

virulence is controlled by the Rgg2/Rgg3 system in response to the short hydrophobic peptides SHP2 and SHP3 (Chang et al., 2011). The effects of SHP have been witnessed in GAS biofilm development with potentiation of surface-associated biofilms forming in concentrations of synthetic SHP pheromone as low as 5 nM (Aggarwal et al., 2014). Rgg-SHP-mediated QS has also been hypothesised to promote interspecies signaling between common residents of the nasopharynx; *S. pneumoniae*, *S. dysgalactiae*, and GAS (Chang et al., 2011). Interspecies signaling utilising the orthologous Rgg/SHP systems has been further investigated and shown to be bidirectional between GAS, GBS, and *Streptococcus dysgalactiae* subsp. *equisimilis,* however, the implication for the role of this particular bidirectional communication using QS systems in multispecies biofilm formation and virulence warrants further analysis (Cook et al., 2013).

Lastly, Autoinducer-2 synthesised by LuxS, an enzyme present in several biofilm forming bacteria, including GAS, is necessary for biofilm formation (Jimenez and Federle, 2014). Although this QS system has yet to be thoroughly investigated, it is thought to control some virulence mechanisms (haemolytic and proteolytic activity), and importantly *emm* gene expression and SpeB production, which have both been shown to affect biofilm formation and development (Lyon et al., 2001, Marouni and Sela, 2003, Siller et al., 2008, Beema Shafreen et al., 2014).

1.3. Modelling GAS biofilms

Current knowledge of biofilm formation, including basic hallmark characteristics, physiology, and role in antimicrobial tolerance, has come primarily from *in vitro* biofilm

modelling. *In vitro* models aim to depict conditions similar to those *in vivo* considering variables such as growth rate, flow rate, nutrient availability, gas concentrations, and substratum. The simplest and earliest biofilm model was liquid growth media inoculated with bacteria left to colonise the solid surface (Zobell, 1943). However, higher throughput models have since been developed such as multi-well systems using various abiotic growth surfaces (glass, plastic, silicone, and polystyrene). Although these are cost-effective and somewhat easy to implement, the biofilms formed are limited in their ability to truly mimic those in an *in vivo* setting (Marks et al., 2014). Moreover, while *in vitro* GAS biofilms have provided important insight into GAS biofilm formation, GAS colonisation and infection *in vivo* is a complex process involving multiple interactions with the host. Such interactions initiate and alter GAS gene expression in a way that is difficult to mimic in most *in vitro* models. It has been demonstrated that a lack of host factors resulted in highly differential virulence gene expression between biofilms produced *in vitro* to those present *in vivo* (Cho and Caparon, 2005), highlighting the importance of mimicking the host environment as closely as possible. Alternative approaches to biofilm formation include the use of epithelial cells as a substratum for GAS biofilm growth to compensate for host factor presence. However, the inherent toxicity of broth grown GAS strains renders long term biofilm-epithelial modelling difficult (Håkansson et al., 2005). A more recent study that utilised both live and pre-fixed epithelial substrata successfully integrated aspects of the necessary environment, closely mirroring *in vivo* GAS colonisation (Marks et al., 2014). Specifically, GAS was

able to form micro-colonies, resemblant of biofilms *in vivo*, as opposed to dense biofilm sheets typical of biofilms grown on abiotic surfaces. Additionally, biofilms were non-toxic to the live human keratinocyte substratum. Overall, this study confirmed that an epithelial substratum potentiates biofilm formation, with bacterial morphology resemblant of *in vivo* GAS biofilms, a result not achievable for GAS biofilms grown on abiotic surfaces like glass or plastic (Marks et al., 2014). Another *in vitro* study investigated the ability of 2 dominating *emm*-types involved with NSTI, (*emm* 1 strain 8157, and *emm* 3 strains 5626 and 8003) to form biofilms using standard polystyrene and glass surfaces (Siemens et al., 2016). Both *emm* 3 strains formed biofilms on uncoated and fibronectin-coated polystyrene surfaces. In contrast, only strain 5626 was able to form a biofilm on glass surfaces. The *emm* 1 strain 8157 did not form biofilms under the tested plate conditions. A 3D organotypic skin model was also generated using human keratinocyte cells (N/TERT-1) and normal human dermal fibroblasts (NHDF) to mimic key anatomical/functional features of the skin. This model had the advantage of dermal and epidermal layers being formed, and key epidermal structural proteins included. The *emm* 1 strain 8157, and *emm* 3 strains 5626 and 8003 were all able to initiate tissue infection in this model, and after 8 hours of incubation, the bacteria were found to predominate the stratum cornium. Upon further incubation the bacteria were dispersed throughout the whole tissue, with bacterial aggregates that developed typical of biofilm upon immunostaining. Further investigation of these aggregates utilising confocal laser scanning microscopy confirmed the presence of hallmark biofilm features of the EPS

including exopolysaccharides, lipids, and extracellular DNA associated with the bacterial community (Flemming and Wingender, 2010, Siemens et al., 2016). At present, GAS existing in the biofilm phenotype is not recognised as a potential component of NSTIs. This comprehensive study by Siemens et al. (2016) supports the need for further investigation into the role biofilms play in GAS NSTIs, and by extension, other GAS associated skin infections.

Future studies using similar epithelial-GAS biofilm models are necessary, with a focus on establishing the interaction between GAS and the local host environment to provide a more accurate understanding of the underlying mechanisms in which GAS may adhere, colonise and persist in the host. Whilst much of the work has focused on the role of host proteins in GAS biofilm formation, host glycans are yet to be studied in the context of GAS biofilm formation.

1.4. Glycans in bacterial pathogenesis

Glycans are carbohydrates present on more than half of all human proteins, with their ubiquitous presence in mucosal fluid, on secreted molecules, immune cells, and a variety of epithelial cell surfaces, making glycosylation one of the most common post-translational modifications (Apweiler et al., 1999, Christiansen et al., 2014).

Glycans exist as saccharides attached to a lipid or protein backbone, they can be linear or branched, and consist of monosaccharides linked glycosidically (Belický et al., 2016). Glycans can occur either as *N*- or *O*-linked and are distinguished by the amino acids they are added to; with *N*-linked glycans attached at the nitrogen of asparagine and *O*-linked

glycans attached at the oxygen of serine or threonine amino acid residues (Fig 1.2) (Belický et al., 2016).

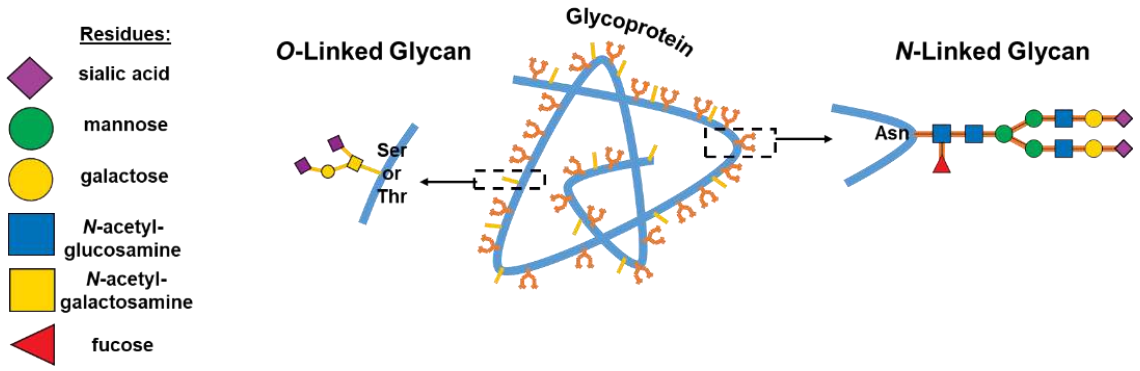

Figure 1.2. Glycoprotein and its *O*- and *N*-linked glycans. The simplified diagram depicts a protein backbone (blue) decorated with *O*- and *N*-linked glycans attached at serine (Ser)/threonine (Thr) or asparagine (Asn) residues respectively.

Glycans have several important biological roles; structural and modulatory roles (e.g. protein folding and membrane organisation), intrinsic intra-species roles (e.g. immune recognition via self-associated molecular patterns), and extrinsic inter-species host-pathogen roles (e.g. pathogen-associated molecular patterns and immune modulation of host by pathogen) (Varki, 2016).

The host cell surface is a landscape rich in an assortment of glycan structures, with access to these glycans making for an interesting and complex environment for pathogens to bind and utilise for a variety of purposes. Within the last decade, considerable advancements have been made in the field of glycobiology such as the development of lectin and glycan microarrays that provide high-throughput screening with increased sensitivity and accuracy. These technologies have enabled the unveiling and identification of these novel glyco-interactions occurring at the bacterial-host interface (Poole et al., 2018). Findings strongly suggest glycans are the initial point of contact with

the host for many bacteria, mediating attachment and colonisation, and can consequently facilitate infection and disease (Poole et al., 2018). Despite the growing evidence and appreciation of the role glycans play in the pathogenesis of several bacteria (Poole et al., 2018), investigation into glycans and their involvement in mediating GAS disease remains comparatively under-investigated.

1.4.1. Glycans are implicated in bacterial adherence at the oropharynx

The oropharynx comprising of the oral cavity and contiguous regions of the tonsils, pharynx, and oesophagus, together the tissues of these distinct sites have a cumulative role in both human health and disease (Dewhirst et al., 2010). The oropharynx further connects to the respiratory and gastrointestinal tract, and as such it is a critical port of entry for several pathogens. Hence, considerable efforts have been made into understanding the interplay between both the naturally residing microflora and pathogenic bacteria to the glycoproteins of saliva and the oropharyngeal epithelia as a means of mediating host-microbe interactions in both healthy and diseased states (Poole et al., 2018).

Saliva is a protein rich liquid environment that bathes the oropharynx, and it contains a variety of protein families (e.g. salivary amylase, mucins, agglutinin, basic and acidic proline rich proteins, immunoglobulins etc), many of which are heavily glycosylated (Helmerhorst and Oppenheim, 2007). Mucins are an example of a glycan rich protein predominated by *O*-linked (and some *N*-linked) glycans, and have a considerable role in host immunity and defense (Hollingsworth and Swanson, 2004, Varki, 2016). Several

bacteria, fungi, and viruses have been found to use lectin-like adhesins to adhere to these salivary mucins. *Helicobacter pylori* is a prime example of a well characterised pathogenic bacteria that has demonstrated effective binding to Lewis B glycan motifs on a major salivary mucin, MUC5B, which otherwise has important roles in host defense. It is hypothesised that this binding mechanism employed by *H. pylori* enables it to camouflage from host defense via molecular mimicry, where it can successfully migrate from the oral cavity to its preferred site of colonisation, the stomach. Once established in the stomach, *H. pylori* causes a variety of gastrointestinal diseases such as peptic ulcers and gastritis (Walz et al., 2005, Issa et al., 2010).

Similarly, attachment to host tissues at the oropharynx is also in part mediated by glycans. The diversity of the glycans that cover the oropharynx has been thought to contribute to distinct tissue tropisms of microbes, sometimes leading to site specific colonisation and infection even within spaces of close proximity (e.g. differential microfloral colonisation of the tooth versus microbial communities present at the tongue) (Cross and Ruhl, 2018). This is particularly evident for *Streptococcus mutans* which exclusively colonises the tooth surface via agglutinin binding, where it consumes a variety of monosaccharides (e.g. mannose, fructose, lactose, and galactose) available at the site. Metabolised monosaccharides are converted into acids that accumulate and cause considerable dental decay, carries, and disease (Mitchell, 2003).

Streptococcus pneumoniae is another well-characterised member of the streptococci family that is found in the mucosa of the nasopharynx. At the mucosal surface,

*S. pneumonia*e expresses several glycosidases that facilitate both adherence and modification of a variety of glycan structures (glycosaminoglycans and both *N*- and *O*-linked glycans) of the airway. Given the prevalence of sialic acid in the oronasopharynx, it is perhaps unsurprising that *S. pneumonia*e is equipped with three neuraminidases (NanA, NanB, and NanB), each of which sequentially cleave terminal sialic acid residues off mucosal glycan structures. Liberated sialic acid is utilised by *S. pneumoniae* for metabolic consumption as well as successful pneumococcal adherence, colonisation, and subsequent disease (King, 2010).

Several other pathogens (e.g. *Candida albicans, P. aeruginosa*, and *E. coli*) involved in a variety of mild to severe infections and diseases have been found to bind glycans of the oropharynx (Lewis and Lewis, 2012, Everest-Dass et al., 2017, Olsen, 2020). Taken together, these findings cement the importance of host glycans in mediating microbial pathogenesis in oropharyngeal disease.

1.4.2. Glycans in GAS adherence

GAS possesses several adhesins and virulence factors (previously outlined) that are important in mediating initial bacterial attachment and adherence to the epithelial surfaces of the throat and skin. Exploitation of host cell surface glycans is a recognised component that drives pathogenesis for several microbes (Poole et al., 2018). However, the investigation into glycan binding and utilisation by GAS is comparatively underexplored. To date, some glycan targets have been established, with much of the work focusing on

the adhesin-like properties of M protein, a major surface expressed protein and virulence factor of GAS (Frick et al., 2003, De Oliveira et al., 2017, De Oliveira et al., 2019).

1.4.2.1. M protein is implicated in glycan binding

The M protein is a highly expressed virulence factor of GAS, and it is implicated in adherence (Walker et al., 2014). Due to its preeminence, the M protein has been of primary focus for identifying GAS-host glycan interactions, and efforts to characterise these interactions continue to be explored.

Some of the earliest research has been conducted on glycosaminoglycans (GAGs) as targets for M protein binding (Bergey and Stinson, 1988, Wadstrom and Ljungh, 1999, Frick et al., 2003). GAGs are abundantly present in the extracellular matrix of all eukaryotic surfaces, and have been recognised as binding points for several bacteria, viruses, and protozoa (Wadstrom and Ljungh, 1999). Bergey and Stinson (1988) found exogenous GAGs, heparin, and heparin sulfate when added in excess, acted as competitive inhibitors of M6 GAS serotype binding to heparin natively present on the basement membranes of kidney tissue samples. Other GAGs were similarly assessed (dermatan sulfate, chondroitin sulfate, and hyaluronic acid), with inhibition of GAS binding occurring to a lesser degree. Wadstrom and Ljungh (1999) described heparin binding to GAS surface molecules, albeit at a low affinity, which they attributed to non-specific binding arising from various charged molecules reducing opportunities to bind heparin. However, only recently was the M protein determined as the adhesin binding these various GAGs. Specifically, Frick et al. (2003) investigated the ability of M proteins

from 49 GAS serotypes to associate with various pharyngeal- and dermal-associated GAGs (including heparin, heparin sulphate, and dermatan sulphate). The study concluded that GAGs mediated GAS adhesion to human cells in an M protein-dependent manner (Frick et al., 2003).

M protein has also been shown to bind other glycans. A study of a throat tropic M6 GAS strain found that fucose containing glycoproteins were essential for M-mediated GAS adherence to pharyngeal epithelia (Wang and Stinson, 1994). More recently, De Oliveira et al. (2019) have shown differential GAS binding affinities of three pharyngitis associated GAS serotypes M1, M3, and M12 towards ABO(H) blood group antigen glycan structures are underpinned by differences in M protein affinity towards blood group antigen structures.

Taken together, these data suggest M protein has an important role in mediating GAS-host glycan interactions and could serve as a potential avenue for therapeutic targeting in the form of glycomimetics that block GAS adherence.

1.4.3. Glycans in oropharyngeal biofilm formation

The oropharynx and its epithelial cell surfaces, mucosal layers, immune cells, secreted molecules, and the saliva which bathes the entirety of the oropharynx are heavily glycosylated. Microbes utilise and modify these glycans for metabolic processes, microbial growth, crossing mucosa, and deactivation/reducing the activity of host immune molecules (Collin and Olsén, 2001, Iyer and Camilli, 2007, Lewis and Lewis, 2012, Garbe et al., 2014). Moreover, as previously explored, glycans are necessary for

microbial attachment and adherence, both crucial initiatory steps towards biofilm formation and biofilm establishment within the host.

S. pneumoniae, an opportunistic pathogen of the oronasopharynx, is perhaps the most characterised for its interactions with host glycans and subsequent biofilm forming abilities. Several reports have suggested that glycan modification and utilisation are necessary mechanisms in biofilm formation for pneumococcal colonisation (King, 2010, Lewis and Lewis, 2012). Although it is likely to be a multifactorial process, the ability of *S. pneumoniae* to form biofilms has been attributed to glycosidase action exerted by neuraminidases NanA and NanB, both of which cleave and liberate sialic acid residues abundantly present in the pharynx and airway of the host (Parker et al., 2009, Lewis and Lewis, 2012). One study found that *S. pneumoniae nanA* and *nanB* mutant strains displayed diminished biofilm forming abilities *in vitro* (Parker et al., 2009). NanA and NanB were further implicated in biofilm formation in a study by Trappetti et al. (2009) which found that initial adherence to the well surface increased only in the presence of sialic acid, and the other 26 sugars assessed exerted no effect. The study further found that biofilm increased in the presence of exogenous sialic acid, with biofilm forming abilities diminishing upon the addition of sialic acid analogs or inhibitors of the neuraminidases tested. Another study described NanA to be particularly active during cluster formation and biofilm maturation *in vitro* (Parker et al., 2009). Thus, host glycans play an important role in the various stages of biofilm formation for *S. pneumoniae*. Other pathogens of the oropharynx such as *Porphyromonas gingivalis*, *Tannerella forsythia,*

and *Haemophilus influenza* have been known to exploit and be dependent on sialic acid for biofilm formation (Bouchet et al., 2003, Roy et al., 2011, Li et al., 2012). Taken together, it is evident that glycans of the oropharynx are an important component of microbial adherence and subsequent biofilm formation. However, the role of host glycans in the context of GAS biofilm formation is an area of research that has previously remained unexplored.

1.5. Aims and Objectives

Despite GAS remaining sensitive to penicillin, antibiotic treatment failure rates of 20-40% have been reported. GAS biofilm formation has previously been investigated in the context of virulence factor involvement using models that do not effectively mimic the host. Improved models of GAS biofilm formation that utilise host factors to mimic *in vivo* conditions will ensure biofilms generated in the lab more accurately reflect those occurring during a clinical infection.

Moreover, host glycans have been implicated in planktonic GAS adherence. However, it is clear that there is gap in the field surrounding their role in GAS biofilm formation. Improved understanding of the way in which GAS interacts, and forms biofilms at the GAS-tissue interface will enhance our understanding of GAS biofilms and pathogenesis. As such, the aims of this project were to investigate the role pharyngeal cell surface glycans play in GAS biofilm formation and subsequent penicillin tolerance.

Specifically, the aims of this project were to:

I. Develop and optimise a GAS biofilm-host cell model

II. Assess the role pharyngeal cell surface glycans play in throat tropic M12 GAS biofilm formation

III. Assess the role pharyngeal cell surface glycans play in GAS biofilm formation for a diverse set of GAS serotypes

Chapter 2: Developing and optimising a GAS biofilm-host cell model

A part of this work has been published in Scientific Reports, Nature.

Overview: GAS causes 700 million infections and accounts for half a million deaths per year. Biofilm formation has been implicated in both pharyngeal and dermal GAS infections. *In vitro*, plate-based assays have shown that several GAS M-types form biofilms, and multiple GAS virulence factors have been linked to biofilm formation. Although the contributions of these plate-based studies have been valuable, most have failed to mimic the host environment, with many studies utilising abiotic surfaces. GAS is a human specific pathogen, and colonisation and subsequent biofilm formation is likely facilitated by distinct interactions with host tissue surfaces. As such, a host cell-GAS biofilm model has been optimised to support and grow GAS biofilms of a variety of GAS M-types. Improvements and adjustments to the crystal violet biofilm biomass assay have also been tailored to reproducibly detect delicate GAS biofilms. 72 h was determined as an optimal growth period for yielding detectable biofilm biomass. Using the established method, GAS biofilms formed are robust and durable, and can be reproducibly assessed via staining/washing intensive assays such as crystal violet with the aid of methanol fixation prior to staining. Lastly, SEM imaging of GAS biofilms formed by this model are resemblant of those previously found on excised tonsils of patients suffering chronic pharyngo-tonsillitis. Taken together, an efficacious GAS biofilm host-cell model has been developed that can support long-term GAS biofilm formation, with biofilms formed closely resembling those seen *in vivo*.

2.1. Introduction

GAS is a Gram-positive human pathogen known to cause an array of infections ranging from mild infections of the skin and throat, to more serious and life threatening conditions such as necrotising fasciitis and numerous autoimmune sequelae (Walker et al., 2014). GAS poses a considerable global burden, with high rates of patient mortality and morbidity (Carapetis et al., 2005).

GAS has been found to form biofilms in the tonsillar crypts of GAS pharyngitis tonsillectomy patients, and in the skin lesions of GAS impetigo sufferers (Akiyama et al., 2003, Roberts et al., 2012). *In vitro*, it has been demonstrated that GAS biofilm formation is strain dependent. Among isolates of the same serotype, biofilm forming capacities are oftentimes found to differ considerably (Baldassarri et al., 2006). Furthermore, *in vitro* plate-based studies have implicated several GAS virulence factors (M protein, capsule, pili, SpeB, CovS, and quorum sensing peptides) in biofilm formation (Vyas et al., 2019). These findings have contributed substantially to our current understanding of GAS biofilms and their involvement in GAS pathogenesis and disease. However, much of this work has been conducted on abiotic surfaces (plastic, glass, and silicone) which GAS does not naturally colonise. To date, few studies have used host matrix components like collagen, fibronectin, or fibrinogen as surface coatings (Cho and Caparon, 2005, Lembke et al., 2006, Sugareva et al., 2010, Oliver-Kozup et al., 2013). Moreover, there is currently no gold standard methodology or protocol in the GAS field for biofilm formation. The variability among methods, and limited use of host factors in *in vitro* plate-based GAS biofilm models found in previous studies has been summarised in Table 2.1. This table highlights that only three *in vitro* plate-based studies utilising epithelial monolayers to grow and support GAS biofilms have been published.

There is a need for GAS biofilm models to better incorporate host factors, as it has been found that failure to do so has significant effects on the biofilms formed, with the overall arrangement and architecture of biofilms and their virulence gene expression, found to noticeably differ from that of biofilms formed *in vivo* (Cho and Caparon, 2005). Moreover, tissue tropism displayed by differing GAS isolates towards the throat and skin, which are vastly different epithelial landscapes and environments (Bessen and Lizano, 2010), will influence GAS adherence, colonisation, and subsequent biofilm formation. Thus, the incorporation of relevant host epithelial substratum, and an overall mimicking of the host environment should be a consideration in GAS biofilm modelling.

Here, a GAS-pharyngeal cell model has been optimised to cultivate robust 72 h GAS biofilms that can be used for a diverse set of GAS M-types. We also propose some optimised steps and tips for increased biofilm integrity and reproducibility when performing crystal violet staining assays. This model has since been used to effectively assess the role pharyngeal cell surface glycans play in GAS biofilm formation (Vyas et al., 2020).

Table 2.1. Examples of *in vitro* plate-based models used for the study of GAS biofilm formation.

Growth Substratum	Time	Media conditions	Biofilm Inoculum*	*emm*-type	Purpose of the study	Ref.
Polystyrene	Up to 96 h	C medium, 23°C	0.1:10	*emm*14	Biofilm forming abilities of WT GAS compared to mutants (capsule, *mga* virulence regulon, M-protein, and *covR*)	Cho and Caparon (2005)
Polystyrene	48 h	THY - 0.5% yeast, 37°C	1:40	*emm*1, 2, 4, 5, 6, 24, and 49	Relationship between M family proteins (M-protein, M-related protein, and M-like protein) and lipoteichoic acid in hydrophobicity and subsequent biofilm formation	Courtney et al. (2009)
Polystyrene	24 h	THY - 0.2% yeast supplemented with 0.5% glucose, 37°C	1:100	*emm*14	Microcolony-dependent and -independent biofilm formation, with a focus on the role of GAS capsule	Matysik and Kline (2019)
Glass and cellular form of fibronectin (cFn) coated glass	1 or 24 h	Brain heart infusion (BHI) and THY + 0.2% yeast, 37°C	Exponential phase GAS	*emm*1, 28, and 41	Streptococcal collagen-like protein-1 (Scl1) binding wound associated cFn (with extra domain A) involvement in biofilm formation	Oliver-Kozup et al. (2013)
Fibronectin or laminin coated polystyrene	24 h	THY - 0.2% yeast, 37°C	Exponential phase GAS	*emm*3	Scl1 and the *scl1.3* locus in adhesion and subsequent biofilm formation	Bachert et al. (2016)
Fibronectin, collagen coated, or uncoated polystyrene	Up to 72 h	BHI - 0.5% glucose, 37°C	Not defined	*emm*2, 6, 18, and 49	*covS* sensor kinase and its role in biofilm formation	Sugareva et al. (2010)

Human: fibronectin, fibrinogen, laminin, collagen coated, or uncoated polystyrene	12 to 120 h	Luria Broth, THY - 0.5% yeast, BHI, or chemically defined medium, 37°C	$1x10^4$ CFU/ml	*emm*1, 2, 3, 6, 12, 14, 18, 28, and 49	Effect of coating with human matrix components in potentiating biofilm formation.	Lembke et al. (2006)
				*emm*14 and *emm*18	Investigating quorum sensing signaling peptide SilC in mediating biofilm density and structure	
Polylysine coated glass coverslips	72 h	C medium, 37°C	1:10		Pili involvement in mature biofilm formation	Manetti et al. (2007)
Pharyngeal: Detroit 562 monolayers	2 h	THY, 37°C	0.6 OD_{600nm}	*emm*1	Pili involvement in initial adhesion and its role in microcolony development	
Pharyngeal: Detroit 562 monolayers	72 h	THY, 34°C	1:20	*emm*1, 3, 9, 12, 44, 53, 90, 98, 108	Assessing the role of pharyngeal cell surface glycans in GAS biofilm formation in the context of GAS pharyngitis	Vyas et al. (2020)
Skin: SCC13 monolayers cells	48 h	THY- 0.5% yeast, 34°C	2×10^4 CFU/0.5mL	*emm*3 and *emm*6	Pre-formed 48 h mature biofilms grown on fixed epithelia, diluted, and re-grown on live epithelia for 48 h. Resultant biofilms examined for colonisation, virulence, and genetic diversity	Marks et al. (2014)

*Inoculums listed as ratios (bacteria: bacterial media), growth phase, or optical density.

2.2. Materials and methods

2.2.1. GAS and culture conditions

GAS strains used in this study (Table 2.2) are clinical GAS isolates, with each strain representative of a discrete GAS *emm*-type (Johnson et al., 2002, Aziz et al., 2004, McKay

et al., 2004, Sanderson-Smith et al., 2014). GAS was grown on horse blood agar (HBA) plates (Oxoid, UK) or Todd Hewitt agar supplemented with 1% (w/v) yeast (THYA) (Difco, Australia) (for media compositions see Appendix A). Static cultures of GAS were grown overnight in Todd Hewitt broth supplemented with 1 % (w/v) yeast (THY) (for enumeration (CFU/mL) details of GAS overnight cultures see Appendix B). GAS was cultured and maintained at 34°C (Marks et al., 2012).

Table 2.2. GAS strains utilised in this study, their *emm*-types, and clinical source (Johnson et al., 2002, Aziz et al., 2004, McKay et al., 2004, Sanderson-Smith et al., 2014, De Oliveira et al., 2019).

M-type	Strain	Clinical source
M1	5448	Invasive infection: Necrotising fasciitis and toxic shock
M12	PRS-8	Superficial infection: persistent Pharyngeal pus/sinusitis
M3	90254	Invasive infection
M98	NS88.2	Invasive infection: Blood (bacteraemia)
M108	NS50.1	Superficial infection: Wound

2.2.2. Human pharyngeal cell culture conditions

Detroit 562, a human pharyngeal epithelial cell line (CellBank Australia, Australia), was cultured in Dulbecco's Modified Eagle Medium (DMEM) F12 (Invitrogen, Australia), supplemented with 2 mM L-glutamine (Gibco, Life Technologies, UK) and 10 % (v/v) heat inactivated foetal bovine serum (FBS) (Bovogen Biologicals, Australia) in cell culture flasks at 37˚C, 5% CO_2 – 20% O_2 atmosphere. For tissue culture cell media composition see Appendix A.

2.2.2.1. Pharyngeal cell monolayer formation

Fixed Detroit 562 pharyngeal cell monolayers form the substratum for GAS biofilm growth. An outline of the optimised process and the monolayers formed are as depicted in Fig 2.1. Firstly, the wells of a 96-well flat bottom cell culture microtiter plate (Greiner Bio-One, Germany) was coated with 50 µL of 300 µg/mL Collagen I from rat tail (Gibco, Life Technologies, UK) prepared in pre-chilled, sterile 17.4 mM acetic acid solution. The plate was incubated for 1 h at 37˚C (5% CO_2 – 20% O_2 atmosphere) to facilitate collagen coating.

After 1 h, the excess collagen was removed from the wells and the wells were seeded with 150 µL Detroit 562 cell suspension ($2x10^5$ cells/mL) and cultured for 48 h (achieving ~95% confluency). Once a ~95% confluent Detroit 562 pharyngeal cell monolayer was achieved, the media containing debris/non-attached Detroit 562 cells was removed, and the wells washed once with 200 µL of phosphate buffer solution (PBS) (for buffer compositions see Appendix A). The Detroit 562 pharyngeal cell monolayers were then fixed with 50 µL sterile 3.7% paraformaldehyde (PFA) (Sigma-Aldrich, USA) for 20 min (RT). Once fixed, the PFA was removed and the monolayers were washed twice with 200 µL of PBS. Monolayers can be used immediately or stored at 2-8°C for up to two weeks (with monolayers kept wet via submersion in 200 µL of PBS) until required for use.

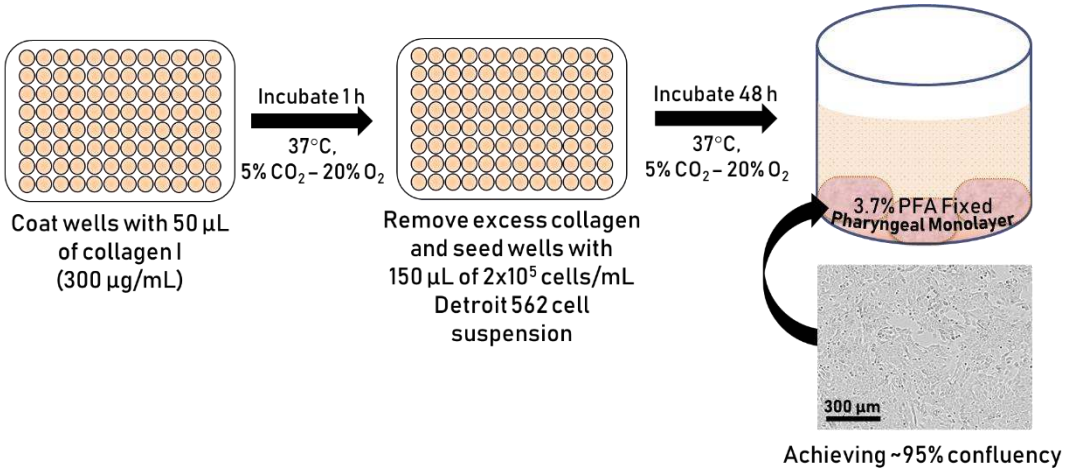

Figure 2.1. Schematic outlining the optimised process of Detroit 562 pharyngeal cell monolayer formation. Schematic shows collagen coating, seeding with Detroit 562 pharyngeal cells, and finally an example well containing a 3.7% PFA fixed ~95% confluent monolayer of Detroit 562 pharyngeal cells. Example monolayer image taken at 10x objective at the Incucyte.

2.2.3. GAS biofilm formation

An outline of the optimised process for GAS biofilm formation using the GAS-pharyngeal cell model is as depicted in Fig 2.2. Wells containing fixed pre-formed Detroit 562 pharyngeal cell monolayers were inoculated with 150 µL of overnight GAS culture diluted 1:20 in THY-glucose (0.5% glucose v/v) (THY-G). Wells containing 150 µL sterile

THY-G (no bacteria) served as media sterility controls and blanks. The plate was incubated for 2 h (34°C, 50 rpm) to facilitate GAS interaction and adherence to the pharyngeal cell monolayer substratum. At 2 h, non-adhered GAS was removed, and the wells replenished with 150 µL sterile THY-G media and the plate incubated (34°C, 50 rpm). Every 24 h, the media was refreshed with 150 µL sterile THY-G until a robust 72 h GAS biofilm was formed.

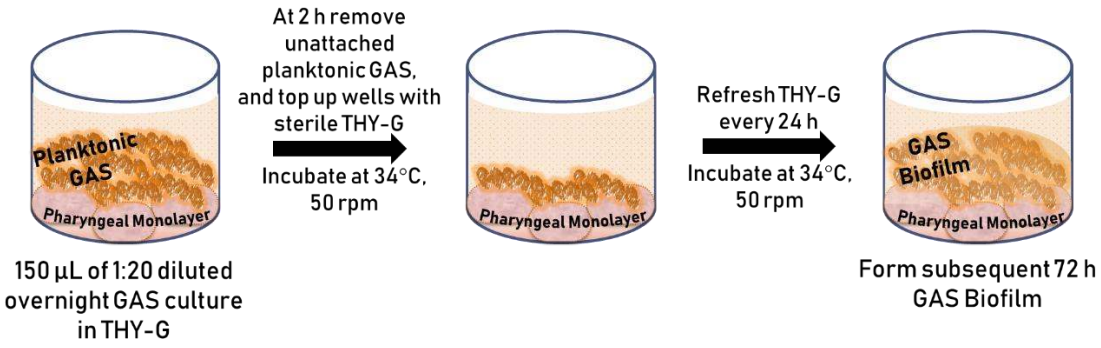

Figure 2.2. Schematic outlining the optimised process of GAS biofilm formation upon the fixed Detroit pharyngeal cell monolayers. Schematic shows fixed Detroit 562 pharyngeal monolayers co-cultured with planktonic GAS cells (cocci chains) left to adhere for 2 h. 72 h GAS biofilms are formed directly from adhered GAS.

2.2.4. GAS biofilm biomass crystal violet staining

Biofilms were detected for their biomass via crystal violet staining modified from Burmølle et al. (2006) and Barraud et al. (2012). To do so, the media was gently and slowly pipetted off from the biofilms formed, and thoroughly air dried (30-40 mins, or until fully dried). Dried biofilms were fixed with 150 µL of 99% methanol for 15 min as per Peeters et al. (2008). Once fixed, the methanol was removed, and the biofilms were further thoroughly air dried to evaporate any remnant methanol. Biofilms were then stained with 150 µL of 0.2% crystal violet (w/v) (Sigma-Aldrich, USA) supplemented with 1.9% ethanol (v/v) for 10 min (RT, static). Upon staining, excess crystal violet was removed, and the biofilms gently washed twice with 200 µL of PBS. Crystal violet stain that had incorporated into the biofilm was re-solubilised upon the addition of 150 µL of 1% sodium dodecyl sulphate

(SDS) (w/v) (Sigma-Aldrich, USA). To ensure thorough release of the crystal violet stain, the biofilms were left to de-stain in the SDS solution for 10 min (RT, static). Monolayers with THY-G (no GAS biofilm) served as plate blanks. Resultant released crystal violet stain was diluted 1:5 in 1% SDS solution and biofilm biomass determined spectrophotometrically at OD_{540nm} (SpectraMax Plus 384 microplate reader).

2.2.5. Scanning electron microscopy

M1 and M12 GAS biofilms were grown on Detroit 562 pharyngeal cell monolayers pre-formed on 13 mm plastic Nunc Thermanox coverslips (Proscitech, USA) in a 12-well polystyrene plate. Biofilms were air dried, and prepared for SEM using methods adapted from (Williams and Bloebaum, 2010) with the following modifications. In brief, biofilms were pre-fixed in 2.5% glutaraldehyde, 50 mM L-lysine monohydrochloride, and 0.001% ruthenium red solution prepared in 0.1 M HEPES buffer (pH 7.3) (30 min, 4°C). Following pre-fixation, biofilms were fixed in fixative solution (2.5% glutaraldehyde and 0.001% ruthenium red prepared in 0.1 M HEPES buffer, pH 7.3) for 1.5 h (4°C) and washed twice in 0.1M HEPES buffer. 2% osmium tetroxide vapour was used post-fixation (2 h) followed by three washes with distilled water (each 15 mins). A graded ethanol series (30%, 50%, 70%, 90%, and 3x 100%) was then used to remove all water from the biofilms before they were critical point dried (Leica CPD 030, Austria). Dried biofilms were then sputter coated with 20nm platinum (Edwards Vacuum coater, USA) and visualised using a JEOL JSM-7500 microscope (JEOL, Japan) at 15 000 x magnification. Detroit 562 pharyngeal monolayer controls (without biofilms) were also imaged at 5000 x magnification. Images were taken at random positions within the samples by an UOW Electron Microscopy Centre technician blinded from the study in an effort to reduce bias.

2.2.6. Statistical analysis

All statistical analysis was performed using GraphPad Prism (version 8.4.0, GraphPad Software, USA). Datasets were checked for normal distribution prior to analysis and subsequently compared using a student T-test. A *p*-value of ≤ 0.05 was considered significant.

2.3. Results

2.3.1. Detroit 562 monolayer development

Most GAS biofilm studies utilise abiotic surfaces such as plastic, glass, or silicone, and very few incorporate host factors like ECM matrix components (collagen, laminin, fibronectin) as surface coatings. As such, these models poorly represent the human environment to which GAS naturally colonises. Here, Detroit 562 pharyngeal cell monolayers serve as the substratum for GAS biofilm growth.

Detroit 562 pharyngeal cells were seeded at a concentration of $2x10^5$ cells/mL on collagen I coated and uncoated surfaces of a 96-well plate. At 28 h of growth, the Detroit 562 pharyngeal cells are most confluent on the collagen I coated wells (Fig 2.3A-C), whereas cells seeded on uncoated wells (Fig 2.3D-F) are of significantly lesser confluency at 28 h despite having been seeded with the same concentration of Detroit 562 pharyngeal cells.

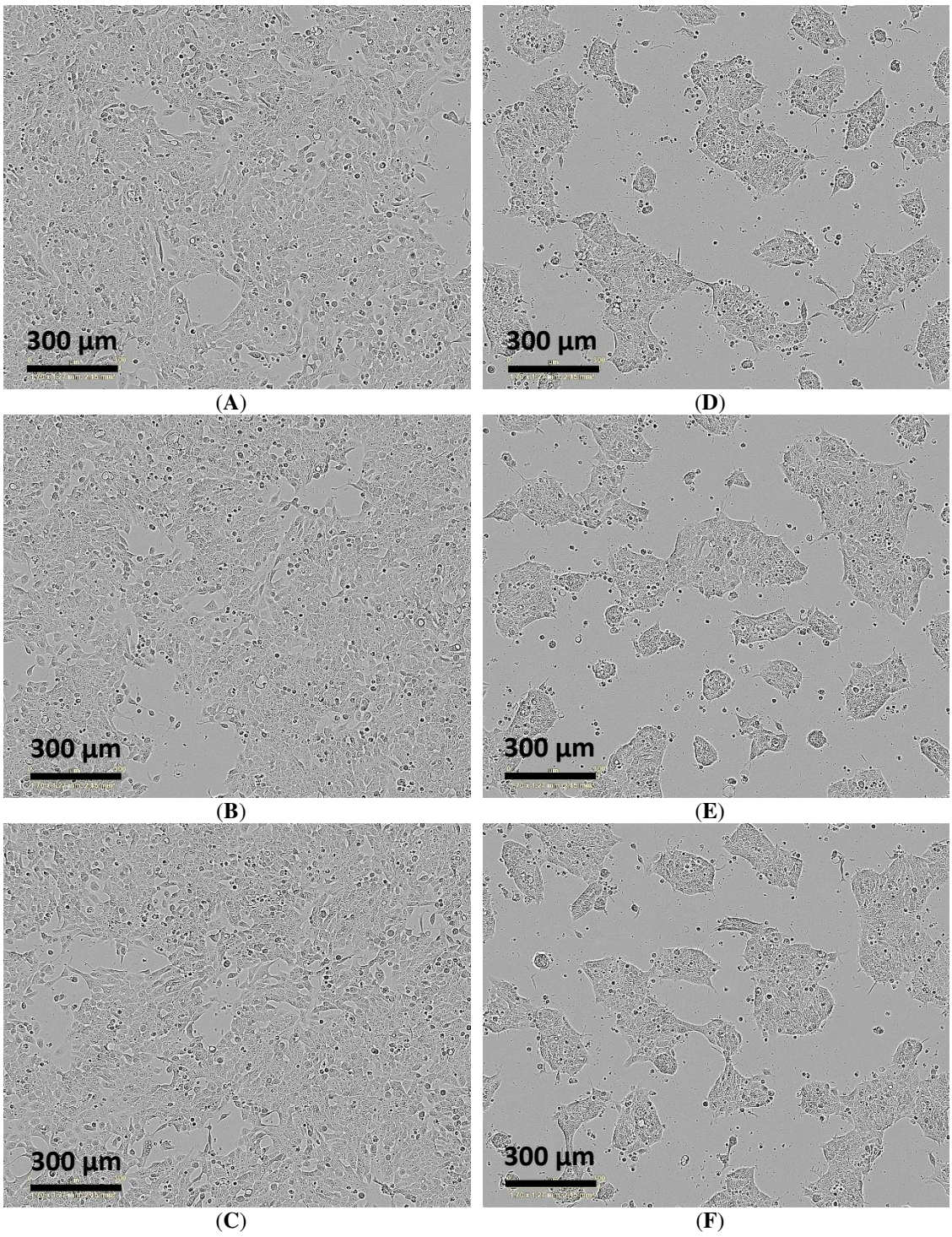

(**A**) (**D**)

(**B**) (**E**)

(**C**) (**F**)

Figure 2.3. 28 h Detroit 562 monolayer development on collagen I coated (A-C) vs uncoated (D-F) well surface. Images taken at 10x objective at the Incucyte. Presented here are 3 biological replicates with 1 representative technical replicate each. Each well was initially seeded with $2x10^5$ Detroit 562 cells/mL.

The Detroit 562 pharyngeal cells were further incubated for a total growth period of 48 h with the aim of reaching monolayers of ≥ 95% confluency. It is important to have a highly confluent monolayer to ensure that subsequent GAS biofilms that form are consistent across the entirety of the biofilm, as opposed to biofilms for example having altered architecture/structure/arrangement in regions lacking Detroit 562 cell presence.

It is evident by 48 h, Detroit 562 pharyngeal cells grown on the collagen I coated well surface reached the desired confluency (Fig 2.4A-C), covering the well surface thoroughly. However, Detroit 562 cells grown on uncoated well surface did not reach the desired confluency, with considerable gaps seen in the monolayer (Fig 2.4D-F).

As such, collagen I coating is a necessary component in the formation of Detroit 562 monolayers for this model.

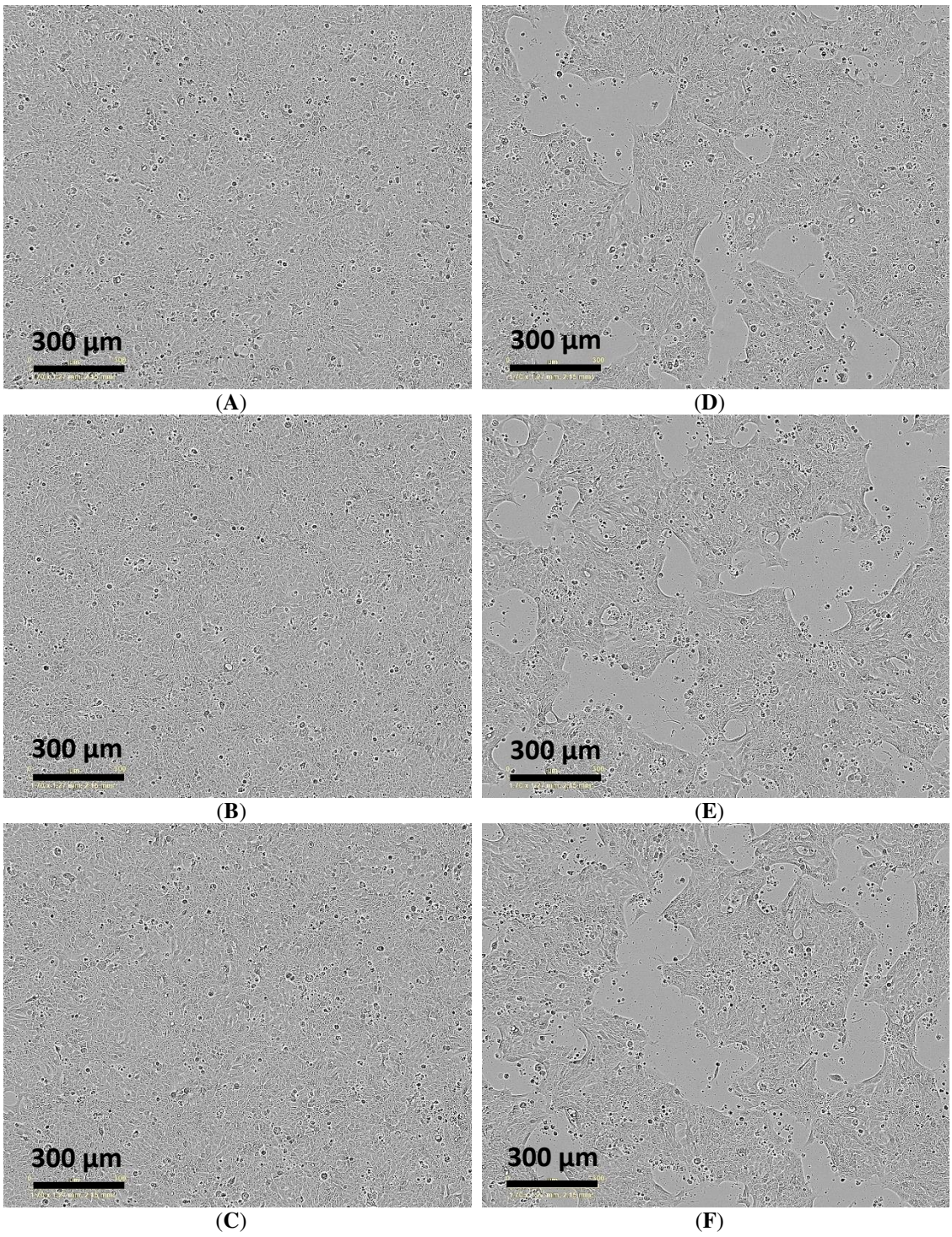

(**A**) (**D**)

(**B**) (**E**)

(**C**) (**F**)

Figure 2.4. 48 h Detroit 562 monolayer development on collagen I coated (A-C) vs uncoated (D-F) well surface. Images taken at 10x objective at the Incucyte. Presented here are 3 biological replicates with 1 representative technical replicate each. Each well was initially seeded with $2x10^5$ Detroit 562 cells/mL.

Broth-grown GAS has been previously found to be inherently toxic towards live epithelial cells (Marks et al., 2014). Therefore, co-culturing GAS biofilms atop live epithelial cells for extended periods of time is not possible. Detroit 562 pharyngeal cell monolayers were fixed with 3.7% paraformaldehyde prior to use for biofilm production. To ascertain if this treatment induces any phenotypic or morphological changes or visible damage to the monolayers, the 48 h Detroit 562 pharyngeal cell monolayers were imaged pre- and post-fixation (Fig 2.5). Fixation does not appear to induce any noticeable changes in the morphology of the pharyngeal cells, nor does it damage the monolayers and their confluency. To further exemplify this, 48 h monolayers grown on uncoated wells with a lower confluency were included (Fig 2.5C and D).

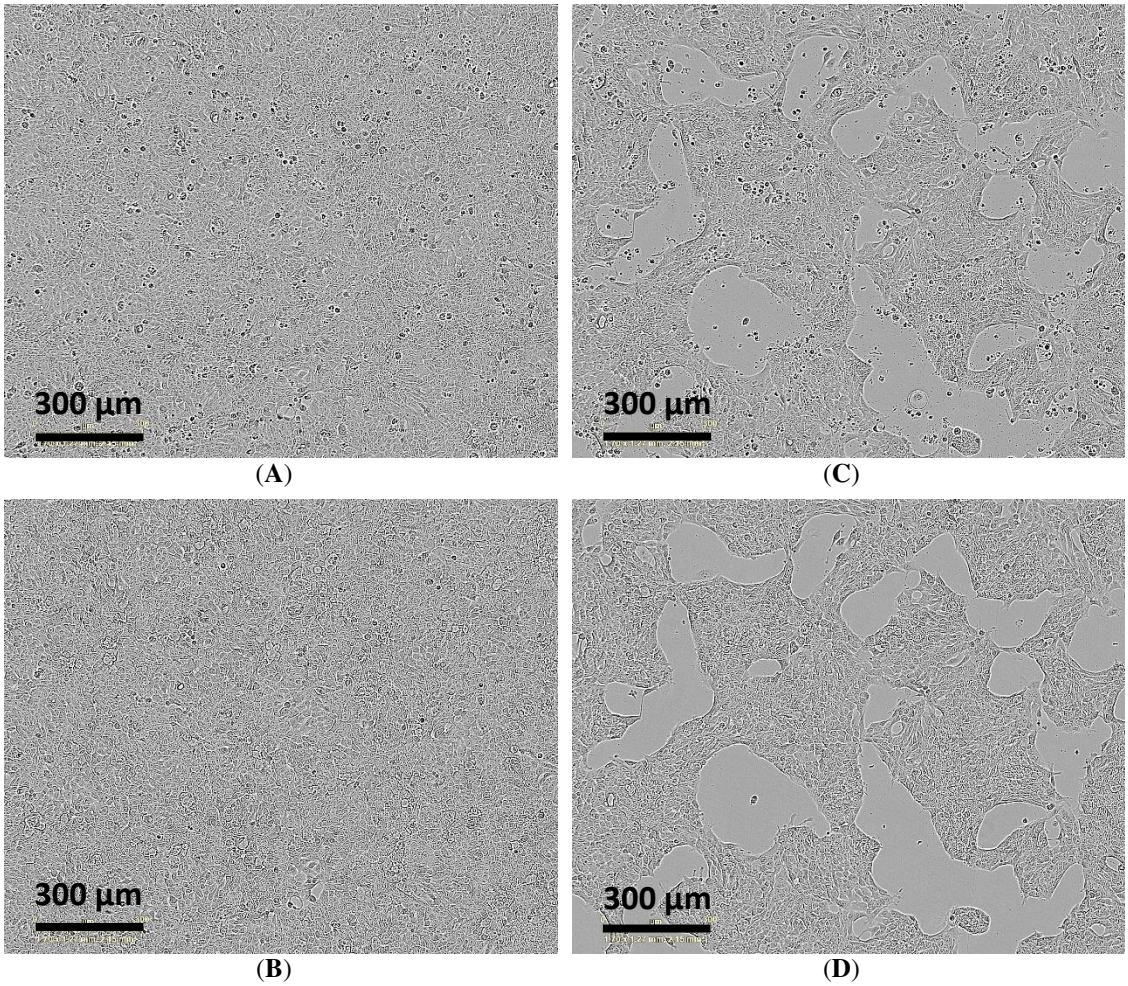

(**A**) (**C**)

(**B**) (**D**)

Figure 2.5. PFA fixation does not alter the morphology of Detroit 562 pharyngeal cells within the monolayers achieved at 48 h. Images show monolayers on collagen coated well surfaces pre-fixation (**A**) and post-fixation (**B**) and monolayers on uncoated well surfaces pre-fixation (**C**) and post-fixation (**D**). Images were taken at 10x objective at the Incucyte.

2.3.2. GAS biofilm formation optimisation

2.3.2.1. 48 h GAS biofilms are potentiated on Detroit 562 pharyngeal cell monolayers

To exemplify and highlight the need for a more physiologically relevant substratum for GAS biofilm growth, two commonly studied GAS isolates, M1 and M12, implicated in GAS pharyngitis were assessed and were the primary focus of this study (Walker et al., 2014). Specifically, 48 h M1 and M12 GAS biofilms were assessed for their biofilm forming abilities on both a plastic substratum and PFA fixed Detroit 562 pharyngeal cell

monolayers via crystal violet staining (Fig 2.6). Both GAS M-types were found to exhibit significantly greater biofilm biomass when grown on the Detroit 562 pharyngeal cell monolayers.

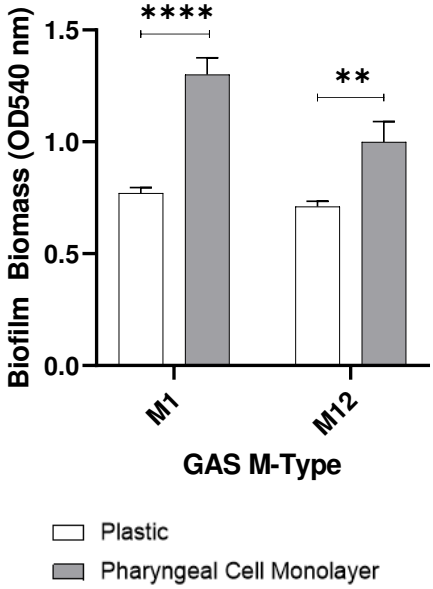

Figure 2.6. M1 and M12 GAS was assessed for its ability to form biofilm on plastic and Detroit 562 pharyngeal cell monolayers. Biofilms were formed for 48 h and biofilm biomass ascertained via crystal violet staining. Data represents mean ± SEM, ** ($p \leq 0.01$) and **** ($p \leq 0.0001$); n = 3 biological replicates, with 3 technical replicates each.

2.3.2.2. Methanol fixation improves reproducibility of crystal violet staining on GAS biofilms

Crystal violet assays were first described by Christensen et al. (1985) as a means of quantifying biofilm. Crystal violet has proven useful in that it detects biofilm in its entirety, staining a biofilms biomass which comprises live and dead cells, as well as EPS matrix. Taken together with its overall ease of use and relatively low cost it has since become a routinely used biofilm stain and detection method (Wilson et al., 2017). Despite these attributes, there are some drawbacks and limitations to crystal violet use, with concerns around reproducibility (Pantanella et al., 2013, Azeredo et al., 2017). Reproducibility can be influenced by a biofilms overall durability and stability, especially

during the wash steps (Azeredo et al., 2017). As such, more delicate biofilms may require additional precautions to ensure biofilm retention during the various washing, staining, and de-staining steps of the assay.

In the current study, to minimise disruption and damage to the GAS biofilms, biofilm plate layout/growth conditions and overall handling were optimised according to the following specifications; growing biofilms at the inner-most wells of a plate with unused wells filled with water to avoid dehydration; adjusting pipetting volume for media removal to account for dehydration during incubations; placing the plate inside a container containing additional water to reduce media evaporation from the wells; gradual media changes (50 µL at a time, as opposed to the entire 150 µL). Furthermore, to improve the durability of the biofilms during crystal violet assaying, 48 h biofilms grown on the Detroit 562 pharyngeal monolayers were either fixed with methanol or left unfixed and assessed for biofilm biomass (Fig 2.7).

Methanol fixation was found to significantly increase retention of biofilm biomass following crystal violet staining (Fig 2.7). Hence, for GAS biofilms, we recommend methanol fixation as an additional step prior to crystal violet staining.

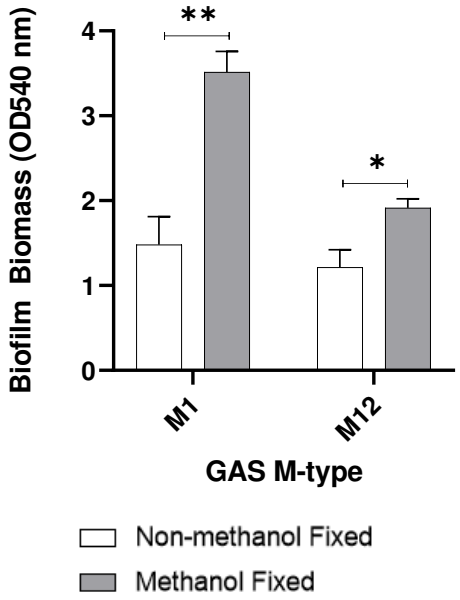

Figure 2.7. Methanol fixation improves M1 and M12 GAS biofilm biomass detection. 48 h GAS biofilms were formed from planktonic GAS that had initially adhered to the monolayer after 2 h incubation. Biofilm biomass was ascertained via crystal violet staining. Data represents mean ± SEM, * ($p \leq 0.05$) and ** ($p \leq 0.01$); n = 3 biological replicates, with 3 technical replicates each.

2.3.2.3. 72 h growth yields optimal biofilm biomass

After optimising the crystal violet assay for GAS biofilms, M1 and M12 GAS biofilm formation on the Detroit 562 pharyngeal cell monolayers was further assessed at extended growth periods of 72 and 96 h to see if greater biofilm biomass was achievable (Fig 2.8). Both M1 and M12 formed significantly more biofilm at 72 h compared to 96 h where biofilm biomass seemed to diminish. The biofilm biomass at 72 h was also greater than the biofilm biomass formed previously at 48 h.

To build upon this and assess the utility of the optimised methodology, additional GAS M-types (M3, 98, and 108) were also assayed for biofilm formation under the same conditions (Fig 2.9). As per M1 and M12, both M98 and M108 formed significantly greater biofilm at 72 h compared 96 h. However, biofilm biomass remained relatively unchanged for M3 at both 72 h and 96 h growth periods.

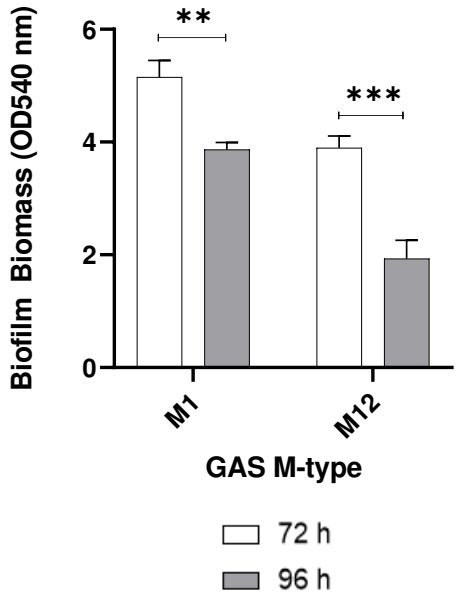

Figure 2.8. 72 h is an optimal period for GAS biofilm formation. M1 and M12 were assessed for GAS biofilm formation at 72 and 96 h. 72 h yielded significantly more biofilm than 96 h. Biofilm biomass was determined via crystal violet staining. Data represents mean ± SEM, ** ($p \leq 0.01$) and *** ($p \leq 0.001$); n = 3 biological replicates, with 3 technical replicates each.

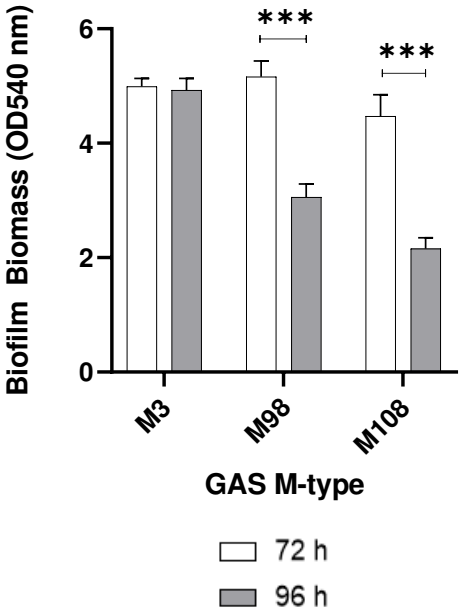

Figure 2.9. Assessing the utility of the optimised methodology on additional GAS M-types (M3, 98, and 108). Biofilm biomass was determined via crystal violet staining. Data represents mean ± SEM, ** ($p \leq 0.01$) and *** ($p \leq 0.001$); n = 3 biological replicates, with 3 technical replicates each.

2.3.3. SEM imaging reveals 72h M1 and M12 GAS biofilms formed in the host cell-GAS model closely resemble those *in vivo*

M1 and M12 72 h biofilms grown on Detroit 562 pharyngeal cell monolayers were visually observed by SEM for their overall biofilm architecture, arrangement, and structure. Both M1 and M12 GAS biofilms show cocci chains arranged in three-dimensional aggregated communities atop the Detroit 562 pharyngeal cell monolayers (Fig 2.10). However, M1 biofilms were found to arrange in tightly packed aggregates of cocci chains on the Detroit 562 monolayers (Fig 2.10 A and B), whereas M12 biofilms were more loosely arranged atop of the monolayers (Fig 2.10 C and D). Both M1 and M12 biofilms produced noticeable EPS that was found closely associated with the cocci chains. Detroit 562 pharyngeal cell monolayers (without biofilm) are also shown (Fig 2. 10 E and F) depicting the pharyngeal cells arranged in confluent monolayers, with pharyngeal cells displaying their cell surface projections.

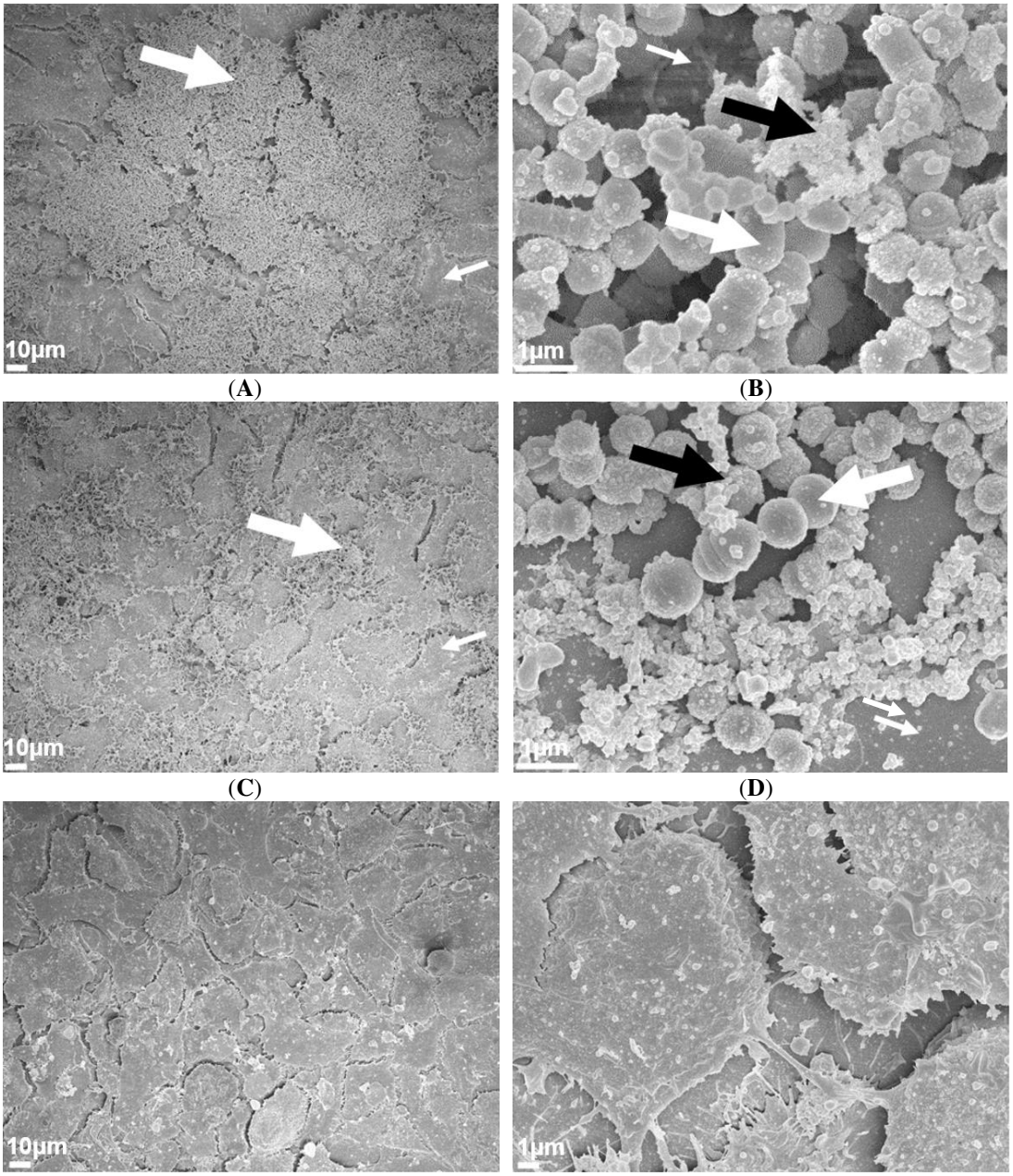

Figure 2.10 Representative 72 h M1 (A and B) and M12 (C and D) GAS biofilms visualised by scanning electron microscopy at 500 and 15 000 x magnification. GAS biofilms show chained cocci (white arrows) arranged into three dimensional aggregated structures with EPS (black arrows) upon the Detroit 562 monolayers (smaller white arrows). Detroit 562 monolayers (without biofilm) were also imaged at (**E**) 500 and (**F**) 5000 x magnification. Images represent 3 biological replicates, with 3 technical each.

2.4. Discussion

GAS is a human pathogen, reliant on several host factors to prompt and facilitate dynamic and unique interactions necessary for successful colonisation and persistence. Most *in vitro* plate-based GAS biofilm models used previously do not mimic the host environment. Moreover, the use of an epithelial substratum for growth is rare. Given the importance of the GAS-host tissue interface in mediating the earlier stages of GAS association and adherence, it is likely that these interactions are also crucial for various stages of subsequent biofilm formation and establishment within the host. Thus, modelling in the absence of host factors and/or relevant host epithelial substratum in *in vitro* plate-based biofilm models may result in biofilms that do not accurately represent the GAS biofilms *in vivo*. Here we report an optimised method for GAS biofilm formation using Detroit 562 pharyngeal cell monolayers as a model for GAS-host interaction.

In the current study, an optimised method for culturing GAS biofilms on pharyngeal cell monolayers was developed. Despite not being a primary cell line, Detroit 562 pharyngeal cells were considered suitable for this model for the following reasons; i) they are derived directly from human pharyngeal tissue, a site which GAS readily colonises, ii) they retain surface structures for adherence (e.g. carbohydrate epitopes) representative of native pharyngeal cells, and iii) they have been used extensively in planktonic GAS adherence assays (Barthelson et al., 1998, Ryan et al., 2001, Frick et al., 2003, Bessen and Lizano, 2010, Ryan and Juncosa, 2016). Future research may wish to adapt this model further, considering the use of other relevant cell types, such as alternative pharyngeal cell lines, primary oropharyngeal tissue and keratinocyte cell lines, as substratum for biofilm formation. Overall, utilisation of pharyngeal epithelial substratum within this model better recreated the host environment compared to most of the previously reported in *vitro* models.

When grown on Detroit 562 pharyngeal cell monolayers, GAS biofilm biomass increased significantly compared to biofilms grown on abiotic plastic substratum. This highlights the difference in biofilm potentiation, as a direct result of substratum for biofilm growth. This supports the utility for GAS biofilm modelling to include epithelia as a substratum for biofilm growth over an abiotic plastic surface.

Whilst various staining techniques have been developed to assess biofilm biomass, crystal violet staining remains one of the most common techniques within the field. Here, we propose optimisation of this method at the biofilm formation steps preceding crystal violet staining, as well as additional considerations required during the crystal violet assay that are tailored to the GAS biofilms formed using this model. Specifically, to further improve biofilm yield, durability, and subsequent reproducibility of the commonly used biofilm biomass crystal stain assay, methanol fixation was assessed. 48 h GAS biofilms that were methanol fixed prior to crystal violet staining yielded greater biofilm biomass, with less biofilm loss during the intensive staining and washing steps. In turn, reducing error, and increasing reproducibility.

Broth grown GAS is inherently toxic to epithelial cells, as such, there have previously been no models that explore or support long-term GAS biofilm-epithelia co-culture in a plate-based model (Marks et al., 2014). Here, we show that GAS biofilm formation is attainable upon the fixed pharyngeal cell monolayer beyond 48 h. However, of the three time points assessed, 72 h is the optimal biofilm growth period for yielding the greatest biofilm biomass for M1, M12, M98, and M108 GAS. Biofilm biomass was seen to diminish at 96 h, likely resulting from partial disintegration of biofilm. This may be indicative of a mature or older biofilm reaching the final step of the biofilm life cycle - dispersal. Dispersal is thought to be triggered by nutrient exhaustion at the site, which in a host enables bacteria to shift to a motile planktonic state for biofilm re-establishment elsewhere (Gjermansen et al., 2005, Lembke et al., 2006, McDougald et al., 2012). These

results conferred with a previous study of M6 and M49 biofilms grown on abiotic plastic well surfaces of a 96 well plate-based system, whereby biofilms had greater biomass at 72 h, and exhibited partial disintegration at 96 h with authors attributing this to the age of the biofilm and nutrient limitation (Lembke et al., 2006).

Finally, visual inspection of the GAS biofilms via SEM imaging found M1 and M12 formed biofilm atop the Detroit 562 pharyngeal cell monolayers. Cocci chains, typical of GAS, can be seen arranged in three dimensional aggregated structures coated in EPS matrix for both GAS M-types. Importantly, biofilms formed in this GAS-epithelial cell model appear similar to SEM images captured of GAS biofilms found at the surface of tonsils removed from patients with recurrent GAS tonsillo-pharyngitis (Roberts et al., 2012). In conclusion, we have demonstrated an efficacious GAS biofilm-pharyngeal cell model that can support long-term biofilm formation, with biofilms formed resembling those seen *in vivo*.

Chapter 3: Assessing the role pharyngeal cell surface glycans play in throat tropic M12 GAS biofilm formation

A part of this work has been published in Antibiotics, MDPI.

Overview: The role host cell glycans play in GAS biofilm formation in the context of GAS pharyngitis and subsequent antibiotic treatment failure has not been previously investigated. GAS serotype M12 GAS biofilms were assessed for biofilm formation on Detroit 562 pharyngeal cell monolayers following enzymatic removal of all *N*-linked glycans from pharyngeal cells with PNGase F. Removal of *N*-linked glycans resulted in an increase in biofilm biomass compared to untreated controls. Further investigation into the removal of terminal mannose and sialic acid residues with α1-6 mannosidase and the broad specificity sialidase (Sialidase A) also found that biofilm biomass increased significantly when compared to untreated controls. Increases in biofilm biomass were associated with increased production of extracellular polymeric substances (EPS). Furthermore, it was found that M12 GAS biofilms grown on untreated pharyngeal monolayers exhibited a 2500-fold increase in penicillin tolerance compared to planktonic GAS. Pre-treatment of monolayers with exoglycosidases resulted in a further doubling of penicillin tolerance in resultant biofilms. Collectively, these data demonstrate that pharyngeal cell surface glycan structures directly impact GAS biofilm formation in a glycan specific fashion.

3.1. Introduction

GAS pharyngitis is the most common disease state, with global incidence estimated at 600 million cases per year (Carapetis et al., 2005). Currently, penicillin remains the antibiotic of choice for treating GAS infections, with no reports of penicillin resistance among clinical GAS isolates. However, antibiotic treatment failure has been well-documented at rates of 20–40% for GAS pharyngitis (Facinelli et al., 2001, Conley et al., 2003, Baldassarri et al., 2006). Biofilms enable bacteria to survive and tolerate both host immunity and antimicrobial treatment. As a result, biofilm-associated infections are oftentimes chronic and recurrent, and particularly difficult to clear and treat (Conley et al., 2003, Baldassarri et al., 2006, Ogawa et al., 2011). Recently, it has been proposed that GAS may form biofilms, contributing to antibiotic treatment failure (Conley et al., 2003). There is evidence of bacterial biofilm formation in human tonsils (Kania et al., 2007), and in a study of patients suffering from recurrent GAS pharyngo-tonsillitis, the presence of GAS biofilms in tonsillar crypts was identified in all 30 patients (Roberts et al., 2012). Furthermore, in a study assessing GAS isolated from pharyngitis patients non-responsive to antibiotics, all 99 GAS isolates demonstrated biofilm-forming ability *in vitro*, with 60% of these displaying increased penicillin tolerance once in the biofilm phenotype (Conley et al., 2003). However, most of these studies utilised abiotic surfaces (glass, plastic, polystyrene) and very few incorporated surface coating with extracellular matrix components such as fibronectin, fibrinogen, laminin, or collagen (Lembke et al., 2006, Manetti et al., 2007, Sugareva et al., 2010, Bachert et al., 2016). The host cell surface is integral in initial host-pathogen interactions, bacterial cell adherence, and subsequent biofilm formation (Kostakioti et al., 2013). Thus, there is a need to better understand the role of host cell surface receptors in GAS biofilm formation.

Glycans are carbohydrates present on more than half of all human proteins, with their ubiquitous presence in mucosal fluid, on secreted molecules, immune cells, and a variety

of epithelial cell surfaces, making glycosylation one of the most common post-translational modifications (Apweiler et al., 1999, Christiansen et al., 2014). Glycans are the initial point of contact with the host for many bacteria, mediating attachment and colonisation, and can consequently facilitate infection and disease. Several human bacterial pathogens such as *Pseudomonas aeruginosa*, *Enterococcus faecalis*, *Helicobacter pylori*, *Streptococcus gordonii*, and *Streptococcus pneumoniae* have proven adept at adhering to and utilising glycan structures for pathogenesis (Aspholm et al., 2006, King, 2010, Garbe et al., 2014, Wong et al., 2018, Wheeler et al., 2019). Bacterial modification of host glycan structures enables binding to otherwise inaccessible host receptors for adherence, modulation of host immune molecules, acquisition of carbohydrate substrates for non-glucose fermentation, facilitation of interspecies competition, and promotion of biofilm formation (Aspholm et al., 2006, King, 2010, Garbe et al., 2014, Wong et al., 2018, Wheeler et al., 2019). An example of a well-characterised glycan-utilising system is the NanA neuraminidase of *S. pneumoniae,* which cleaves off terminal sialic acid residues from glycans. NanA has been shown to be particularly active during cluster formation and biofilm maturation *in vitro* (Parker et al., 2009). Another study found increased *S. pneumoniae* biofilm formation was seen only for biofilms exposed to sialic acid, but not in the presence of other glycans (Trappetti et al., 2009).

The utilisation of glycans by GAS remains poorly understood, despite GAS possessing an array of adhesins capable of binding structures on the richly glycosylated epithelial surfaces and in the fluids of the oropharynx. Studies to date have focused on planktonic GAS-host glycan interactions in the context of the M protein, a major surface-expressed protein which has a role in the adherence of GAS to host tissues (Wang and Stinson, 1994, Frick et al., 2003, De Oliveira et al., 2017, De Oliveira et al., 2019). Investigation of the ability of M proteins from 49 GAS serotypes to associate with various pharyngeal- and

dermal-associated glycosaminoglycans (GAGs) revealed that GAGs mediated GAS adhesion to human cells in an M protein-dependent manner (Frick et al., 2003). Recently, M1 GAS was shown to bind glycans via the M protein, including the ABO(H) blood group antigens, which are oligosaccharides abundant on the epithelia of most individuals, including the pharynx (De Oliveira et al., 2017). Similar trends were observed in two other prevalent GAS M-types, M3 and M12 (De Oliveira et al., 2019). Interestingly, this study showed that modification of the cell surface glycome via treatment with a range of exoglycosidases altered GAS-host cell interactions (De Oliveira et al., 2019). Taken together, these findings further highlight the role of glycans in mediating GAS adherence. Whilst the role of host glycans in GAS adherence has been investigated, their role in GAS biofilm formation has yet to be examined. Investigation of glyco-interactions at the GAS-tissue interface in the context of biofilms will enhance our understanding of GAS biofilms and GAS pathogenesis. Consequently, findings of such studies may inform and support the development of novel anti-biofilm strategies as well as biofilm-specific antibiotic treatments. Herein, we examine the role of human pharyngeal *N*-glycans in M12 GAS biofilm formation and subsequent penicillin tolerance.

3.2. Materials and methods

3.2.1. GAS and culture conditions

M12 GAS used in this study is commonly associated with pharyngeal disease (Sanderson-Smith et al., 2014, De Oliveira et al., 2017, De Oliveira et al., 2019). GAS was grown on horse blood agar (HBA) plates (Oxoid, UK) or Todd Hewitt agar supplemented with 1% (*w*/*v*) yeast (THYA) (Difco, Australia). Static cultures of GAS were grown overnight in Todd Hewitt broth supplemented with 1% (*w*/*v*) yeast (THY). GAS was cultured and maintained at 34 °C (Marks et al., 2012).

3.2.2. Human pharyngeal cell culture conditions and monolayer formation

Detroit 562, a human pharyngeal epithelial cell line (CellBank Australia, Australia), was cultured in Dulbecco's Modified Eagle Medium (DMEM) F12 (Invitrogen, Australia), supplemented with 2 mM L-glutamine (Gibco, Life Technologies, UK) and 10% (*v*/*v*) heat inactivated foetal bovine serum (FBS) (Bovogen Biologicals, Australia) in cell culture flasks at 37 °C, 5% CO_2 to 20% O_2 atmosphere.

Fixed Detroit 562 pharyngeal cell monolayers form the substratum for bacterial growth for subsequent biofilm experiments. In brief, wells of 96-well flat bottom cell culture microtiter plates (Greiner Bio-One, Germany) were coated with 300 µg/mL Collagen I from rat tail (Gibco, Life Technologies, UK) and incubated for 1 h, 37 °C, 5% CO_2 to 20% O_2 atmosphere. After 1 h, wells were seeded with 150 µL Detroit 562 cell suspension (2×10^5 cells/mL) and cultured for 48 h (or until a monolayer of ~95% confluency was achieved). Monolayers were washed once with PBS and fixed with sterile 3.7% paraformaldehyde for 20 min. Once fixed, wells were washed twice with PBS, and monolayers were kept wet via submersion in PBS until required for use.

3.2.3. Characterisation of Detroit 562 pharyngeal cell surface *N*-linked glycans

Characterisation of the Detroit 562 pharyngeal cell surface *N*-linked glycans purified from cell surface glycoproteins was conducted as per the methods developed by Everest-Dass et al. (2012) with slight modification. In brief, 3 different passages derived from the same vial of the Detroit 562 cells (representative of 3 biological replicates) were pelleted and washed once in 14 mL PBS by centrifugation (20 min, 1000g, 4°C) in a Heraeus Multifuge X3R centrifuge (Thermofisher Scientific, USA). Cells were counted using a haemocytometer and cell concentration adjusted to $2x10^8$ cells/mL and pelleted by centrifugation (5 min, 1000g, 4°C). The pellet was re-suspended in 2 mL of lysis buffer and thoroughly homogenised using a Branson 250 digital sonicator (Branson, USA) (30% amplitude, 6 watts, 5-s pulses for 2 min) followed by syringe lysis with a 23-gauge needle. Supernatant

containing the cellular proteins was collected from the centrifuged homogenate and further diluted with lysis buffer and sedimented by ultracentrifugation (1 h, 100 000g, 4°C) with a Sorvall MTX 150 Micro-Ultracentrifuge (Thermofisher Scientific, USA) (Ryan et al., 2001). Resultant membrane protein pellet was re-suspended in 1 mL lysis buffer containing 1% Triton X-114 (v/v), and the pellet completely homogenised. Samples were heated at 37°C for 20 min, and phase partitioned by centrifugation (5 min, 300 g, RT). The Triton X-114 layer containing the membrane proteins were precipitated with 9 volumes of ice-cold acetone and incubated overnight at -20°C. The precipitated membrane proteins were re-solubilised in 100 µL of 8 M urea, and protein quantified by DC assay. 20 µg of protein lysate from each of the 3 passages were independently dot blotted in triplicate onto EtOH-wetted PVDF membrane (20 µg of BSA and bovine fetuin were included as glycan negative and positive controls respectively) and dried overnight (RT). Dried dot blots were then washed in MeOH (15 min, shaking, RT) and further washed in water (15 min, shaking, RT). To qualitatively confirm and visualise immobilised protein, the dot blotted membrane was stained with Coomassie blue for 3 min, and then de-stained, and the membrane placed in water. Protein-laden spots of 6mm diameter were excised from the PVDF membrane and submerged into wells containing 100 µL 1% PVP40 where they were incubated for 5 min, and then washed three times with 200 µL water. For the removal of *N*-linked glycans, 2 µL of PNGase F (1000 U) (NEB) and 8 µL water was added to each well and incubated overnight at 37°C. After incubating overnight, the 96-well plate was sonicated for 5 min in an Ultrasonic Cleaner sonicating water bath (Unisonics, Australia). The wells were then rinsed with 20 µL water, and the solutions collected. The samples were then acidified with 10 µL 100 mM ammonium acetate (pH 5) and incubated for 1 h, RT. Released *N*-glycans were reduced in alkaline conditions by the addition of 20 µL of 1.25 M $NaBH_4$ in 100 mM KOH, incubated for 3 h at 50°C. After cooling to RT, the reaction was neutralised with 2 µL of glacial acetic acid.

Sodium salts of *N*-glycan solutions were removed by passage through and subsequent washing of cation exchange microcolumns constituted by packing 25 µL of Dowex® 50W X8 (Sigma-Aldrich, USA) in a ZipTip® C18 tip (Merck Millipore), activated with 50 µL of 1 M HCl prior to addition of sample. Solutions were passed through columns using a benchtop micro-centrifuge at full speed for 15-30 s. Sodium-desalted samples were vacuum dried in a Savant® SPD131DDA SpeedVac™ Concentrator (ThermoFisher). Samples were then washed and dried three times with 100 µL of methanol to remove residual borate.

Desalted samples were further purified by porous graphitised carbon (PGC) chromatography. Columns were constituted with 5 µL of PGC material from HyperSep® Hypercarb® cartridges (ThermoFisher) in methanol, deposited in a ZipTip® C18 tip. Prior to addition of sample, columns were washed with elution buffer (80% v/v acetonitrile (ACN), 0.1% v/v trifluoroacetic acid (TFA)) and subsequently equilibrated in loading buffer (0.1% v/v TFA). Dried samples were dissolved in 50 µL loading buffer and passed through columns, with flow through re-loaded into the columns. Enriched glycans were eluted in 50 µL of elution buffer and vacuum dried. Dried, purified enriched glycans were stored at –20 °C.

Dried glycans were reconstituted in 20 µL of water immediately prior to LC-MS/MS analysis. Sample handling and injections were performed using an Ultimate 3000 UHPLC (Thermo Scientific). Samples were injected in running buffer (10 mM NH_4HCO_3) through a PGC pre-column (3 µm Hypercarb, 320 µm ID x 100 mm) at a flow rate of 6 µL/min and subsequently a PGC analytical column (3 µm Hypercarb, 75 µm ID x 100 mm) at a flow rate of 1 µL/min. Chromatographic separation was achieved using a 120 min gradient for *N*-glycans (0 – 70% v/v ACN). The HPLC system was directly connected to an electrospray ionisation source (AmaZon Speed Ion-Trap, Bruker Corporation, UK) with a capillary voltage of 3 kV. MS spectra were obtained in negative mode between m/z 400 and 1800 with an accumulation time of 200 ms.

Data analyses were carried out in Compass Data Analysis 4.2 (Bruker Corporation) for structural assignment and in Skyline 20.1 (MacLean et al., 2010) for quantitation. Quantitation was performed for each isomer identified by MS^2 spectra and retention time by calculating the area under the curve (AUC). This was expressed as a percentage of total AUC yielding relative abundance for each replicate.

3.2.4. Detroit 562 pharyngeal cell monolayer pre-treatment

3.2.4.1. PNGase F treated monolayers

Wells of the 96-well microtiter plates containing pre-formed fixed Detroit 562 pharyngeal cell monolayers were blocked with 1% PVP40 solution and incubated for 5 min. Once blocked, the PVP40 was removed, and the wells washed three times with distilled water. For the removal of *N*-linked glycans, 5 µL of PNGase F (50 U) (Promega, Madison, WI, USA) and 10 µL PBS was added to each well and incubated overnight at 37 °C. After incubating with PNGase F, released *N*-linked glycans were removed and the wells washed once with PBS. Untreated PBS wells representing the whole glycome of the Detroit 562 pharyngeal cell monolayers were also included as a control. *N*-linked glycan removal was confirmed via Concanavalin A Alexa fluor 647 lectin binding assay (Appendix D, Figure D). In brief, untreated and PNGase F pre-treated pharyngeal cell monolayers were incubated with 5 µg/mL Concanavalin A Alexa fluor 647 for 15 min (RT, dark). Unbound lectin removed, and monolayers washed twice with 100 µL PBS. Untreated and PNGase F pre-treated monolayers incubated without lectin (PBS) served as background/auto-fluorescence controls and were subtracted from sample reads. Samples were read spectrofluorometrically at excitation 625–30 nm/emission 680–30 nm.

3.2.4.2. Exoglycosidase: α1-6 mannosidase, α1-2, 3 mannosidase, and Sialidase A treated monolayers

Pre-formed fixed Detroit 562 pharyngeal cell monolayers of the 96-well microtiter plate were treated with 30 µL/well reaction volumes of each of the exoglycosidases. For mannosidases, the reaction volume comprises 3 µL 1 × GlycoBuffer 1 (NEB), 0.3 µL 100 µg/mL purified BSA (NEB), 0.2 µL α1-6 mannosidase (8 U) or α1-2,3 mannosidase (8 U) (NEB), and 26.5 µL PBS. For Sialidase A, 6 µL 5 × Reaction Buffer B (250 mM sodium phosphate pH 6.0) (Prozyme, Hayward, CA, USA), 0.2 µL Sialidase A (1×10^{-3} U) (Prozyme, Hayward, CA, USA), and 23.8 µL PBS. Untreated PBS wells representing the intact surface glycome of the fixed Detroit 562 pharyngeal cell monolayers were also included as a control. The plate was incubated for 2 h, 37 °C. Once incubated, the wells were washed once with PBS. Glycan removal was confirmed via lectin binding assay as per (De Oliveira et al., 2019), with exoglycosidase pre-treated pharyngeal cell monolayers incubated with either biotinylated *Hippeastrum hybrid* lectin (binding mannose residues) (Vector Laboratories, Australia) or biotinylated *Sambucus nigra* lectin (binding sialic acid residues) (Vector Laboratories, Australia) (Appendix E, Figure E).

3.2.5. Initial adherence of planktonic GAS

Pre-formed fixed Detroit 562 pharyngeal cell monolayers were inoculated with 150 µL of stationary phase GAS culture diluted 1:20 in THY (*v*/*v*) supplemented with sterile 0.5% glucose (THY-G) and incubated for 2 h to promote initial attachment (34 °C, slow shaking at 50 rpm). At 2 h, non-adherent GAS was removed, and the wells washed three times with PBS. To detach Detroit 562 cells from the bottom of the microtiter plate, 0.05% trypsin-EDTA (1×) (Gibco, USA) was added to each well and incubated (15 min, 37 °C). To lyse the now-detached Detroit 562 cells containing internalised bacteria, 0.025% Triton X-100 was added and pipetted vigorously. To enumerate the adherent

GAS population, 10-fold serial dilutions of the cell suspensions were performed in PBS and aliquots spot plated onto THYA (incubated overnight, 34 °C) for subsequent colony counting and CFU/mL determination.

3.2.6. GAS biofilms

96-well microtiter plates containing pre-formed fixed Detroit 562 pharyngeal cell monolayers untreated and pre-treated with either PNGase F or the exoglycosidases were inoculated with 150 µL of overnight GAS culture diluted 1:20 in THY-G. The inoculum was incubated for 2 h (34 °C, 50 rpm). At 2 h, non-adherent GAS was removed, and wells replenished with sterile THY-G. Subsequent 72 h GAS biofilms were produced (34 °C, 50 rpm), with sterile THY-G media refreshment performed every 24 h.

3.2.6.1. GAS biofilm biomass crystal violet staining

Biofilm biomass was assessed via crystal violet staining. Biofilms were air dried for 30 min (or until completely dried), and fixed with 99% methanol for 15 min. Once fixed, the biofilms were thoroughly air-dried and stained with 0.2% crystal violet (*w*/*v*) (Sigma-Aldrich, St Louis, MO, USA) supplemented with 1.9% ethanol (*v*/*v*) for 10 min (RT, static). Once stained, excess crystal violet was removed and each well gently washed twice with PBS. Crystal violet stain that had incorporated into the biofilm was re-solubilised in 1% sodium dodecyl sulphate (SDS) (*w*/*v*) (Sigma-Aldrich, St Louis, MO, USA), and incubated (10 min, RT). Monolayers with THY-G (no GAS biofilm) served as media sterility controls and background staining controls, with absorbance values subtracted from those of biofilm samples. Biofilm biomass quantification was performed by diluting the released dye 1:5 in the 1% SDS solution, and subsequently measured at OD_{540nm} using a SpectraMax Plus 384 microplate reader.

3.2.6.2. GAS biofilm cell viability

GAS biofilms were assessed for viability via i) live cell populations determined via enumeration of serially diluted biofilms and ii) live/dead staining with Syto9/PI.

3.2.6.2.1. Enumeration of live cells within GAS biofilms

GAS biofilms were assessed for the live cell populations via enumeration of serially diluted biofilms. Briefly, biofilms were washed once in PBS and thoroughly re-suspended in fresh PBS via vigorous scraping of biofilms from the well surface, followed by a 5 min sonication. The population of live cells within these biofilms were enumerated via 10-fold serially diluting in PBS, and spot plating onto THYA (incubated overnight, 34 °C) for subsequent colony counting and CFU/mL determination.

3.2.6.2.2. Determining percentage live/dead within the GAS biofilms

Biofilms were washed once in PBS and thoroughly re-suspended in fresh PBS. Viable cells were enumerated via 10-fold serially diluting in PBS, and spot plating aliquots of the dilutions onto THYA (incubated overnight, 34°C) for subsequent colony counting and CFU/mL determination. Live/dead staining with Syto9/PI was based off Bac Light bacterial viability staining kit L7012 (Invitrogen, Molecular Probes, USA) manufacturer's instructions with some modifications. In brief, biofilms were washed once with 0.9% NaCl buffer (w/v) and stained with Syto9/PI combined (3µM and 18µM respectively) for 15 min in the dark. Controls were also included (0.9% NaCl buffer, Syto9 alone, and PI alone). Fluorescence was measured in a CLARIOstar (BMG Labtech, Germany) microtiter plate reader at 485-15 nm excitation, and emissions of 530-20 nm and 630-20 nm collected for Syto9 and PI respectively. Results are expressed as percentages of live/dead populations by:

1) $$\%\, Dead = \frac{Value\ of\ PI}{Value\ of\ Syto9} \times 100\ \%$$

2) $$\%\, Live = 100\ \% - \%\, Dead$$

3.2.6.3. GAS biofilm EPS

To assess a biofilms EPS, the i) EPS-GAGs and ii) common EPS components (eDNA and protein) were examined. Briefly, EPS associated GAGs were quantified by 1,9-dimethyl methylene blue (DMMB) dye based EPS assay adapted from methods described elsewhere (Peeters et al., 2008). EPS components (eDNA and protein) were fluorescently stained with Sytox Blue, a cell membrane-impermeant nucleic acid stain (Molecular Probes, Invitrogen, Eugene, OR, USA) and FilmTracer SYPRO Ruby biofilm matrix stain that labels most classes of proteins (Molecular Probes, Invitrogen, Eugene, OR, USA). In brief, biofilms were fixed with 99% methanol for 15 min, and subsequently air dried. Biofilms were individually stained for 30 min in the dark with 5 µM Sytox Blue and 0.5× concentration FilmTracer SYPRO Ruby biofilm matrix stain, with PBS as a control. Fixed Detroit 562 pharyngeal monolayers without biofilm were also stained and served as controls for background staining, with resultant absorbance values subtracted from biofilm EPS measurements. Fluorescence was measured using a CLARIOStar (with 6 × 6 matrix well scanning of the non-homogenous biofilms). Sytox Blue was read with an excitation of 440–15 nm and emission of 484–20 nm, and FilmTracer SYPRO Ruby biofilm matrix read with an excitation of 450–15 nm and emission of 610–20 nm.

3.2.7. M12 GAS penicillin susceptibility

As per accepted guidelines and standard protocols the MIC and MBC values were determined for penicillin activity against planktonic M12 GAS (Oliva and Chopra, 1992, Pankey and Sabath, 2004). Briefly, M12 planktonic GAS suspension (1×10^6 CFU/mL) was challenged with serially diluted penicillin and incubated (24 h, 34 °C). The MIC was defined as the lowest concentration of penicillin required to completely inhibit bacterial growth (indicated by clear wells), and further confirmed by measuring OD_{600nm} using a SpectraMax Plus 384 microplate reader (See Appendix F, Figure F). MBC was defined as the lowest concentration of penicillin required to induce complete killing of bacteria

as determined upon spot plating on THYA. For biofilm susceptibility, MBEC was determined by challenging the pre-formed biofilms with 2-fold dilutions of penicillin in THY, 2% G (*v*/*v*) (24 h, 34 °C). Biofilms were washed once in PBS and thoroughly re-suspended in fresh PBS. Viable cells were enumerated via 10-fold serially diluting in PBS, and spot plating onto THYA (incubated overnight, 34 °C) for subsequent colony counting and CFU/mL determination. The MBEC was determined as the lowest concentration of penicillin required to induce complete eradication of the GAS biofilms (Ceri et al., 1999).

3.2.8. Scanning electron microscopy

M12 GAS biofilms were grown on untreated and PNGase F or exoglycosidase pre-treated fixed Detroit 562 pharyngeal monolayers on 13 mm plastic Nunc Thermanox coverslips (Proscitech, Rochester, NY, USA) in a 12-well polystyrene plate. Biofilms were air dried, and prepared for SEM using methods adapted from (Williams and Bloebaum, 2010) with the following modifications. In brief, biofilms were pre-fixed in 2.5% glutaraldehyde, 50 mM L-lysine monohydrochloride, and 0.001% ruthenium red solution prepared in 0.1 M HEPES buffer (pH 7.3) (30 min, 4 °C). Following pre-fixation, biofilms were fixed in fixative solution (2.5% glutaraldehyde and 0.001% ruthenium red prepared in 0.1 M HEPES buffer, pH 7.3) for 1.5 h (4 °C) and washed twice in 0.1 M HEPES buffer. Post-fixation (2 h), 2% osmium tetroxide vapour was used, followed by three washes with distilled water (each 15 min). A graded ethanol series (30%, 50%, 70%, 90%, and 3 × 100%) was then used to remove all water from the biofilms before they were critical point dried (Leica CPD 030, Austria). Dried biofilms were then sputter coated with 20 nm platinum (Edwards Vacuum coater, USA) and visualised using a JEOL JSM-7500 microscope (JEOL, Japan) at 15 000x magnification. Untreated and PNGase F or exoglycosidase pre-treated fixed Detroit 562 pharyngeal monolayer controls (without biofilms) were also imaged at 500× magnification. Images were taken at random positions

within the samples by an UOW Electron Microscopy Centre technician blinded from the study in an effort to reduce bias.

3.2.9. Statistical analysis

All statistical analysis was performed using GraphPad Prism (version 8.4.0, GraphPad Software, USA). A student's t-test or a one-way ANOVA was performed with a Tukey's multiple comparisons post hoc test where relevant. A *p*-value of ≤ 0.05 was considered significant.

3.3. Results

3.3.1. Indiscriminate removal of *N*-linked glycans from the pharyngeal cell surface via PNGase F treatment results in increased M12 GAS biofilm biomass

M12 GAS, an M-type frequently associated with GAS pharyngitis (Cunningham, 2000, Walker et al., 2014), was investigated for its biofilm-forming ability on PFA fixed Detroit 562 pharyngeal monolayers following removal of *N*-linked glycans via peptide-*N*-glycosidase F (PNGase F) treatment. Initial adherence of planktonic M12 GAS was determined by colony forming units, and biofilms were assessed for biofilm biomass and live bacterial cell count by crystal violet staining and colony forming units determination, respectively (Fig 3.1A). In the absence of *N*-linked glycans, planktonic M12 GAS displayed a significant decrease in initial adherence ($p \leq 0.05$) when compared to adherence to untreated cells (Fig 3.1B). Despite a reduction in initial GAS adherence, M12 GAS biofilm biomass increased significantly ($p \leq 0.0001$) on the surface of PNGase F treated cells compared to the untreated control (Fig 3.1C). However, PNGase F pre-treatment of monolayers did not significantly affect the GAS CFU within the biofilms (Fig 3.1D).

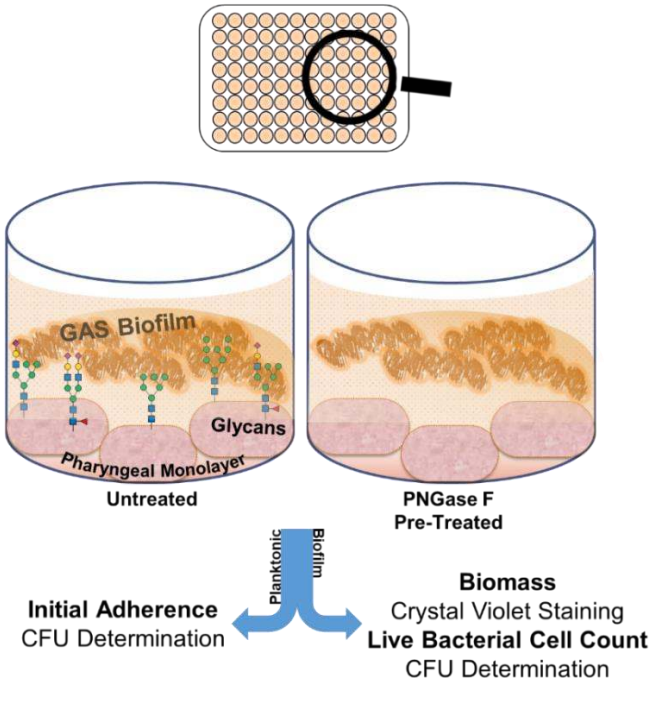

(**A**)

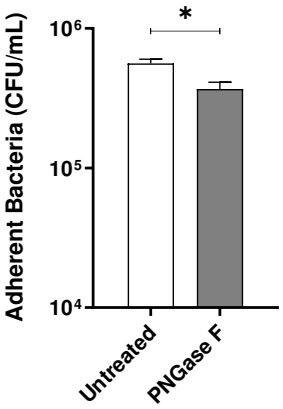

(**B**)

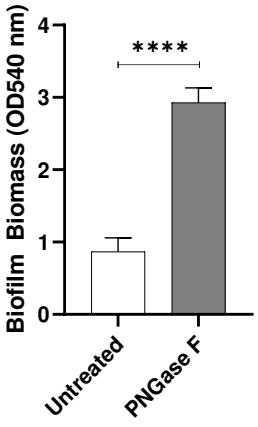

(**C**)

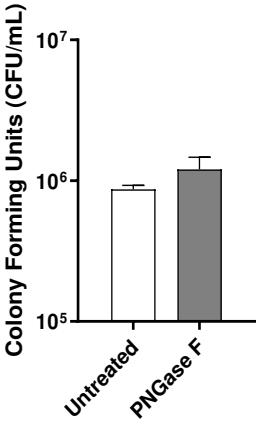

(**D**)

Figure 3.1. Indiscriminate removal of *N*-linked glycans from the pharyngeal cell surface via PNGase F treatment results in increased M12 Group A *Streptococcus* (GAS) biofilm biomass. (**A**) Assay schematic for 72 h M12 GAS biofilms formed on PNGase F pre-treated and untreated pharyngeal monolayers. (**B**) Initial adherence enumerated for planktonic GAS following 2 h incubation with Detroit-562 cell monolayers. 72 h biofilms were assessed for (**C**) biofilm biomass via crystal violet staining and (**D**) colony forming units via enumeration. Data represents mean ± SEM, with statistical analysis performed, * ($p \leq 0.05$) and **** ($p \leq 0.0001$); n = 3 biological replicates, with 3 technical replicates each.

To visually investigate the effect of PNGase F pre-treated pharyngeal monolayers on M12 GAS biofilm formation, SEM imaging was conducted. Biofilms formed on both untreated and PNGase F pre-treated monolayers show M12 GAS chained cocci arranged into three dimensional aggregated structures with extracellular polymeric substances (EPS) matrix material present (Fig 3.2). Biofilms formed on PNGase F pre-treated pharyngeal monolayers (Fig 3.2C) appear to have more EPS matrix compared to biofilms formed on untreated cells (Fig 3.2A). EPS matrix material is associated with the aggregated GAS cocci. Interestingly, the EPS produced on the GAS biofilms seemed to come in two distinct forms, a web-like mesh matrix (small black arrows) and a more globular matrix (large black arrows).

Untreated and PNGase F pre-treated Detroit 562 pharyngeal monolayers (without biofilm) were also imaged as controls to ensure that PNGase F treatment did not affect pharyngeal cell morphology (Fig 3.2B and D).

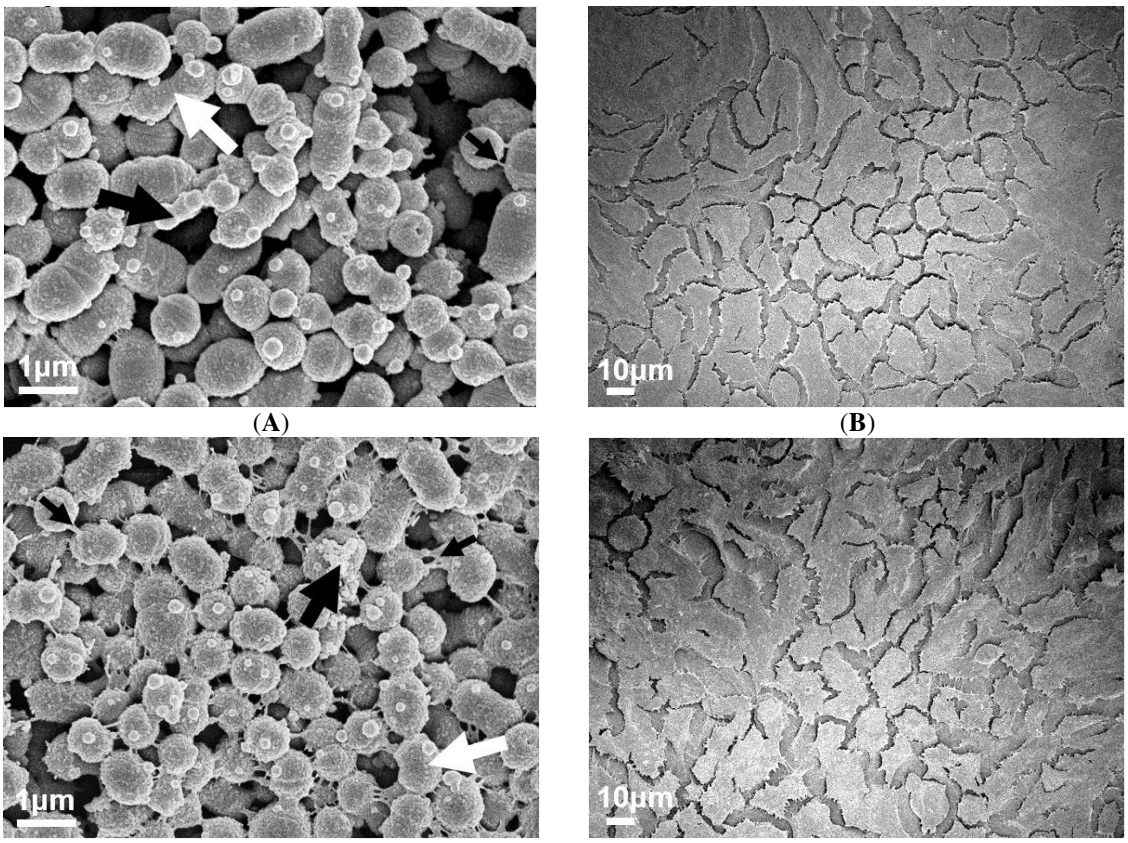

Figure 3.2. Visual inspection of 72 h M12 GAS biofilms captured via SEM revealed substantial extracellular polymeric substances (EPS) present in biofilms formed on PNGase F pre-treated pharyngeal cell monolayers. Images are representative of biofilms formed on (**A**) untreated and (**C**) PNGase F pre-treated pharyngeal monolayers. GAS biofilms show chained cocci (white arrows) arranged into three dimensional aggregated structures with EPS matrix material present (big and small black arrows). SEM images of (**B**) untreated and (**D**) PNGase F pre-treated Detroit 562 pharyngeal cell monolayers (without biofilm) are also included. Biofilms and Detroit 562 pharyngeal cell monolayers (without biofilm) were imaged using the JEOL JSM-7500 microscope at 15 000× and 500× magnification, respectively. SEM images were randomly selected and represent two biological replicates with two technical replicates each.

3.3.2. Characterisation of *N*-linked glycans from Detroit 562 Pharyngeal cell surface reveals abundance of mannose and sialic acid terminating glycan structures

To further examine the role of host *N*-glycans on the surface of pharyngeal monolayers in GAS biofilm formation, a comprehensive profile of the Detroit 562 pharyngeal cell surface *N*-glycome was determined. Membrane proteins were purified from pharyngeal cell culture lysates and treated with PNGase F. Released *N*-glycans were identified using porous graphitised carbon liquid chromatography (PGC-LC) and tandem mass spectrometry by electrospray ionisation (ESI-MS/MS). A total of 19 unique structures were detected, not including linkage isomers (see Appendix C, Table C).

Quantitation by relative abundance revealed oligomannose structures to be the predominant class of *N*-glycans, comprising 82.03% of the Detroit 562 pharyngeal cell surface *N*-glycome (Fig 3.3A) with further analyses confirming that mannose was by far the most abundant terminal monosaccharide, followed by sialic acid and galactose (Fig 3.3B). Terminal *N*-acetylglucosamine was detected at a very low abundance (<0.01%). Core fucosylation was observed in 14% of structures. Glycans were identified based primarily on MS^2 fragmentation data with representative spectra of the most abundant *N*-glycans of each class (Fig 3.3C) provided in Fig 3.3D–F.

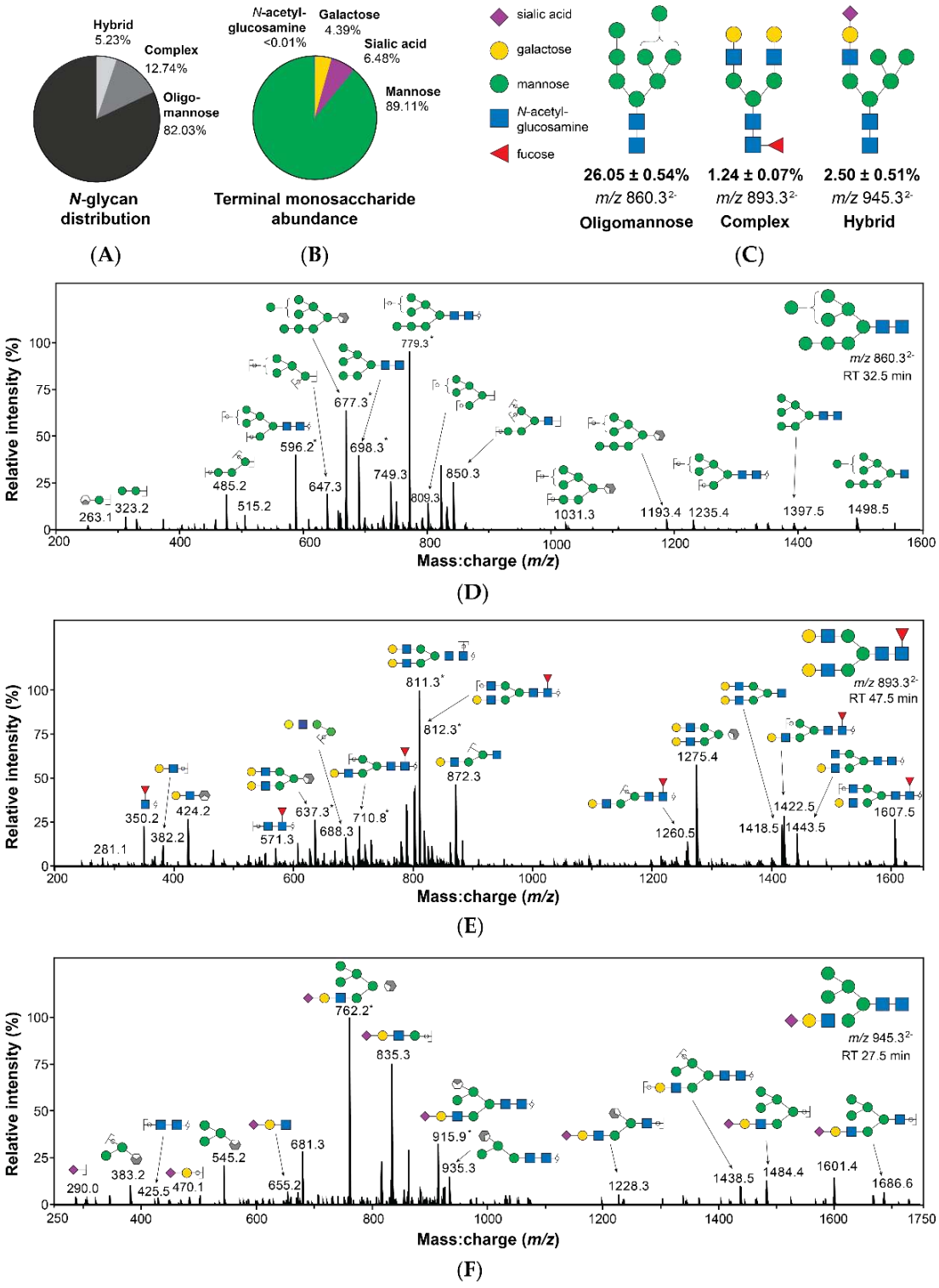

Figure 3.3. Structures bearing terminal mannose predominate the surface of Detroit 562 pharyngeal cells as determined by PGC-LC-ESI-MS/MS. (**A**) Surface *N*-glycans are primarily oligomannose structures. (**B**) Mannose is the most abundant terminal monosaccharide of *N*-glycans. (**C**) Examples of oligomannose, complex, and hybrid *N*-glycans are provided, including relative abundance and mass-to-charge ratio (*m/z*) as detected by MS. Structures were identified primarily using MS^2 spectra (**D**–**F**) (Ceroni et al., 2008, Harvey et al., 2008, Everest-Dass et al., 2012, Everest-Dass et al., 2013) in addition to precursor mass:charge ratio (*m/z*) and retention time. Structural isomers sharing the same *m/z*, composition, and terminal monosaccharide presentation were combined in evaluation of abundance, calculated by integration of area under of the curve from extracted ion chromatograms. Abundance values are relative and are presented as combined mean ± SEM from 3 biological replicates, each with 3 technical replicates. * Denotes doubly charged fragments. Glycans are represented using conventional graphical nomenclature (Varki et al., 2015).

3.3.3. Removal of terminal mannose and sialic acid residues from pharyngeal cell surface glycans differentially impacts the capacity of M12 GAS to form biofilm.

3.3.3.1. Initial adherence, biofilm biomass, and bacterial colony forming units

Oligomannose, sialic acid, and galactose were found to comprise the major *N*-linked glycans on the surface of Detroit 562 pharyngeal cells. Sialic acid is utilised by several pathogens at the nasopharynx in colonisation and biofilm formation (Parker et al., 2009, Trappetti et al., 2009). Due to the abundance of mannose, and the previously described importance of sialic acid in bacterial virulence, the role of these structures in GAS biofilm formation was further explored.

To do so, Detroit 562 pharyngeal monolayers were first pre-treated with specific exoglycosidases; α1-6 mannosidase (removes α1-6 linked mannose residues), α1-2,3 mannosidase (removes α1-2 and α1-3 linked mannose residues), and the broad specificity sialidase (which will be referred to as Sialidase A) (removes linear and branched terminal α2-3, α2-6, α2-8, and α2-9 linked sialic acid); and monosaccharide removal was confirmed by lectin binding assays (see Appendix E, Figure E). Initial adherence of planktonic GAS after 2 h incubation with the untreated and exoglycosidase pre-treated monolayers was determined. The biofilms formed on these monolayers were assessed for biofilm biomass and bacterial colony forming units (Fig 3.4A). Investigation into the initial adherence of planktonic M12 GAS interacting with the exoglycosidase pre-treated and control monolayers found no significant differences (Fig 3.4B). Despite this, the 72 h M12 GAS biofilms exhibited increased biomass on the exoglycosidase pre-treated monolayers compared to the untreated control (Fig 3.4C). Notably, α1-6 mannosidase and Sialidase A pre-treatment of monolayers resulted in significant increases ($p \leq 0.05$) in biofilm biomass. The number of colony forming units within the biofilms did not differ significantly between treatments (Fig 3.4D). Despite this, live/dead staining with

Syto9/PI (Fig 3.4E) revealed a significant increase in the number of dead cells within biofilms formed on α1-6 mannosidase and Sialidase A pre-treated monolayers ($P \leq 0.05$).

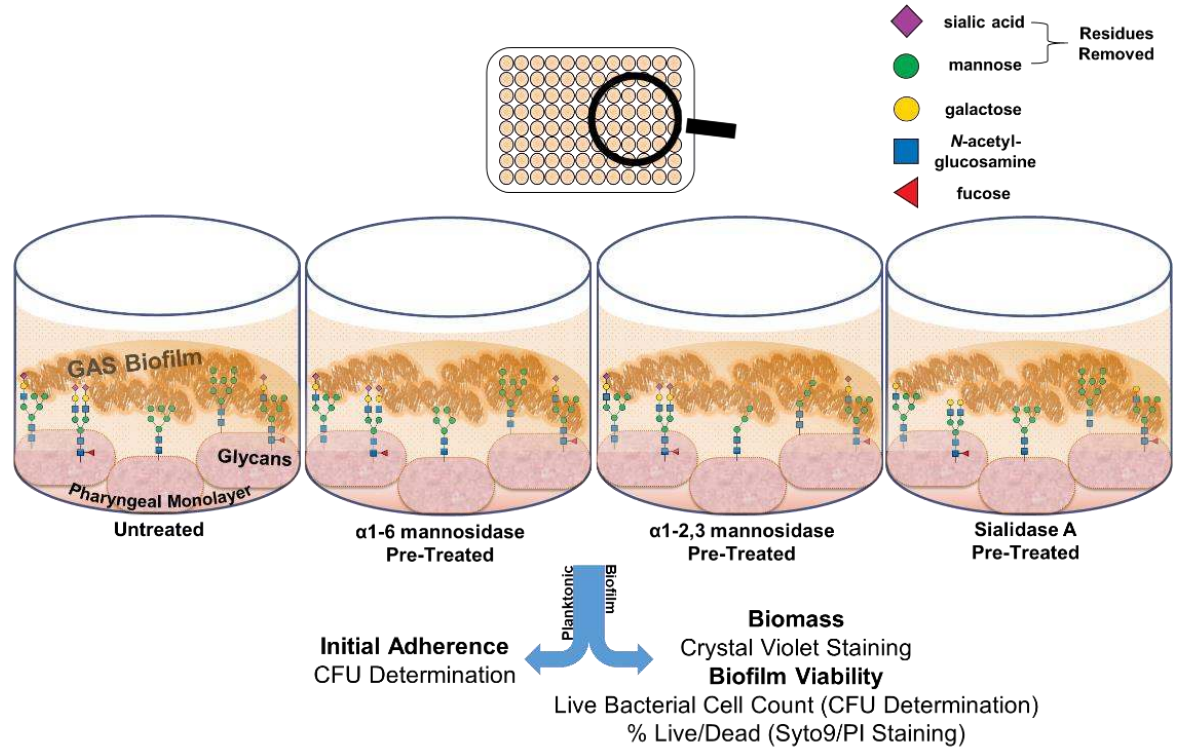

(**A**)

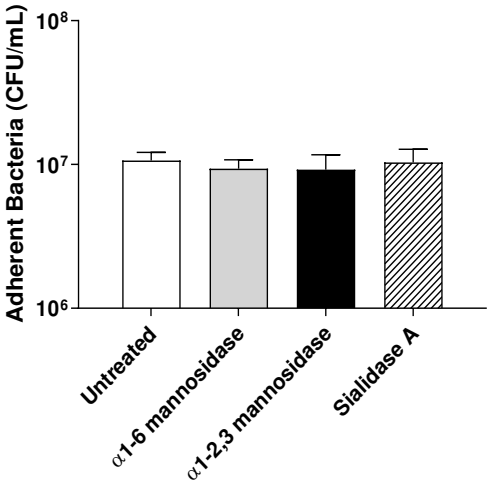

(**B**)

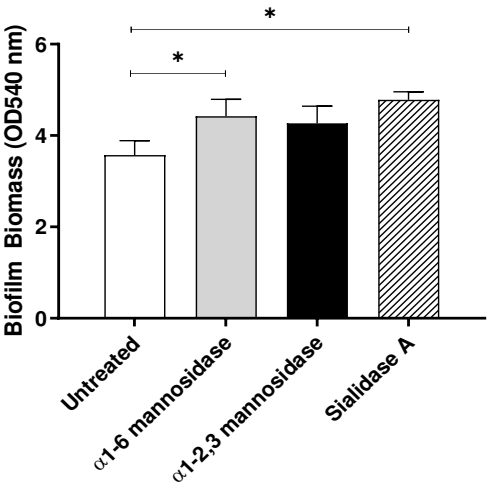

(**C**)

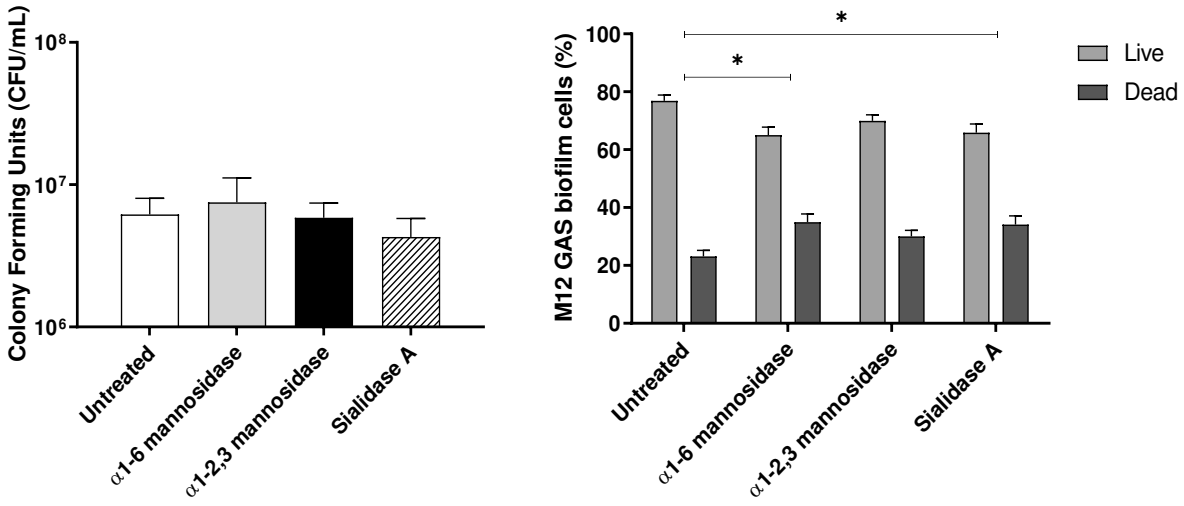

(**D**) (**E**)

Figure 3.4. Pre-treatment of pharyngeal cell surface with α1-6 mannosidase and Sialidase A results in significantly increased M12 GAS biofilm biomass. (**A**) Assay schematic for the characterisation of biofilms formed on each of the exoglycosidase (α1-6 mannosidase, α1-2,3 mannosidase, and Sialidase A) pre-treated pharyngeal monolayers vs. untreated. (**B**) Initial adherence enumerated for planktonic GAS upon 2 h incubation. 72 h biofilms are assessed for (**C**) biofilm biomass via crystal violet staining and viability by (**D**) colony forming units via enumeration and (**E**) live/dead staining with Syto9/PI. Data represents mean ± SEM, with statistical analysis performed using a one-way ANOVA with Tukey's multiple comparisons test * ($p \leq 0.05$); $n = 3$ biological replicates, with 3 technical replicates each.

3.3.3.2. Biofilm EPS

Biofilms are comprised of bacterial cells and EPS. To further determine what may be contributing to the observed changes in biofilm biomass, EPS associated sulphated GAGs, extracellular DNA (eDNA), and protein was assessed (Fig 3.5A).

1,9 dimethyl methylene blue (DMMB) staining was used to detect EPS-associated sulphated GAGs (Peeters et al., 2008, Pantanella et al., 2013). EPS associated sulphated GAGs increased significantly for M12 GAS biofilms formed on α1-6 mannosidase ($p \leq 0.01$) and Sialidase A ($p \leq 0.05$) pre-treated pharyngeal cell monolayers compared to the untreated control (Fig 3.5B). This result supports the findings from crystal violet staining, suggesting EPS production increases in response to modification of cell surface glycans. Lastly, EPS was examined for common EPS components (eDNA and protein), via fluorescent stains Sytox Blue and SYPRO Ruby (Fig 3.5C). There were no significant differences in the presence of EPS associated eDNA or protein in biofilms formed.

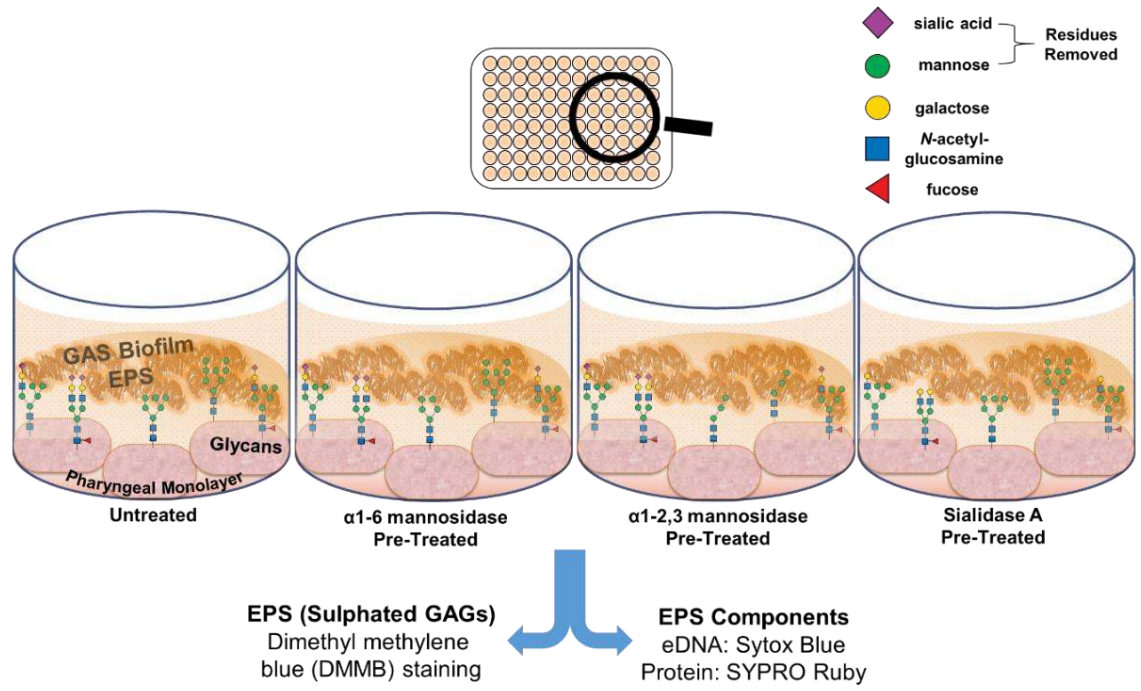

(**A**)

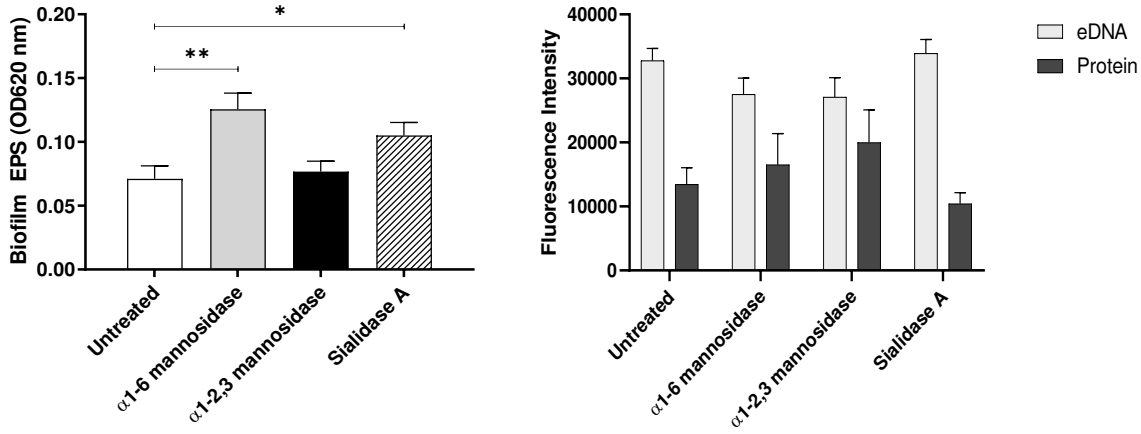

(**B**) (**C**)

Figure 3.5. Biofilm EPS increases significantly for biofilms formed on α1-6 mannosidase and Sialidase A pre-treated pharyngeal cell surfaces. (**A**) Assay schematic for the assessment of biofilm EPS resulting from biofilm formed on each of the exoglycosidase (α1-6 mannosidase, α1-2,3 mannosidase, and Sialidase A) pre-treated pharyngeal monolayers vs. untreated. 72 h biofilms were assessed for (**B**) EPS via DMMB staining of sulphated GAGs and (**C**) EPS associated components (eDNA and protein) via fluorescent staining with Sytox Blue and FilmTracer SYPRO Ruby biofilm matrix stain, respectively. Data represents mean ± SEM, with statistical analysis performed using a one-way ANOVA with Tukey's multiple comparisons test * ($p \leq 0.05$) and ** ($p \leq 0.01$); $n = 3$ biological replicates, with 3 technical replicates each.

To visually investigate the effect of exoglycosidase (α1-6 mannosidase, α1-2,3 mannosidase, and Sialidase A) pre-treated pharyngeal monolayers on M12 GAS biofilm formation, SEM imaging was conducted (Fig 3.6). Biofilms formed on both untreated and exoglycosidase pre-treated monolayers show M12 GAS chained cocci arranged into three dimensional aggregated structures with EPS matrix material present (Fig 3.6A, C, E, and G). Biofilms formed on each of the exoglycosidase pre-treated pharyngeal monolayers appear to produce more EPS matrix material associated with the aggregated GAS cocci when compared to GAS biofilms formed on the untreated control. EPS produced on all GAS biofilms display the distinct forms seen previously, a web-like mesh matrix (small black arrows) and a more globular matrix (big black arrows). Both extend from the cocci cell surface of these biofilm cells. Untreated and exoglycosidase pre-treated Detroit 562 pharyngeal monolayers (without biofilms) were also imaged as controls to ensure that each exoglycosidase treatment did not affect pharyngeal cell morphology/structures (Fig 3.6B, D, F, and H).

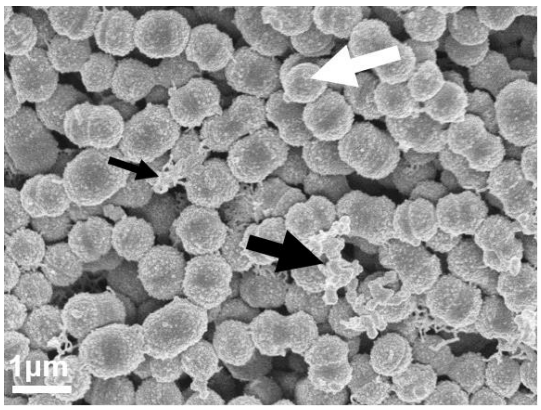

(**A**)

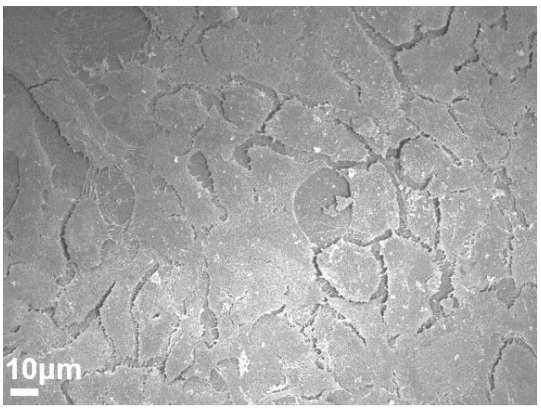

(**B**)

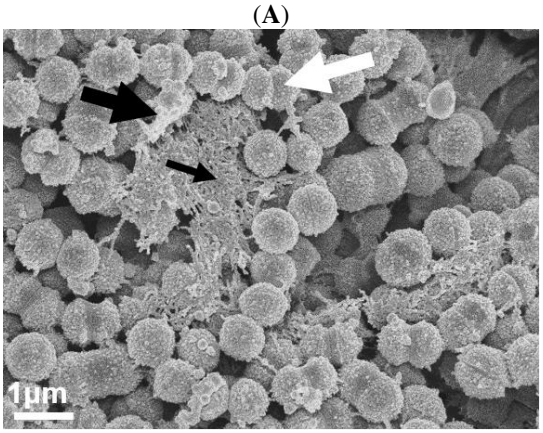

(**C**)

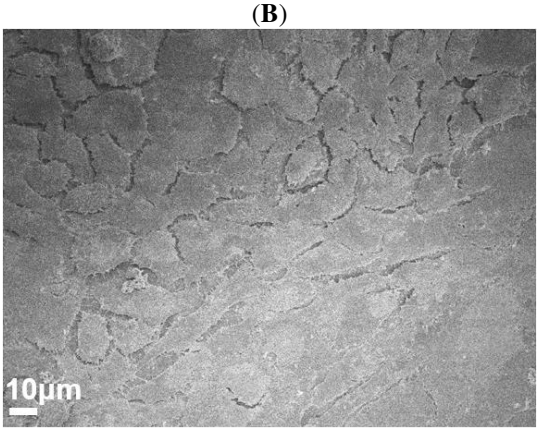

(**D**)

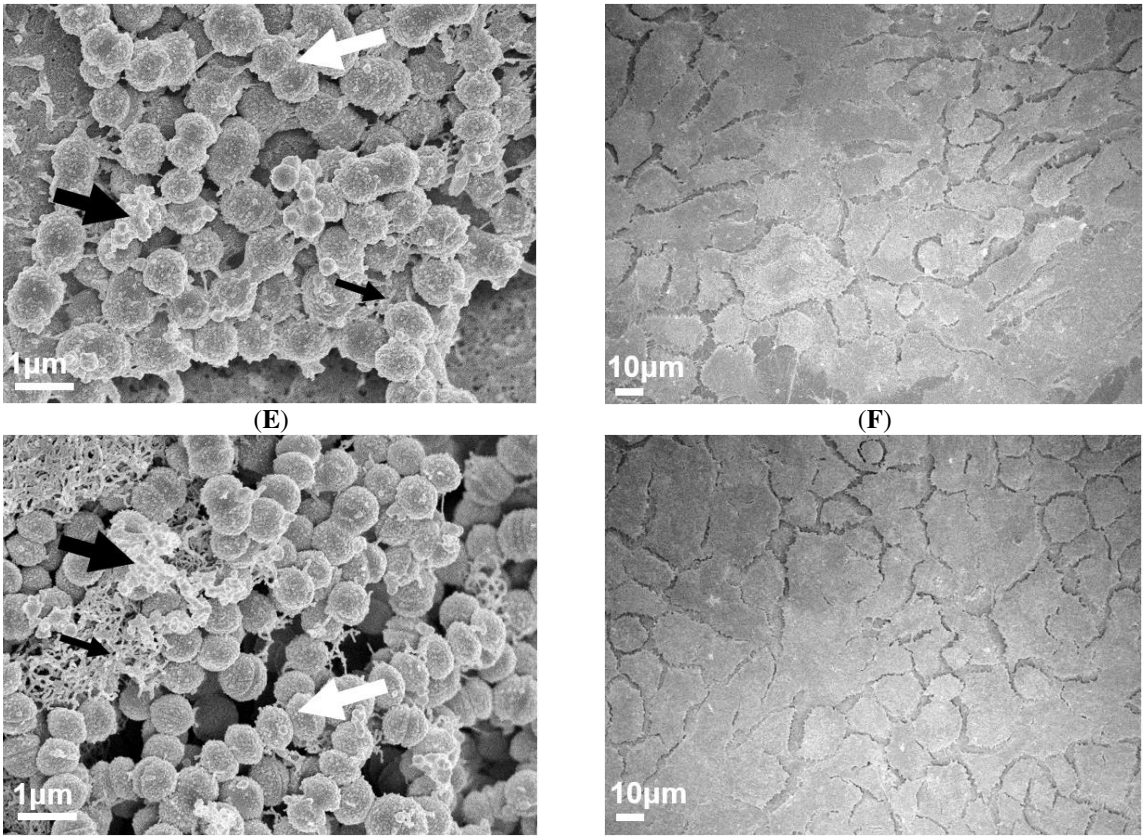

Figure 3.6. Visual inspection of 72 h M12 GAS biofilms captured via SEM revealed substantial EPS present in biofilms formed on exoglycosidase pre-treated pharyngeal cell monolayers. Images are representative of biofilms formed on (**A**) untreated, (**C**) α1-6 mannosidase, (**E**) α1-2,3 mannosidase, and (**G**) Sialidase A pre-treated pharyngeal monolayers. GAS biofilms show chained cocci (white arrows) arranged into three dimensional aggregated structures with EPS matrix material present (big and small black arrows). SEM images of (**B**) untreated, (**D**) α1-6 mannosidase, (**F**) α1-2,3 mannosidase, and (**H**) Sialidase A pre-treated Detroit 562 pharyngeal cell monolayers (without biofilms) are also included. Biofilms and Detroit 562 pharyngeal cell monolayers (without biofilm) were imaged using the JEOL JSM-7500 microscope at 15,000× and 500× magnification, respectively. SEM images were randomly selected and represent two biological replicates with two technical replicates each.

3.3.4. Increased biofilm formation promotes penicillin tolerance

Penicillin is the antibiotic of choice for the treatment of GAS infections (Wessels, 2016). The biofilm phenotype is known to decrease bacterial susceptibility to antibiotics and is suspected to play a role in the observed antibiotic treatment failure rate of 20–40% of GAS pharyngitis cases (Facinelli et al., 2001, Conley et al., 2003, Baldassarri et al., 2006). As such, the penicillin susceptibility of the M12 GAS biofilms was assessed.

Firstly, the susceptibility of planktonic M12 GAS to penicillin was confirmed by determining the minimum inhibitory concentration (MIC) and minimum bactericidal concentration (MBC) values (data not shown, but MIC graphs available at

Appendix F, Figure F). A MIC and MBC of 0.025 μg/mL was established, which is consistent with the reported GAS MIC and MBC range for penicillin (Çiftçi et al., 2003, Sakata, 2013). Notably, minimum biofilm eradication concentration values (MBECs) determined for M12 GAS biofilms formed on untreated and exoglycosidase pre-treated monolayers (Table 3.1) were all considerably higher than the MIC for planktonic M12 GAS, resulting in 2500–5000-fold greater penicillin tolerance. Specifically, biofilms formed on untreated pharyngeal monolayers had an MBEC of 62.5 μg/mL, whereas biofilms formed on exoglycosidase pre-treated monolayers had an MBEC of 125 μg/mL.

Table 3.1. M12 GAS biofilms exhibit enhanced penicillin tolerance when formed upon exoglycosidase-treated pharyngeal cell monolayers. MBECs (μg/mL) determined for M12 GAS biofilms were compared to the planktonic M12 GAS minimum inhibitory concentration (MIC) (0.025 μg/mL). Data represent $n = 3$ biological replicates, with 3 technical replicates each.

Biofilm monolayer	M12 MBEC (μg/mL)	Fold Greater Tolerance Compared to MIC
Untreated	62.5	2500
α1-6 mannosidase	125	5000
α1-2,3 mannosidase	125	5000
Sialidase A	125	5000

3.4. Discussion

Pharyngitis is the most prevalent form of GAS disease (Carapetis et al., 2005, Wessels, 2016). Although other pathogenic agents can cause pharyngitis, GAS is frequently isolated in affected children (20–40%) and adolescents/young adults (5–15%) (Conley et al., 2003, Danchin et al., 2007). Penicillin is the antibiotic of choice due to its narrow spectrum of activity, safety, and accessibility (Wessels, 2016). Most notably, there have been no reported cases of GAS resistance to penicillin to date among clinical isolates. Despite this, antibiotic treatment failure occurs in 20–40% of cases (Kuhn et al., 2001, Conley et al., 2003). Numerous hypotheses have been suggested to explain this treatment failure rate including GAS host-cell internalisation and viral/bacterial co-pathogenicity (Österlund et al., 1997, Pichichero and Casey, 2007). More recently, it has been proposed that GAS may exist as a biofilm, a microbial phenotype that is known to provide protection from both host immunity and antibiotics (Akiyama et al., 2003, Ogawa et al.,

2011, Marks et al., 2014). Numerous studies have since investigated biofilm formation in the context of GAS pharyngitis and treatment failure. However, many of them employ abiotic substrata, and moreover, none have considered the role of host cell surface glycans. Given the increasingly appreciated importance of glycans in the host-pathogen relationship and the abundance of glycosylated structures in the oropharynx, this work contributes to an improved understanding of the role of host glycans in the pathogenesis of GAS pharyngitis and antibiotic treatment failure.

Interactions of planktonic GAS with a variety of glycan structures have been observed in numerous studies, many of which indicate that host glycans are implicated in GAS binding and adhering to host cells (Frick et al., 2003, De Oliveira et al., 2017, De Oliveira et al., 2019). In the current study, removal of *N*-linked glycans from the Detroit 562 pharyngeal cell surface significantly decreased initial adherence of planktonic M12 GAS. Despite this, subsequent M12 GAS biofilms displayed a significant increase in biofilm biomass on PNGase F treated cells. SEM imaging of biofilms formed on both untreated and PNGase F pre-treated monolayers revealed adherent M12 GAS cocci chains arranged in three dimensional aggregated structures intermeshed with EPS matrix. Moreover, biofilms formed on PNGase F pre-treated monolayers were seen to have more EPS matrix. Two varieties of EPS matrix were visible; the globular EPS matrix seen in the current study is phenotypically similar to GAS biofilms imaged via SEM previously on the surface of tonsils removed from patients with recurrent GAS tonsillopharyngitis (Roberts et al., 2012). The web-like EPS matrix projecting from the cocci cell surface of these biofilms has been captured in one previous study of M2 GAS biofilms, with the authors describing the EPS matrix material as “threadlike structures of an as-yet unknown chemical composition” (Lembke et al., 2006).

Although this is an interesting finding, it is unlikely *in vivo* that a host cell surface would be lacking in all or most of its *N*-linked glycans. As such, we focused on the role of

specific *N*-linked glycans that are abundant on the Detroit 562 pharyngeal cell surface in this study. PGC-LC-ESI-MS/MS analysis of the Detroit 562 pharyngeal cell surface *N*-glycome revealed that oligomannose structures are the most abundant class of *N*-glycan, followed by complex and hybrid glycans, with mannose being the predominant monosaccharide on the cell surface. As mannosidases act upon oligomannose *N*-glycans primarily, and hybrid *N*-glycans secondarily, broad-spectrum sialidase treatment was additionally utilised in this study to act upon complex and hybrid *N*-glycans. Removal of terminal mannose and sialic acid residues resulted in an increase of biofilm biomass similar to that induced by total *N*-glycan removal with PNGase F, independent of initial adherence and enumerated biofilm viability. It is possible that removal of these glycans enables access by GAS to otherwise impeded host receptors involved in the host-pathogen interaction, further promoting biofilm formation. The importance of terminal monosaccharides has been demonstrated in a previous study of GAS binding to human buccal epithelial (HBE) cells, whereby expression of terminal galactose and sialic acid residues had significant effects on M1, 3, and 12 associations, whilst terminal fucose and *N*-acetylgalactosamine were of comparatively lesser dependence of binding for all three GAS M-types. It was suggested that fucose and *N*-acetylgalactosamine may have a host-protective effect, sterically hindering access to the preferred galactose residues (De Oliveira et al., 2019). Many pathogens are known to possess their own suite of glycosidases which they utilise to liberate glycan residues for their own metabolic processes, and moreover, to better access preferred glycan structures for adherence (Grewal et al., 2008, Inui et al., 2015). For example, *S. pneumoniae* expresses multiple neuraminidases that cleave off sialic acids, unmasking other receptors for increased binding and virulence (Grewal et al., 2008).

To further assess viability, particularly the dead cell populations within these biofilms, Syto9 and PI staining was used. Syto9 stains nucleic acids of all cells, whereas PI only

stains nucleic acids of cells with compromised membranes. When used together at appropriate concentrations, PI is in excess to Syto9 and with its overall higher binding affinity towards nucleic acids will displace Syto9. As such, dead cells can be distinguished from total cell population (Robertson et al., 2019, Rosenberg et al., 2019). Pre-treatment with α1-6 mannosidase and Sialidase A resulted in biofilms comprising a significantly greater proportion of dead cells. However, these results conflict with the findings of the biofilm viability determined via enumeration. Although Syto9 and PI are routinely used for staining live/dead cells, it is understood that there are some limitations which may lead to an erroneous and inaccurate depiction of viability. Specifically, over or underestimation of live or dead cells may result from poorer penetration of the dyes for bacteria grown in nutrient-rich media and variation in bacterial membrane integrity resulting from differing physiological growth states (Stiefel et al., 2015, Robertson et al., 2019). More importantly, eDNA, which is a well-established component of many microbial biofilms, is also stained by these dyes (Rosenberg et al., 2019). Taken together it is likely that the dead cell population has been overestimated. Future study should consider a combination of methods to accurately estimate viability; utilising stains for metabolic activity and visualisation of these biofilms via confocal laser scanning microscopy (CLSM) or super-resolution microscopy. Additionally, given the limitations presented by culture-based methods (i.e. some species existing in a viable, but non-cultivable state), culture-independent techniques may also be of use. Specifically, quantitative real-time PCR (qPCR) which can rapidly detect these viable but otherwise non-cultivable cells, and thus give a better representation of the biofilm viability (Magalhães et al., 2019).

Given that initial planktonic GAS adherence and the population of live cells as determined via enumeration within the biofilms did not seem to uniquely contribute to the increases in biofilm biomass, EPS was examined. The EPS is an important component

of the biofilm, and it is thought to contribute to around 80–85% of the total biofilm biomass (Cowan, 2011). The removal of glycans did not result in an increase of initial bacterial adherence, and it is possible changed glycan structures modified expression of genes associated with EPS production, although this was not explored in the current study. The EPS matrix has its own complex and dynamic matrixome, which defines the compositional and functional diversity of the EPS. EPS is predominantly comprised of polysaccharides, proteins, eDNA, and lipids. Despite variability in their composition across pathogens, EPS-associated polysaccharides are generally considered the most abundant (Flemming and Wingender, 2010, Bales et al., 2013, Karygianni et al., 2020). Currently, GAS EPS remains poorly defined, with only one study having investigated EPS polysaccharides, determining that L-glucose and D-mannose were the most abundant sugar moieties of the EPS of one M6 strain (Shafreen et al., 2011).

DMMB staining is a simple approach that has been used extensively in staining the EPS GAG polysaccharides of numerous other bacterial biofilms (e.g., *Staphylococcus aureus*, *P. aeruginosa*, *Burkholderia cenocepacia*, and *Propionibacterium acnes*) (Peeters et al., 2008, Pantanella et al., 2013). Here, for the first time, it is demonstrated that DMMB is suitable for detecting GAS biofilm EPS-associated GAGs. Moreover, DMMB staining revealed that biofilms formed on α1-6 mannosidase and Sialidase A pre-treated pharyngeal monolayers exhibited significantly increased EPS polysaccharide production, despite eDNA or protein abundance remaining unchanged. Further assessment of other EPS components such as lipids and a diverse range of polysaccharides should be investigated via other fluorescent stains such as 1,1′-dioctadecyl-3,3,3′,3′-tetramethylindodicarbocyanine perchlorate (DiD'oil) or concanavalin A conjugated to a fluorophore such as tetramethylrhodamine (González-Machado et al., 2018). SEM imaging of biofilms formed on both untreated and each of the exoglycosidase pre-treated monolayers revealed biofilms similar to those seen on untreated and PNGase F pre-treated

monolayers. Biofilms show adherent M12 GAS cocci chains arranged in three dimensional aggregated structures intermeshed with EPS matrix. Similar to results following PNGase F treatment, biofilms formed on exoglycosidase pre-treated pharyngeal cell monolayers showed an increase in EPS matrix. Both varieties of EPS (globular and web-like) were present in biofilms formed.

A critical characteristic of the biofilm phenotype is increased tolerance to antimicrobials, with reports of antimicrobial tolerance anywhere between 10 and >1000 times greater compared to planktonic form (Costerton et al., 1999, Donlan and Costerton, 2002, Hall-Stoodley et al., 2004). Biofilms may be a contributing factor for the antibiotic treatment failure rate of 20–40% reported in cases of GAS pharyngitis. Here we determined if the observed increase in biofilm formation was functionally relevant in the context of penicillin tolerance when compared to planktonic GAS. Penicillin tolerance doubled following removal of mannose and sialic acid residues, respectively, from the pharyngeal monolayer substratum. We have shown that removal of these residues leads to increases in EPS which may have impeded penicillin penetration through the biofilms. Several other features unique to the biofilm phenotype may have further contributed to the increase in penicillin tolerance including differential growth rates of bacterial cells, nutrient gradients, and antibiotic degradation once in the biofilm (Costerton et al., 1995, Stewart and William Costerton, 2001, Høiby et al., 2010, Lewis, 2010). Further study should aim to characterise the specific mechanisms for the enhanced penicillin tolerance described here.

The indiscriminate removal of all *N*-glycans and the targeted removal of terminal mannose and sialic acid, which predominate the surface of Detroit 562 pharyngeal cells, increases biofilm biomass, specifically via increased EPS production. The presence of certain host glycan structures may be a host-protective mechanism, reducing the formation of GAS biofilms *in vivo.* GAS has been shown to modify host glycoproteins

via recently discovered glycosidases endoglycosidase S and α-mannosidase (Collin and Olsén, 2001, Suits et al., 2010). The ability of GAS to modify the host-glycome at different sites and stages of infection has not been characterised. Our findings suggest that modification of the host glycome during the course of infection may increase the ability of GAS to form biofilms.

GAS is commonly attributed to pharyngeal infection with over 600 million cases per year, presenting a considerable global burden (Carapetis et al., 2005). Recurrent GAS infection, persistent carriage, and antibiotic treatment failure remain challenging and unresolved, despite numerous efforts in characterising the consortia of molecular mechanisms underpinning GAS virulence and pathogenesis. Moreover, most of these studies have been conducted only in the context of planktonic GAS. Here GAS biofilm formation has been investigated for the first time, with a particular focus on the effect of altering pharyngeal cell surface glycans. Host cell surface glycans may offer a protective advantage against GAS biofilm formation. We have shown that modulation of the pharyngeal glycome has a direct impact on GAS biofilm formation, with increases in EPS likely to play an important role. Moreover, the increased GAS biofilms displayed significantly greater penicillin tolerance dependent on the host cell glycome. Lastly, this study described the effect of host glycosylation on GAS biofilm formation and GAS biofilm formation as an important proponent in penicillin tolerance.

Chapter 4: Assessing the role pharyngeal cell surface glycans play in GAS biofilm formation for a diverse set of GAS serotypes

Overview: Previously, M12, a prominent pattern A-C GAS M-type contributing to global pharyngeal infection (Walker et al., 2014) was assessed for its biofilm forming abilities in response to changes in Detroit 562 pharyngeal cell surface mannose and sialic acid availability. Here, a diverse range of GAS M-types representative of distinct *emm* patterns A-C, D, and E were similarly assessed for their biofilm formation. Modulation of the pharyngeal glycome directly impacted GAS biofilm formation of all eight GAS M-types in a strain- and glycan- dependent manner. M-types were grouped by their *emm* patterns to identify correlations between *emm* pattern and GAS biofilm formation response to changes in Detroit 562 pharyngeal cell surface glycan profile modifications. With the exception of pattern E GAS M-types, variances in biofilm formation in response to differentially exposed pharyngeal cell surface glycans were not *emm* pattern specific. Further investigation is warranted into other factors that may be contributing biofilm formation at the pharyngeal glycan surface, such as non-M GAS virulence factors, biofilm specific mechanisms (e.g. quorum sensing) and so forth. Overall, the findings of this work suggest that altering the pharyngeal cell surface glycome results in biofilm potentiation of a diverse selection of GAS M-types. These findings underscore the importance of the glycomic landscape of the host in mediating GAS biofilm formation.

4.1. Introduction

Of the plethora of virulence factors produced by GAS, the M protein is a major virulence factor that is abundantly expressed on the surface of GAS (Walker et al., 2014). The M protein is well characterised and has been found to play a role in adhesion to the host cell surface for a variety of GAS strains (Ellen and Gibbons, 1972, Tylewska et al., 1988, Caparon et al., 1991). The 5’ region of the *emm* gene that encodes the M protein has served as a valuable means to distinguish and type GAS strains. This means of *emm*

typing has led to the identification of over 200 differing GAS *emm* types (Smeesters et al., 2010, Walker et al., 2014). Although their distribution is in part impacted by geographic and socioeconomic factors, the predominance of certain *emm* types in discrete geographical locations is widely reported. In industrialised regions, M-types 1, 3, and 12 predominate, and underpin ~40% of GAS disease (Steer et al., 2009). Moreover, epidemiological studies have found distinct M-types have been heavily associated with various disease manifestations, for example, M-types 2 and 44/61 are linked to superficial disease, whereas M-types 1 and 3 are associated with invasive disease (Ekelund et al., 2005, Shea et al., 2011).

The genetic variability in the *emm* gene consequently confers diversity in protein function and binding ligands among each distinct GAS M-type. This can be seen in the varying abilities of differing GAS M-types to adhere to- and internalise at- distinct epithelial tissues of the pharynx and/or skin (Bessen and Lizano, 2010). Decades of epidemiological study have found strong associations between M-types and the bodily niche they occupy, and the subsequent disease manifestations they cause (Wannamaker, 1970, Bessen et al., 1996, Bessen and Lizano, 2010). This has led to the identification of distinct throat, skin, and generalist strains (Bessen and Lizano, 2010). Further investigation has found an association between the *emm* gene and *emm*-family (M-related protein encoded by *mrp* and M-like protein encoded by *enn*) located within the multiple gene activator (Mga) regulon and GAS tissue tropism. This has led to an additional GAS typing system, the '*emm* pattern' typing system, that comprises five distinct patterns (Fig 4.1) (Hollingshead et al., 1994). GAS M-types belonging to Patterns A-C are thought to be associated with pharyngeal infections, Pattern D with infections of the skin, and Pattern E are termed generalist and are associated with infections in both the pharynx and skin (Bessen and Lizano, 2010). This was supported in a 2004 study of over 4000 GAS isolates, in which a strong trend was found, whereby isolates of pattern A-C *emm* types caused infections

of the throat, and those belonging to pattern D *emm* type were highly likely to cause impetigo lesions of the skin (McGregor et al., 2004).

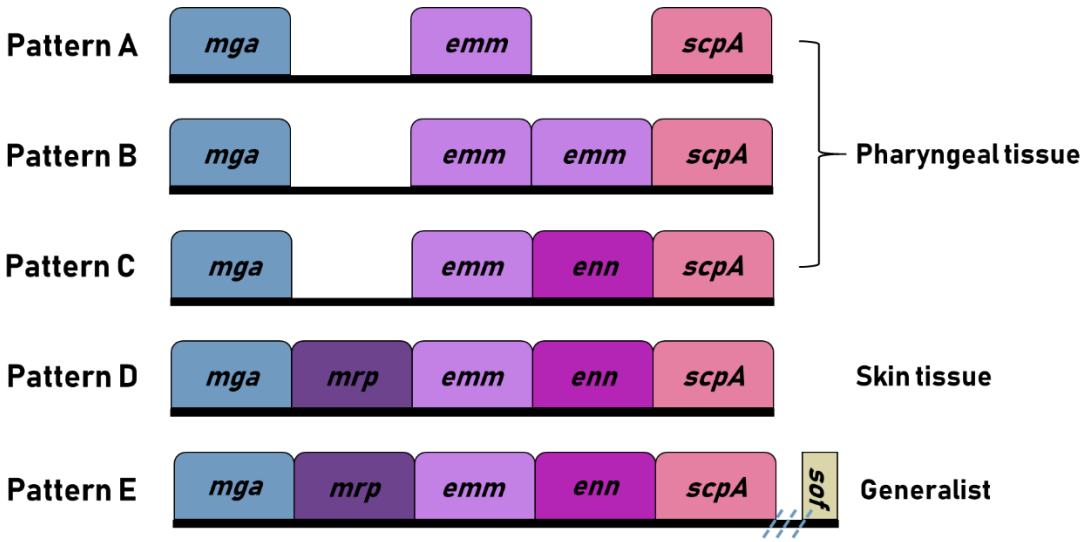

Figure 4.1. GAS *Emm* pattern system is underpinned by the genomic arrangement of the multiple gene activator (Mga) regulon. The Mga regulon comprises of the M protein family; M-related protein (encoded by *mrp*), M-protein (encoded by *emm*), and M-like protein (encoded by *enn*). The *scpA* (encoding c5a peptidase) is located downstream of the M protein family genes. Together these are thought to contribute to tissue tropism and have been assigned to each respective *Emm* pattern as follows; pharyngeal tissue (Pattern A-C), skin tissue (Pattern D), and generalist which can associate to both pharyngeal and skin tissue (Pattern E). Pattern E strains uniquely possess a *sof* gene located downstream of the *mga* regulon, which secretes serum opacity factor. Figure is adapted from Hollingshead et al. (1994), Bessen and Lizano (2010).

The diversity of the *emm* gene also contributes to differential binding of host extracellular matrix components (fibrinogen, fibronectin, albumin etc) and host antibodies (Smeesters et al., 2010, Sanderson-Smith et al., 2014). Interestingly, *emm* patterns can confer exclusive M protein binding profiles which may further contribute to differential tissue tropism (Bessen, 2016). For example, pattern A-C M proteins primarily bind fibrinogen, pattern D M proteins primarily bind plasminogen, and pattern E M proteins primarily bind IgA antibody and the complement component 4 binding protein (Smeesters et al., 2010).

Glycans have been shown to be ligands for a small number of pattern A-C associated M proteins (M1, 3, and 12). Frick et al. (2003) demonstrated that M1 GAS could bind Detroit 562 pharyngeal cells via surface-expressed GAGs dermatan sulfate and/or heparan sulfate. De Oliveira et al. (2017) observed M1 binding human buccal epithelial (HBE)

cells with varying affinities via A, B, and O(H) histo-blood group antigens, with recognition of the H antigen and association of M1 GAS to H-antigen expressing cells notably higher than for other histo-blood group antigens. In a more recent study by De Oliveira et al. (2019), analysis of glycan binding by M proteins was expanded to include A-C M proteins of M3 and M12. It was found that M3 and M12 colonisation of HBE cells was also mediated in part by human histo-blood group antigens and Lewis antigens. M3 and M12 GAS had the greatest association with HBE cells expressing H antigen, followed by HBE cells expressing A antigen (De Oliveira et al., 2019). These studies provide strong evidence that host glycans play an important role in GAS colonisation, however, they are limited to studying planktonic GAS belonging to pattern A-C *emm* types.

As outlined in chapter 3, the removal of distinct mannose and sialic acid residues from the Detroit 562 pharyngeal cell surface via α1-mannosidase and a broad specificity sialidase (Sialidase A) significantly increased the ability of M12 GAS to form biofilms. Given the diversity of M proteins, the known association between *emm* pattern and tropism, and the high rates of disease globally caused by these diverse *emm* types, it is important to study a broader variety of GAS M-types. Here, the biofilm forming abilities of other throat tropic pattern A-C GAS M-types (M1 and M3), as well as several representative pattern D and E M-type strains were assessed in response to pharyngeal cell surface glycan removal.

The aim of this chapter is to determine if changes in biofilm formation in response to an altered pharyngeal glycomic landscape is common to a diverse selection of GAS M-types. GAS M-types were categorised into their representative e*mm* pattern to further understand if the bodily niche associated with these *emm* types elicited any further effects on biofilm formation. Such research will broaden the understanding of GAS biofilms in the context of these complex host glycan-GAS interactions.

4.2. Materials and methods

Methods used for the assessment of other GAS M-types in this chapter are those established and defined in the previous chapter (Chapter 3, Section 3.2) for M12 GAS biofilm formation in response to pharyngeal cell surface glycans. As such, they are presented here in brief. Moreover, the assays used to evaluate the effect pharyngeal cell surface glycans exert on the diverse range of GAS M-types and the *emm* patterns they represent in forming biofilms have further been summarised in the schematic (Fig 4.2).

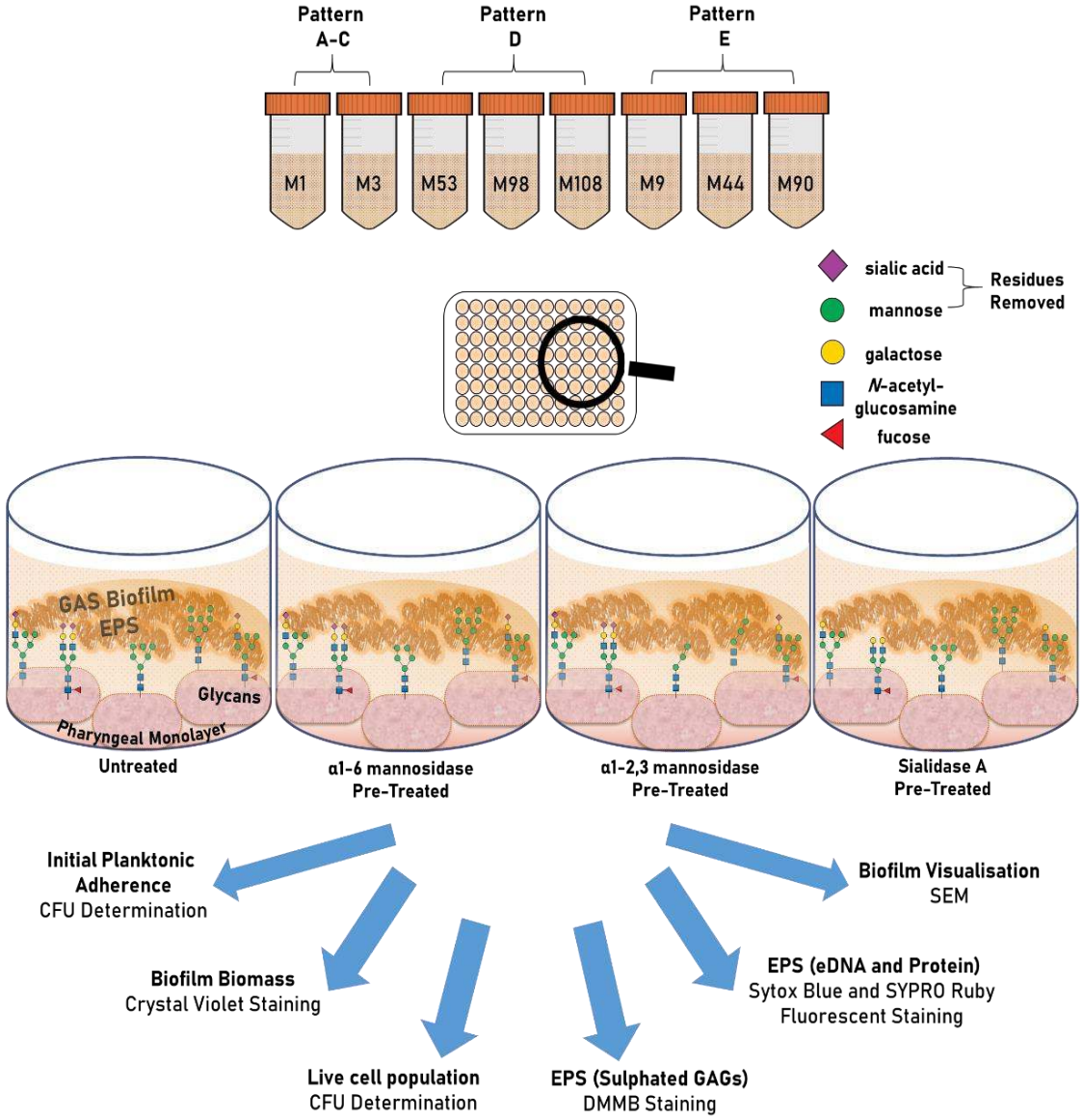

Figure 4.2. Schematic outlining the methods used for the assessment of pharyngeal cell glycan's and their role in biofilm formation for eight diverse GAS M-types.

4.2.1. GAS and culture conditions

GAS strains used in this study (Table 4.1) are clinical GAS isolates, with each strain representative of a discrete GAS *emm*-type (Aziz et al., 2004, McKay et al., 2004, Johnson et al., 2002, Sanderson-Smith et al., 2014). GAS was grown on either HBA plates or THYA where appropriate. Static cultures of GAS were grown overnight in THY. GAS was cultured and maintained at 34°C (Marks et al., 2012).

Table 4.1. GAS strains used in this study have been categorised by their emm patterns; A-C, D, and E. The table further details strain M-types, strain identity, and clinical source (Johnson et al., 2002, Aziz et al., 2004, McKay et al., 2004, Maamary et al., 2010, Sanderson-Smith et al., 2014, De Oliveira et al., 2019).

Pattern	M-type	Strain	Clinical source
A-C	M1	5448	Invasive infection: Necrotising fasciitis and toxic shock
	M3	90254	Invasive infection
D	M53	NS13	Invasive infection: Blood (bacteraemia)
	M98	NS88.2	Invasive infection: Blood (bacteraemia)
	M108	NS50.1	Superficial infection: Wound
E	M9	NS179	Invasive infection: Pustules on foot (bacteraemia)
	M44	NS297	Superficial infection: skin sore
	M90	NS730	Invasive infection: Necrotising fasciitis, hip pus

4.2.2. Human pharyngeal cell culture conditions, monolayer formation, and exoglycosidase pre-treatment

4.2.2.1. Human pharyngeal cell culture conditions

Detroit 562 pharyngeal epithelial cells were cultured in DMEM F12, supplemented with L-glutamine and heat inactivated FBS in cell culture flasks at 37˚C, 5% CO_2 – 20% O_2 atmosphere.

4.2.2.2. Pharyngeal cell monolayer formation

Wells of 96-well flat bottom cell culture microtiter plates were coated with Collagen I from rat tail and incubated for 1 h (37˚C, 5% CO_2 – 20% O_2 atmosphere). After 1 h, wells were seeded with 150 µL Detroit 562 cell suspension ($2x10^5$ cells/mL) and cultured for 48 h to form monolayers. Monolayers were washed once with PBS and fixed with sterile 3.7 % PFA for 20 min. Fixed monolayers were washed with PBS, and monolayers kept wet via submersion in PBS until required for use.

4.2.2.3. Exoglycosidase: α1-6 mannosidase, α1-2,3 mannosidase, and Sialidase A treated monolayers

Fixed pre-formed Detroit 562 pharyngeal cell monolayers of the 96-well microtiter plate were treated with 30 µL/well reaction volumes of each of the exoglycosidases; α1-6 mannosidase, α1-2,3 mannosidase, and Sialidase A. Untreated PBS wells representing the intact surface glycome of the Detroit 562 pharyngeal cell monolayers were also included as a control. The plate was incubated for 2 h, 37°C. Once incubated, the wells were washed once with PBS.

4.2.3. Initial adherence of planktonic GAS

Fixed pre-formed Detroit 562 pharyngeal cell monolayers were inoculated with 150 µL of stationary phase GAS culture diluted 1:20 in THY-G and incubated for 2 h to promote initial attachment (34°C, slow shaking at 50 rpm). At 2 h, non-adherent GAS was removed, and the wells washed thrice with PBS. To detach Detroit 562 cells from the bottom of the microtiter plate, trypsin-EDTA was added to each well and incubated (15 min, 37°C). To lyse the now-detached Detroit 562 cells containing internalised bacteria, Triton X-100 was added and pipetted vigorously. To enumerate the adherent GAS population, 10-fold serial dilutions of the cell suspensions were performed in PBS and aliquots spot plated onto

THYA (incubated overnight, 34°C) for subsequent colony counting and CFU/mL determination.

4.2.4. GAS biofilms

96-well microtiter plates containing pre-formed fixed Detroit 562 pharyngeal cell monolayers untreated and pre-treated with exoglycosidases were inoculated with 150 µL of overnight GAS culture diluted 1:20 in THY-G. The inoculum was incubated for 2 h (34°C, 50 rpm). At 2 h, non-adherent GAS was removed, and wells replenished with sterile THY-G. Subsequent 72 h GAS biofilms were produced (34°C, 50 rpm), with sterile THY-G media refreshment performed every 24 h.

4.2.4.1. GAS biofilm biomass crystal violet staining

Biofilm biomass was assessed via crystal violet staining. Air dried biofilms were fixed with 99% methanol and stained with crystal violet for 10 min (RT, static). Once stained, excess crystal violet was removed and each well gently washed twice with PBS. Crystal violet stain that had incorporated into the biofilm was re-solubilised in 1% SDS (w/v), and incubated (10 min, RT). Monolayers with THY-G (and no GAS biofilm) doubled up as media sterility controls and blanks. Biofilm biomass quantification was performed by diluting the released dye 1:5 in the 1% SDS solution, and subsequently measured at OD_{540nm} using a SpectraMax Plus 384 microplate reader.

4.2.4.2. GAS biofilm cell viability

GAS biofilms were assessed for viability via enumeration of serially diluted biofilms. Briefly, biofilms were washed once in PBS and thoroughly re-suspended in fresh PBS. Viable cells were enumerated via 10-fold serially diluting in PBS, and spot plating onto THYA (incubated overnight, 34°C) for subsequent colony counting and CFU/mL determination.

4.2.4.3. GAS biofilm EPS

To assess biofilm EPS, the i) EPS-GAGs and ii) common EPS components (eDNA and protein) were examined. Briefly, EPS associated S-GAGs were quantified by 1,9-dimethyl methylene blue (DMMB) dye-based EPS assay. EPS components (eDNA and protein) were fluorescently stained with Sytox™ Blue, a cell membrane-impermeant nucleic acid stain and FilmTracer™ SYPRO® Ruby biofilm matrix stain that labels most classes of proteins.

4.2.4.4. Scanning electron microscopy

GAS biofilms were grown on untreated and exoglycosidase pre-treated fixed monolayers on 13 mm plastic Nunc Thermanox coverslips in a 12-well polystyrene plate. Biofilms were pre-fixed for 30 min (4°C), and further fixed for 1.5 h (4°C). Post-fixation of biofilms was conducted using 2% osmium tetroxide vapour (2 h). A graded ethanol series was then used, and samples were critical point dried. Dried samples were then sputter coated with platinum and visualised using a JEOL JSM-7500 microscope at 15 000 x magnification. Untreated and exoglycosidase pre-treated Detroit 562 pharyngeal monolayer controls (without biofilms) were also imaged at 5000 x magnification. Images were taken at random positions within the samples by an UOW Electron Microscopy Centre technician blinded from the study in an effort to reduce bias.

4.2.5. Statistical analysis

All statistical analysis was performed using GraphPad Prism. One-way ANOVA was performed with a Tukey's multiple comparisons post hoc test. A p-value of ≤ 0.05 was considered significant.

4.3. Results

4.3.1. Pattern A-C GAS M-types

4.3.1.1. Initial adherence, biofilm biomass, and bacterial colony forming units

M12 GAS is an *emm* pattern A-C family member (Bessen et al., 1989). Previously, M12 biofilm formation on exoglycosidase (α1-6 mannosidase, α1-2,3 mannosidase, and Sialidase A) pre-treated vs untreated Detroit 562 pharyngeal cell monolayers was investigated. Findings suggested M12 biofilm biomass significantly increased on α1-6 mannosidase and Sialidase A pre-treated surfaces. Whilst this increase in biofilm biomass was independent of initial planktonic M12 GAS adherence and bacterial colony forming units, EPS was found to likely be involved.

M1 and M3, are commonly associated with GAS pharyngitis and have been deemed major contributors to high global pharyngeal infection rates (Walker et al., 2014). Here, these two Pattern A-C GAS M-types have been assessed for biofilm formation to see if pattern classification correlates with changes in biofilm formation following the removal of mannose and sialic acid residues.

Investigation of the initial adherence of planktonic M1 and M3 GAS interacting with the exoglycosidase (α1-6 mannosidase, α1-2,3 mannosidase, and Sialidase A) pre-treated and control monolayers found no significant differences (Fig 4.3A). Despite this, the 72 h M1 and M3 GAS biofilms exhibited increased biomass on the exoglycosidase pre-treated monolayers compared to the untreated control (Fig 4.3B). Notably, for both M1 and M3 GAS biofilms formed on α1-2, 3 mannosidase, there was a significant increase ($p \leq 0.05$) in biofilm biomass. M1 also displayed a significant increase in biofilm biomass when grown on Sialidase A pre-treated monolayers. The number of colony forming units within the biofilms did not differ significantly between treatments (Fig 4.3C).

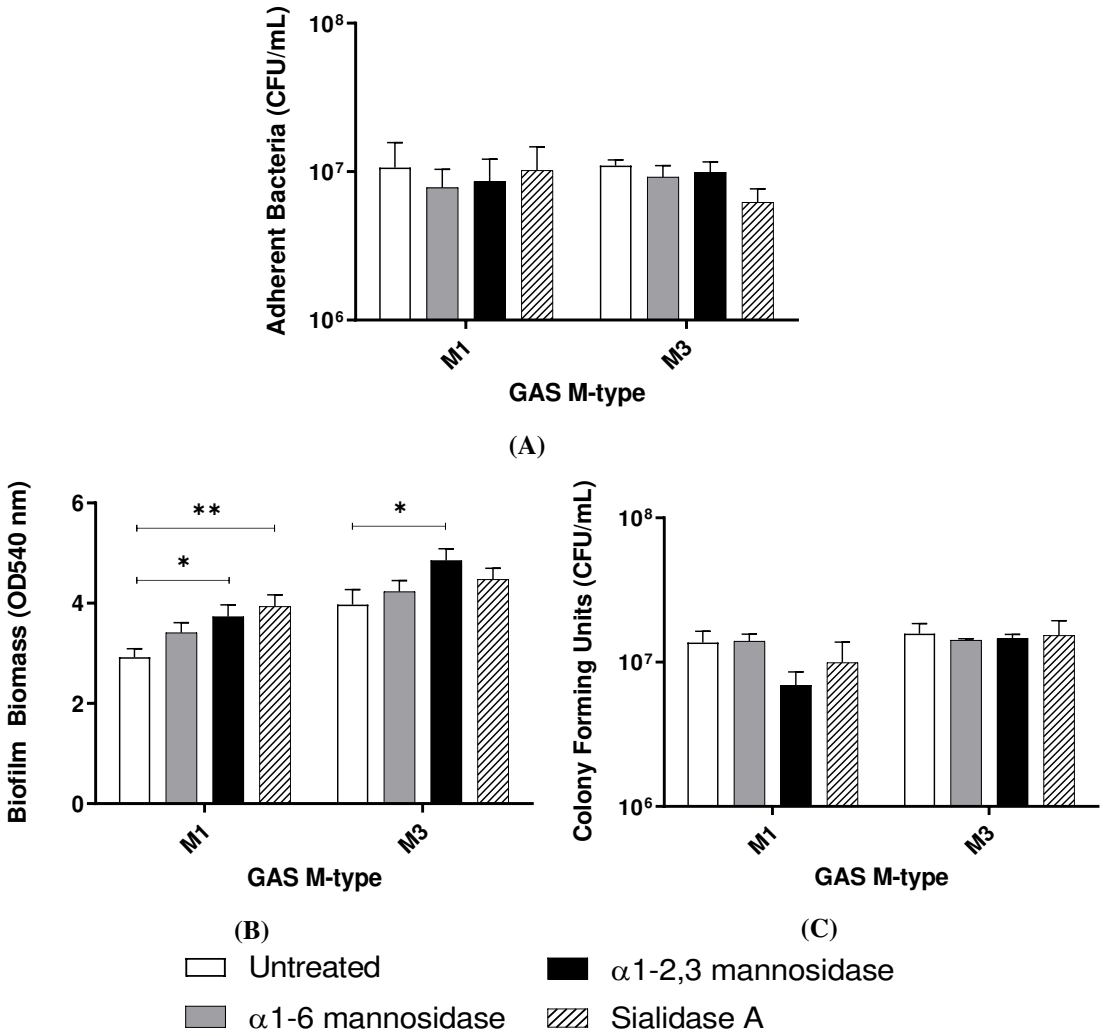

Figure 4.3. Pattern A-C GAS M-types M1 and M3 assessed for their biofilm formation on exoglycosidase pre-treated Detroit 562 monolayers. (**A**) Initial adherence enumerated for planktonic GAS following 2 h incubation. 72 h biofilms were assessed for (**B**) biofilm biomass via crystal violet staining and (**C**) colony forming units via enumeration. Data represents mean ± SEM, with statistical analysis performed using a one-way ANOVA with Tukey's multiple comparisons test * ($p \leq 0.05$) and ** ($p \leq 0.01$); n = 3 biological replicates, with 3 technical replicates each

4.3.1.2. Biofilm EPS

Biofilms are comprised of microbial cells and EPS. To further determine what may be contributing to the observed changes in biofilm biomass, EPS associated sulphated GAGs (S-GAGs), extracellular DNA (eDNA), and protein was assessed.

DMMB staining of EPS associated S-GAGs found no significant differences in EPS for M1 biofilms formed on any of the monolayers (Fig 4.4A). However, M3, was found to increase in EPS S-GAG content for biofilm formed on α1-6 mannosidase pre-treated monolayers (Fig 4.4A). As such, M3 EPS was further examined for eDNA and protein content via Sytox Blue and SYPRO ruby stains (Fig 4.4B). However, there were no

significant differences in the presence of EPS associated eDNA or protein in any of the M3 biofilms formed.

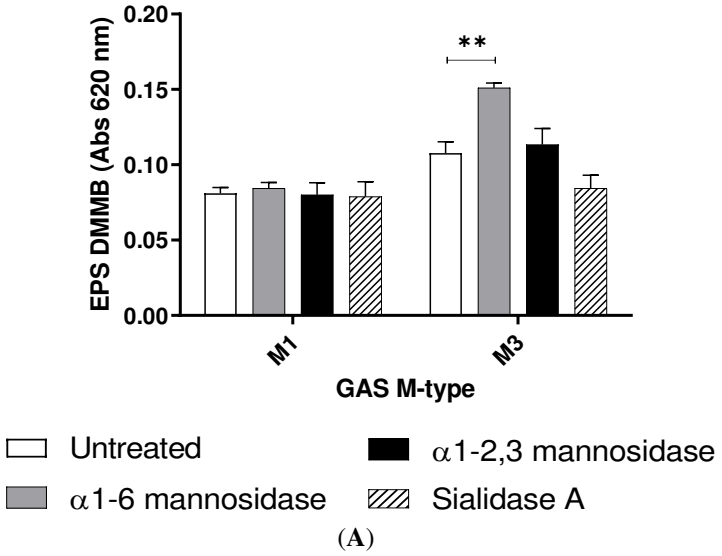

(**A**)

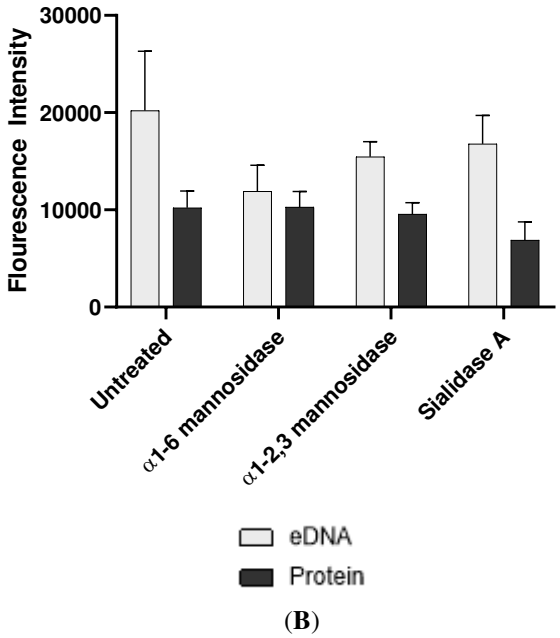

(**B**)

Figure 4.4. M3 has significantly increased EPS (S-GAGs) when biofilms were formed on α1-6 mannosidase pre-treated pharyngeal cell monolayers. M1 and M3 Biofilms were assessed for (**A**) EPS via DMMB staining of sulphated GAGs. (**B**) M3 biofilm EPS was further inspected for its EPS associated components (eDNA and protein) via fluorescent staining with Sytox™ Blue and FilmTracer™ SYPRO® Ruby biofilm matrix stain, respectively. Data represents mean ± SEM, with statistical analysis performed using a one-way ANOVA with Tukey's multiple comparisons test ** ($p \leq 0.01$); n = 3 biological replicates, with 3 technical replicates each.

4.3.1.3. Visualisation of M3 GAS biofilms

Given the significant increases in M3 EPS for biofilms formed on α1-6 mannosidase pre-treated monolayers, M3 biofilms formed on untreated and exoglycosidase pre-treated monolayers were further investigated via SEM imaging. M3 GAS biofilms formed on both untreated and exoglycosidase pre-treated monolayers show distinct, long cocci chains arranged into three dimensional aggregated structures with EPS matrix material present (Fig 4.5A, C, E, and G). Biofilms formed on each of the pharyngeal monolayers appear to produce EPS matrix material associated with the aggregated GAS cocci. However, no significant differences were visually apparent in the amount of EPS present among biofilms formed. Two varieties of EPS were found, the web-like mesh matrix (small black arrows) a more globular matrix (big black arrows). Both appeared to extend from the cocci cell surface of these biofilm cells. Untreated and exoglycosidase pre-treated Detroit 562 pharyngeal monolayers (without biofilms) were also imaged as controls to ensure that each exoglycosidase treatment did not affect pharyngeal cell morphology/structures (Fig 4.5B, D, F, and H).

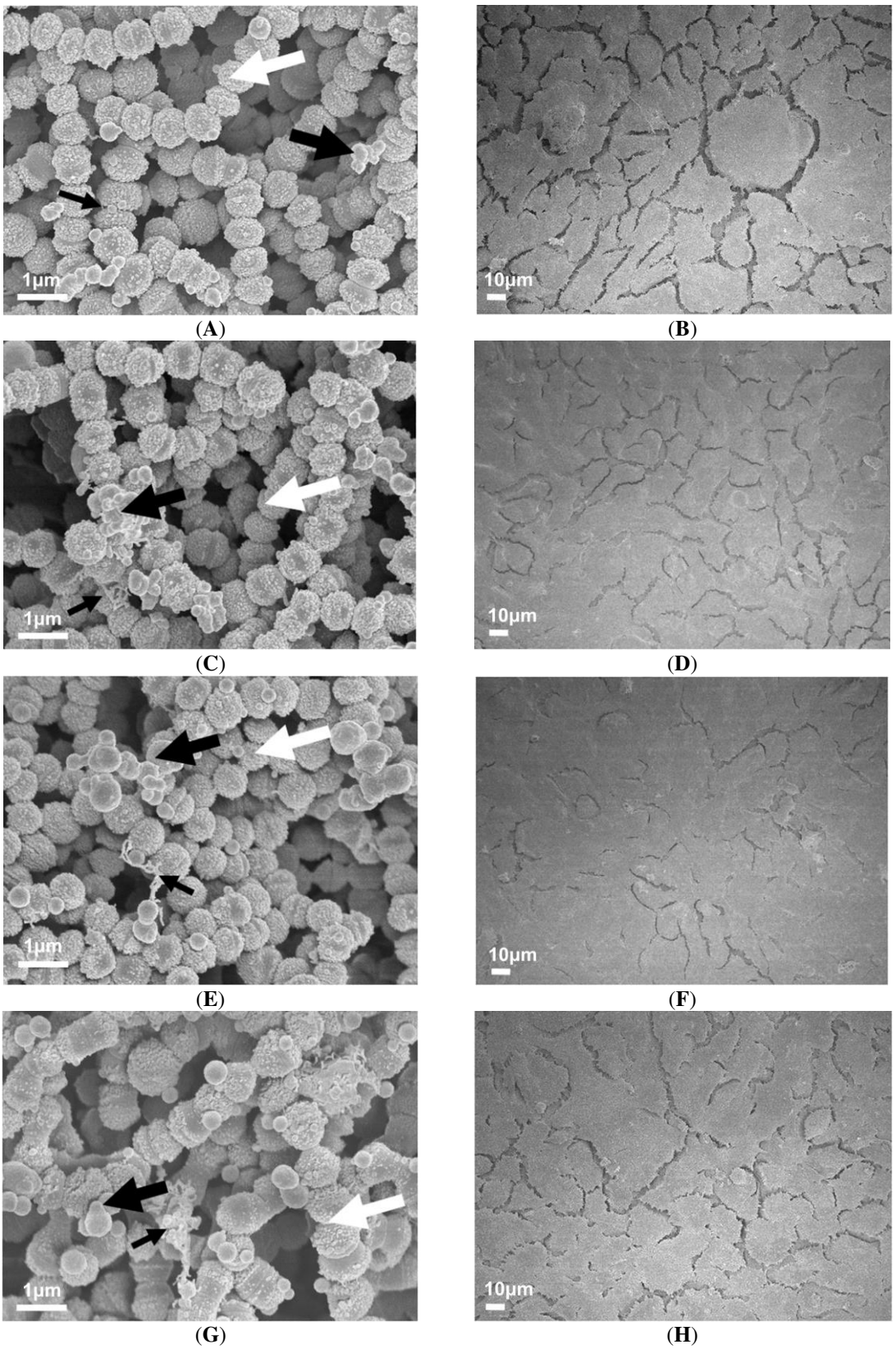

Figure 4.5. Visual inspection of 72 h M3 GAS biofilms captured via SEM reveals substantial EPS present in biofilms formed on exoglycosidase pre-treated pharyngeal cell monolayers. Images are representative of biofilms formed on (**A**) untreated, (**C**) α1-6 mannosidase, (**E**) α1-2,3 mannosidase, and (**G**) Sialidase A pre-treated pharyngeal monolayers. GAS biofilms show chained cocci (white arrows) arranged into three dimensional aggregated structures with EPS matrix material present (big and small black arrows). Biofilms were imaged using the JEOL JSM-7500 microscope at 15 000 x magnification. Respective Detroit 562 pharyngeal cell monolayer controls; (**B**) untreated, (**D**) α1-6 mannosidase, (**F**) α1-2,3 mannosidase, and (**H**) Sialidase A pre-treated were also imaged at 500 x magnification. SEM images were randomly selected and represent two biological replicates with two technical replicates each.

4.3.2. Pattern D GAS M-types

4.3.2.1. Initial adherence, biofilm biomass, and bacterial colony forming units

Pattern D strains of GAS are thought to have preference towards colonisation and infection of the skin (Bessen and Lizano, 2010). M53 is a known dermal isolate implicated in superficial skin diseases (Steer et al., 2009), whilst M98 and M108 are other pattern D GAS isolates (Sanderson-Smith et al., 2014), were also assessed for biofilm formation on the Detroit 562 pharyngeal cell monolayers.

Initial adherence of planktonic M53, 98, and 108 to Detroit 562 pharyngeal cell monolayers did not differ significantly between exoglycosidase (α1-6 mannosidase, α1-2,3 mannosidase, and Sialidase A) pre-treated and untreated monolayers (Fig 4.6A). Despite this, all three Pattern D GAS M-types formed biofilms with an increased biomass on the exoglycosidase pre-treated monolayers compared to the untreated control (Fig 4.6B). M98 biofilms formed on all three exoglycosidase (α1-6 mannosidase, α1-2,3 mannosidase, and Sialidase A) pre-treated monolayers displayed a significant increase ($p \leq 0.001$) in biofilm biomass compared to biofilm biomass found on untreated control. M108 displayed a significant increase in biofilm biomass when grown on α1-2,3 mannosidase pre-treated monolayers but not on α1-6 mannosidase and Sialidase A pre-treated monolayers. Despite increases in M53 biofilm biomass when grown on α1-6 mannosidase, α1-2,3 mannosidase, and Sialidase A pre-treated monolayers, these increases were not significant when compared to biofilm biomass formed on untreated control cells. The number of colony forming units for all biofilms formed found no significant differences between biofilms formed on exoglycosidase pre-treated (α1-6 mannosidase, α1-2,3 mannosidase, and Sialidase A) monolayers compared to colony forming units of biofilm formed on untreated control (Fig 4.6C).

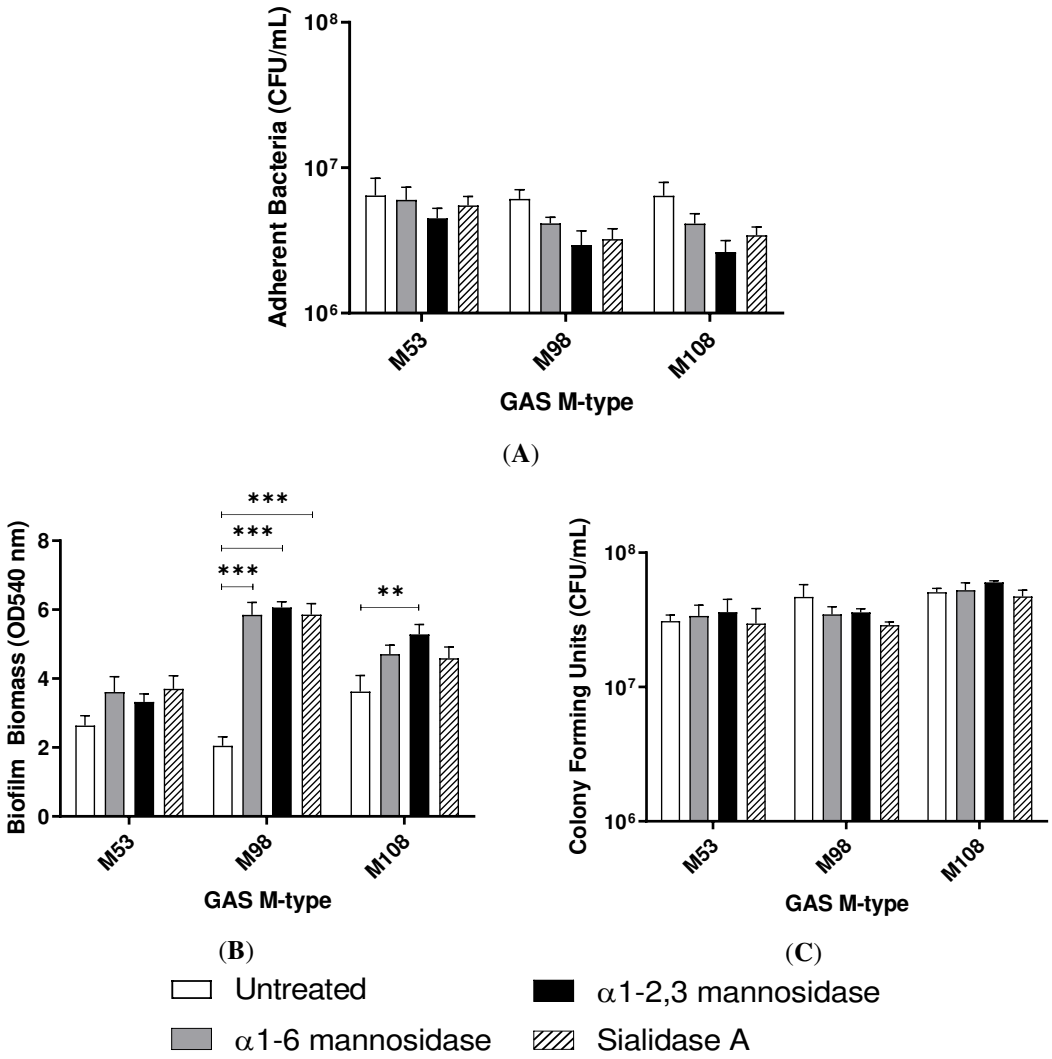

Figure 4.6. Pattern D GAS M-types M53, M98, and M108 assessed for their biofilm formation on exoglycosidase pre-treated Detroit 562 monolayers. (**A**) Initial adherence enumerated for planktonic GAS following 2 h incubation. 72 h biofilms were assessed for (**B**) biofilm biomass via crystal violet staining and (**C**) colony forming units via enumeration. Data represents mean ± SEM, with statistical analysis performed using a one-way ANOVA with Tukey's multiple comparisons test ** ($p \leq 0.01$) and *** ($p \leq 0.001$); n = 3 biological replicates, with 3 technical replicates each.

4.3.2.2. Biofilm EPS

DMMB staining of EPS associated S-GAGs found no significant differences in EPS for M53 or M108 biofilms formed on any of the exoglycosidase (α1-6 mannosidase, α1-2,3 mannosidase, and Sialidase A) pre-treated monolayers when compared to untreated control (Fig 4.7A). However, EPS S-GAGs were found to increase for M98 biofilm formed on α1-6 mannosidase pre-treated monolayers (Fig 4.7A). Hence, M98 EPS was further examined for eDNA and protein content via Sytox Blue and SYPRO ruby stains

(Fig 4.7B). However, there were no significant differences in the presence of EPS associated eDNA or protein in any of the M98 biofilms formed.

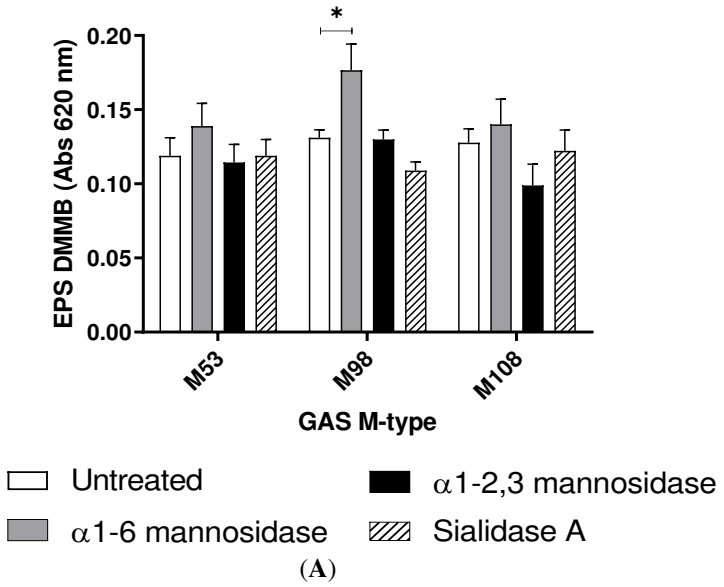

(**A**)

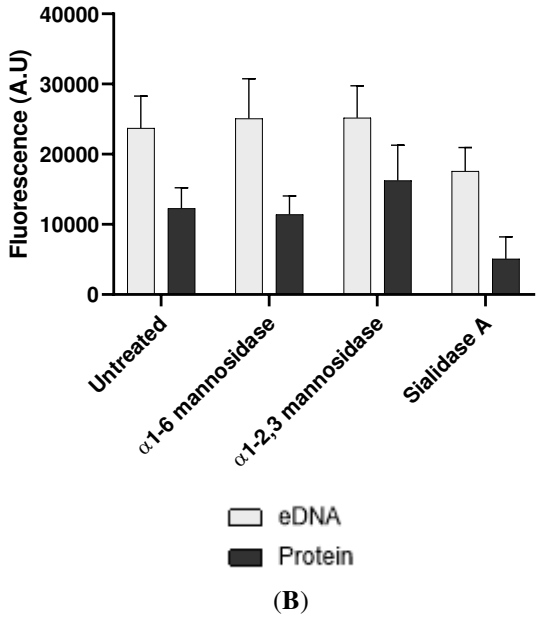

(**B**)

Figure 4.7. M98 has significantly increased EPS (S-GAGs) when biofilms were formed on α1-6 mannosidase pre-treated pharyngeal cell monolayers. M53, 98, and 108 biofilms were assessed for (**A**) EPS via DMMB staining of sulphated GAGs. (**B**) M98 biofilm EPS was further inspected for its EPS associated components (eDNA and protein) via fluorescent staining with Sytox™ Blue and FilmTracer™ SYPRO® Ruby biofilm matrix stain, respectively. Data represents mean ± SEM, with statistical analysis performed using a one-way ANOVA with Tukey's multiple comparisons test * ($p \leq 0.05$); n = 3 biological replicates, with 3 technical replicates each.

4.3.2.3. Visualisation of M98 GAS biofilms

M98 EPS was found to increase significantly for biofilms formed on α1-6 mannosidase pre-treated monolayers. Hence, M98 GAS biofilm formation on each of the exoglycosidase pre-treated and untreated monolayers were further visually inspected via SEM imaging. All M98 GAS biofilms were found have GAS cocci chains arranged into three dimensional aggregated structures with EPS matrix material present (Fig 4.8A, C, E, and G). Biofilms formed on each of the pharyngeal monolayers appear to produce EPS matrix material associated with the aggregated GAS cocci. However, no significant differences were visually apparent in the amount of EPS present among biofilms formed. Two varieties of EPS were found, the web-like mesh matrix (small black arrows) a more globular matrix (big black arrows) that extend from the cocci cell surface of these biofilm cells. Untreated and exoglycosidase pre-treated Detroit 562 pharyngeal monolayers (without biofilms) were also imaged as controls to ensure that each exoglycosidase treatment did not affect pharyngeal cell morphology/structures (Fig 4.8B, D, F, and H).

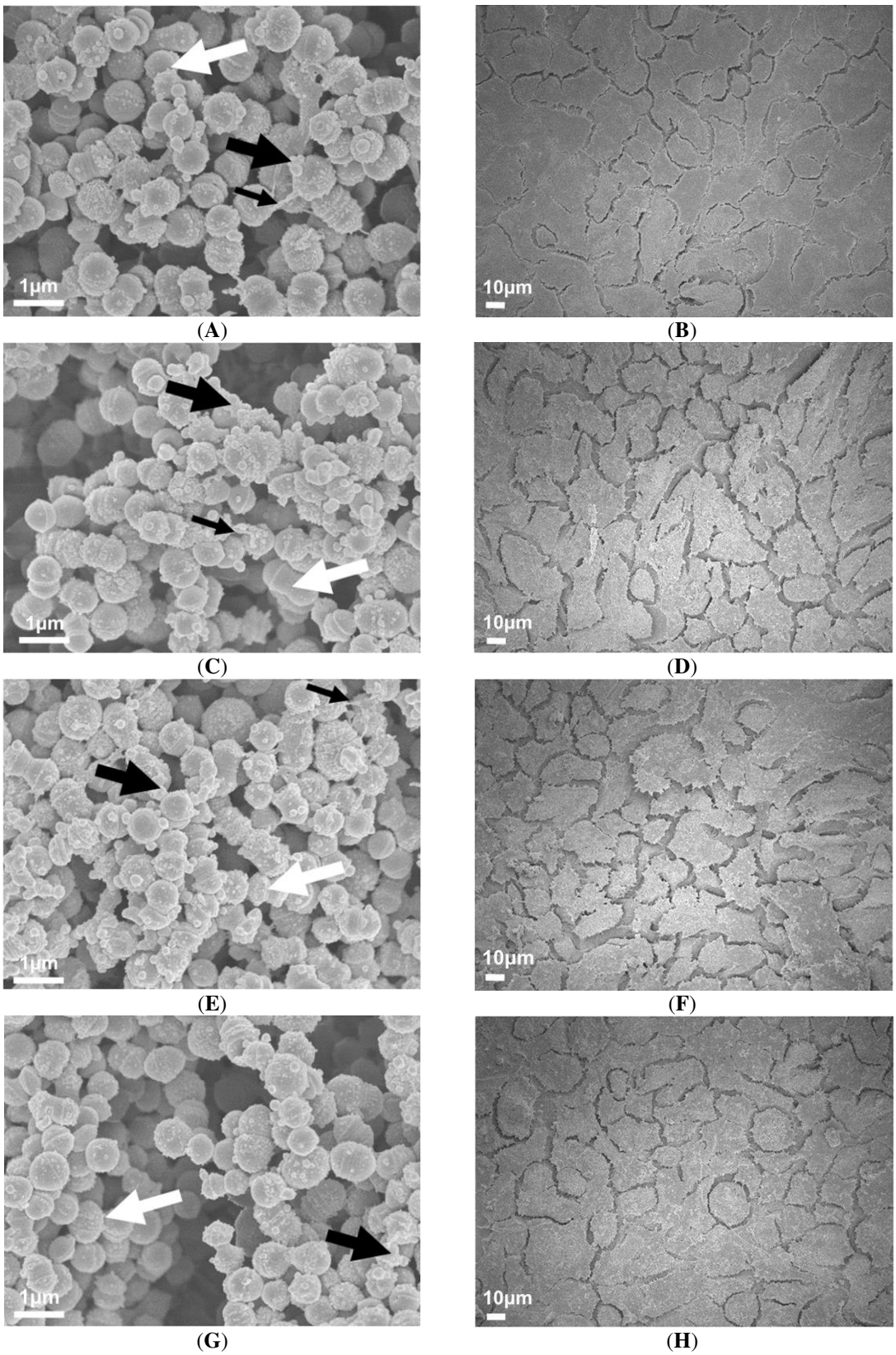

Figure 4.8. Visual inspection of 72 h M98 GAS biofilms captured via SEM reveals substantial EPS present in biofilms formed on exoglycosidase pre-treated pharyngeal cell monolayers. Images are representative of biofilms formed on (**A**) untreated, (**C**) α1-6 mannosidase, (**E**) α1-2,3 mannosidase, and (**G**) Sialidase A pre-treated pharyngeal monolayers. GAS biofilms show chained cocci (white arrows) arranged into three dimensional aggregated structures with EPS matrix material present (big and small black arrows). Biofilms were imaged using the JEOL JSM-7500 microscope at 15 000 x magnification. Respective Detroit 562 pharyngeal cell monolayer controls; (**B**) untreated, (**D**) α1-6 mannosidase, (**F**) α1-2,3 mannosidase, and (**H**) Sialidase A pre-treated were also imaged at 500 x magnification. SEM images were randomly selected and represent two biological replicates with two technical replicates each.

4.3.3. Pattern E GAS M-types

4.3.3.1. Initial adherence, biofilm biomass, and bacterial colony forming units

All three pattern E strains M9, 44, and 90 were assessed for initial adherence to the untreated and exoglycosidase (α1-6 mannosidase, α1-2,3 mannosidase, and Sialidase A) pre-treated monolayers. However, there were no significant differences in the ability of any of the assessed planktonic GAS M-types to adhere/interact with any of the exoglycosidase pre-treated monolayers when compared to untreated monolayers (Fig 4. 9A). Despite this, all three Pattern E GAS M-types formed biofilms with a significantly increased biomass on all three exoglycosidase (α1-6 mannosidase, α1-2,3 mannosidase, and Sialidase A) pre-treated monolayers compared to the untreated control (Fig 4.9B). Despite this, the number of colony forming units within the biofilms did not differ significantly between treatments (Fig 4.9C).

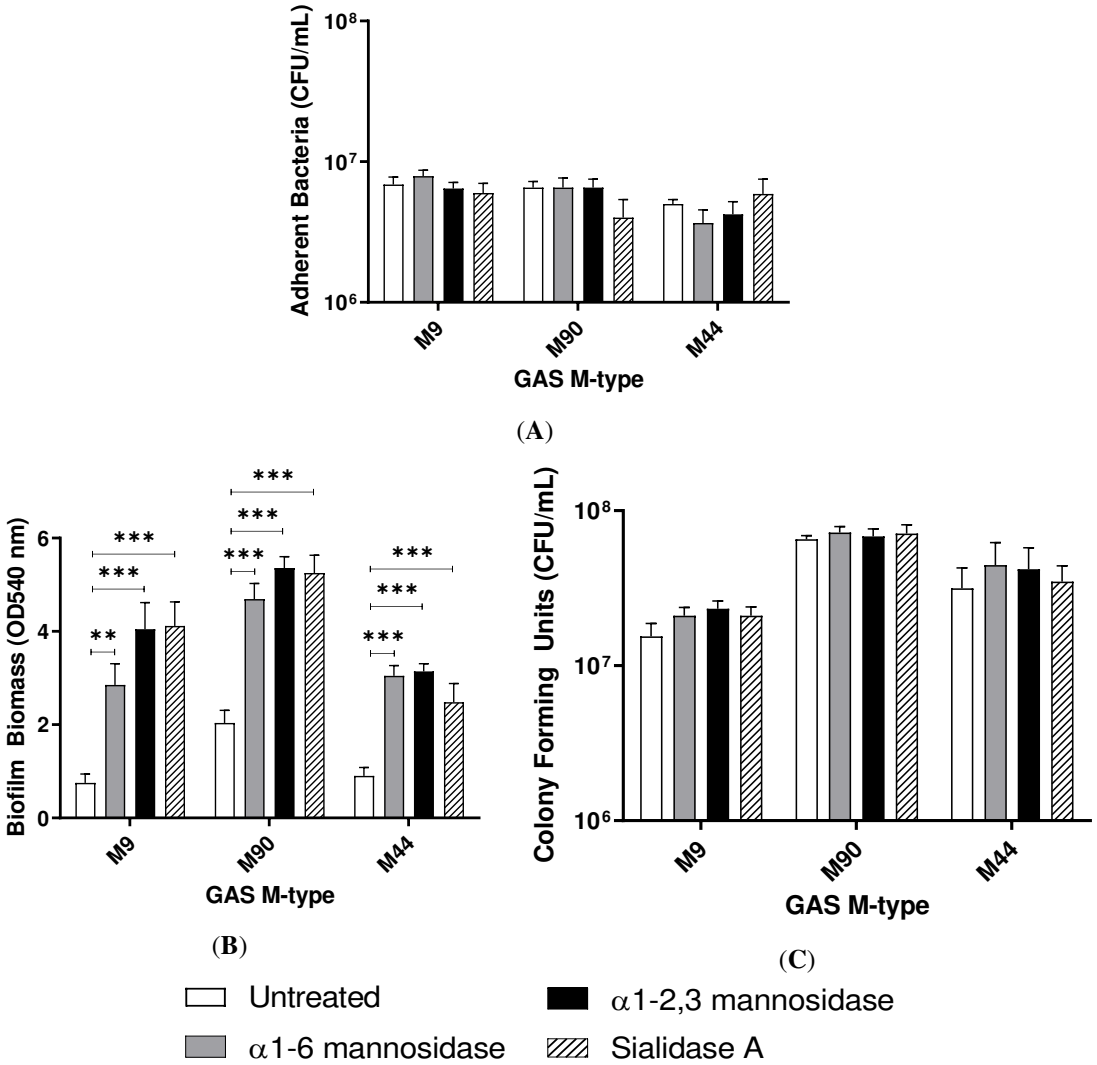

Figure 4.9. Pattern E GAS M-types M9, M44, and M90 assessed for their biofilm formation on exoglycosidase pre-treated Detroit 562 monolayers. (**A**) Initial adherence enumerated for planktonic GAS following 2 h incubation. 72 h biofilms were assessed for (**B**) biofilm biomass via crystal violet staining and (**C**) colony forming units via enumeration. Data represents mean ± SEM, with statistical analysis performed using a one-way ANOVA with Tukey's multiple comparisons test ** ($p \leq 0.01$) and *** ($p \leq 0.001$); n = 3 biological replicates, with 3 technical replicates each.

4.3.3.2. Biofilm EPS

DMMB staining of EPS associated S-GAGs found no significant differences in EPS for M9 or M44 biofilms formed on any of the exoglycosidase (α1-6 mannosidase, α1-2,3 mannosidase, and Sialidase A) pretreated monolayers when compared to untreated control (Fig 4.10A). However, M90, was found to increase in EPS S-GAG content for biofilm formed on α1-6 mannosidase pre-treated monolayers (Fig 4.10A). M90 EPS was further examined for eDNA and protein content via Sytox Blue and SYPRO ruby stains (Fig 4.10B). However, there were no significant differences in the presence of EPS

associated eDNA or protein in any of the M90 biofilms formed on exoglycosidase vs untreated monolayers. Interestingly, compared to other GAS M-types previously assessed, M90 appears to have considerably lesser EPS protein content compared to eDNA content.

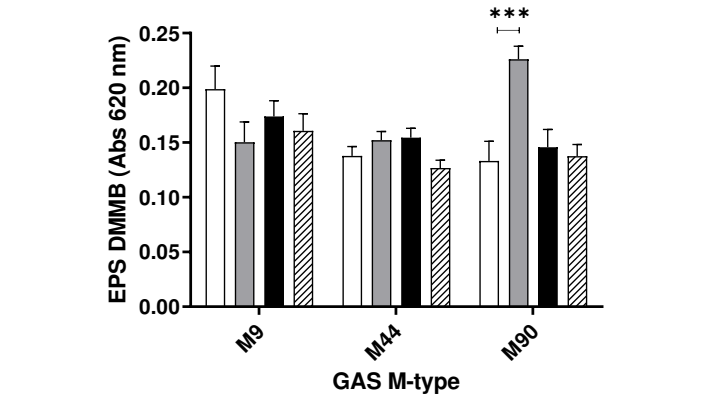

(**A**)

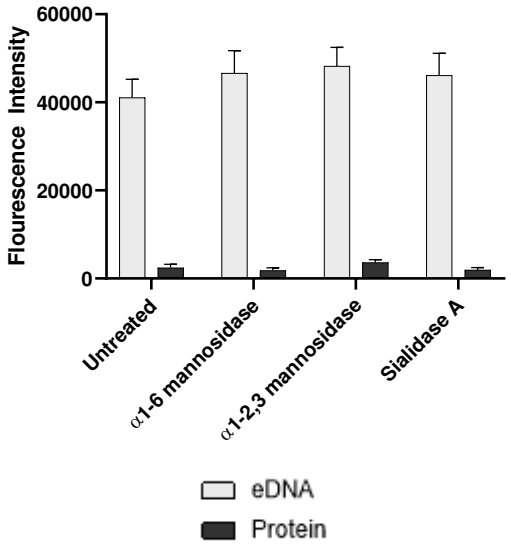

(**B**)

Figure 4.10. M90 has significantly increased EPS (S-GAGs) when biofilms were formed on α1-6 mannosidase pre-treated pharyngeal cell monolayers. M9, 44, and 90 biofilms were assessed for (**A**) EPS via DMMB staining of sulphated GAGs. (**B**) M90 biofilm EPS was further inspected for its EPS associated components (eDNA and protein) via fluorescent staining with Sytox™ Blue and FilmTracer™ SYPRO® Ruby biofilm matrix stain, respectively. Data represents mean ± SEM, with statistical analysis performed using a one-way ANOVA with Tukey's multiple comparisons test *** ($p \leq 0.001$); n = 3 biological replicates, with 3 technical replicates each.

4.3.3.3. Visualisation of M90 GAS biofilms

M90 EPS was found to increase significantly for biofilms formed on α1-6 mannosidase pre-treated monolayers. Hence, M90 GAS biofilm formation on each of the exoglycosidase pre-treated and untreated monolayers were further visually inspected via SEM imaging. Biofilms formed on both untreated and exoglycosidase pre-treated monolayers show M90 GAS cocci chains arranged into three dimensional aggregated structures with EPS matrix material present (Fig 4.11A, C, E, and G). M90 GAS biofilm formed on α1-6 mannosidase pre-treated pharyngeal monolayers (Fig 4.11C) appeared to produce more EPS matrix material associated with the aggregated GAS cocci when compared to GAS biofilm formed on the untreated control or the other exoglycosidase pre-treated monolayers. Two varieties of EPS were found, the web-like mesh matrix (small black arrows) and a more globular matrix (big black arrows) that both extend from the cocci cell surface of these biofilm cells. Untreated and exoglycosidase pre-treated Detroit 562 pharyngeal monolayers (without biofilms) were also imaged as controls to ensure that each exoglycosidase treatment did not affect pharyngeal cell morphology/structures (Fig 4.11B, D, F, and H).

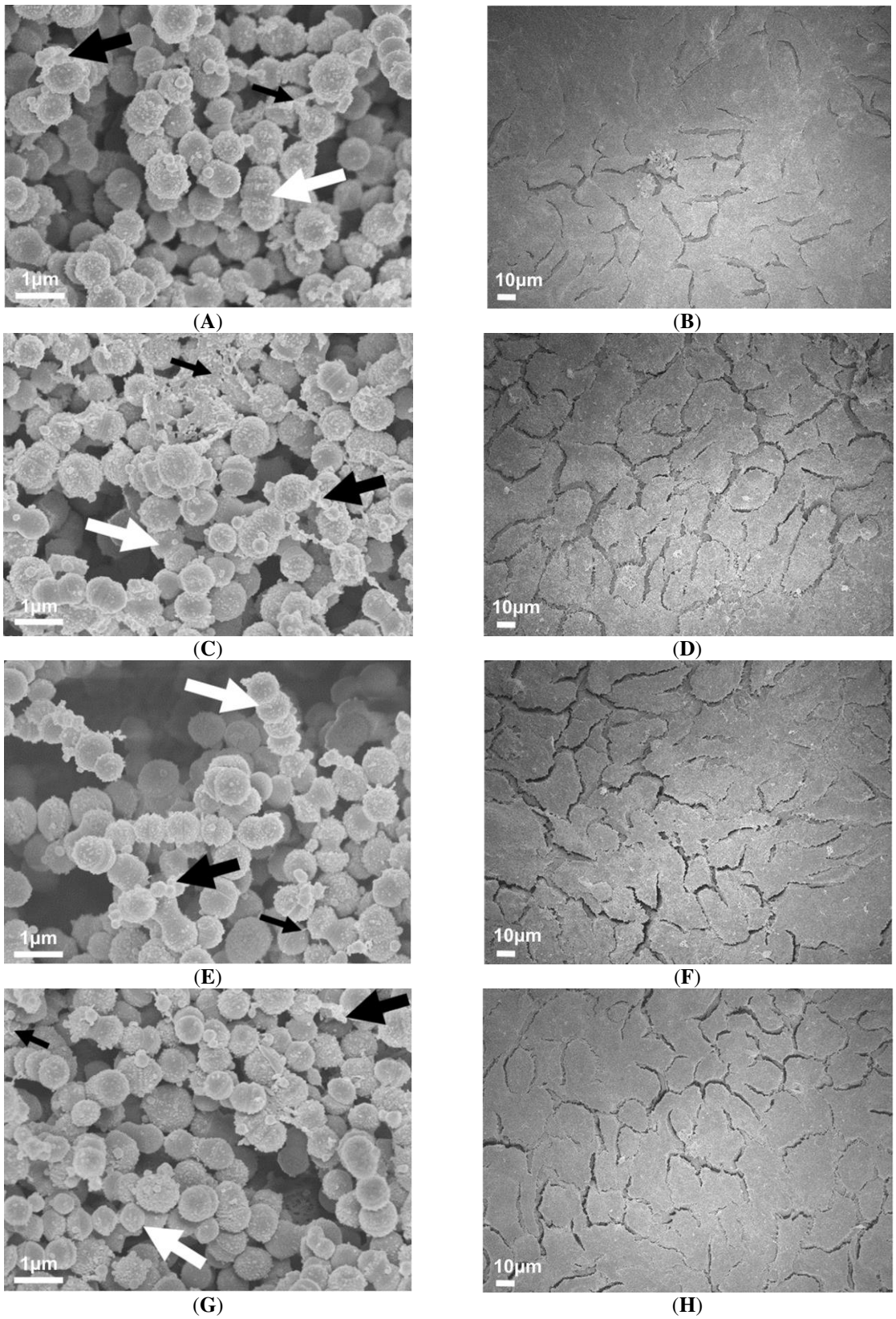

Figure 4.11. Visual inspection of 72 h M90 GAS biofilms captured via SEM reveals substantial EPS present in biofilms formed on exoglycosidase pre-treated pharyngeal cell monolayers. Images are representative of biofilms formed on (**A**) untreated, (**C**) α1-6 mannosidase, (**E**) α1-2,3 mannosidase, and (**G**) Sialidase A pre-treated pharyngeal monolayers. GAS biofilms show chained cocci (white arrows) arranged into three dimensional aggregated structures with EPS matrix material present (big and small black arrows). Biofilms were imaged using the JEOL JSM-7500 microscope at 15 000 x magnification. Respective Detroit 562 pharyngeal cell monolayer controls; (**B**) untreated, (**D**) α1-6 mannosidase, (**F**) α1-2,3 mannosidase, and (**H**) Sialidase A pre-treated were also imaged at 500 x magnification. SEM images were randomly selected and represent two biological replicates with two technical replicates each.

4.4. Discussion

The most common sites of GAS infection are the epithelia of the skin and throat, resulting in superficial infections such as pharyngitis and impetigo respectively. However, GAS can also cause several more serious invasive infections (e.g. bacteremia, sepsis, and necrotising fasciitis) and numerous autoimmune sequelae (e.g. rheumatic heart disease and acute post-streptococcal glomerulonephritis) (Walker et al., 2014). Collectively, these disease etiologies are responsible for an alarming global health burden. The global burden of GAS disease is further compounded by the reported antibiotic treatment failure rate and a lack of vaccine (Walker et al., 2014).

Within the last decade, the appreciation of the host glycome in mediating GAS adherence, colonisation, and its role in subsequent disease manifestation has gained interest. Previously, GAS M proteins of pattern A-C GAS M-types M1, 3, and 12 have been implicated in recognising ABO(H) histo-blood group antigens and Lewis structures found on HBE cells (De Oliveira et al., 2017, De Oliveira et al., 2019). However, this was in the context of planktonic GAS, and these studies only assessed three GAS serotypes – all belonging to the same *emm* pattern. Given the diversity of over 200+ circulating GAS *emm* types, and the growing appreciation of biofilm formation as an important GAS virulence mechanism (Baldassarri et al., 2006, Roberts et al., 2012, Marks et al., 2014, Walker et al., 2014, Vyas et al., 2019), there is an unmet need to increase our understanding of the interactions between GAS and host glycans. Specifically, assessment of GAS biofilm formation in response to pharyngeal cell surface glycans with a broad range of GAS strains representative of all *emm* patterns is warranted.

Previous research presented in this thesis showed that the removal of mannose and sialic acid glycan residues from the surface of Detroit 562 pharyngeal cell monolayers significantly enhanced M12 GAS biofilm formation via EPS production. To explore the impact of host glycan modification on GAS biofilm formation more broadly, an additional

eight GAS isolates were studied using similar methodology. To build upon this, GAS M-types were categorised by their *emm* patterns (pattern A-C, D, and E) to ascertain if there were any trends or correlation between GAS M-types belonging to distinct *emm* patterns and the biofilms formed in response to the de-glycosylated pharyngeal cell monolayers. Overall, the targeted removal of terminal mannose and sialic acid residues that predominate the surface of Detroit 562 pharyngeal cells resulted in increased biofilm biomass independent of initial adherence and biofilm CFU for all eight GAS M-types. This response was in a glycan- and strain-dependent manner and suggests that the influence the host glycome imparts on the GAS biofilm phenotype is not limited to a single strain or M-type. Biofilms of three M-types (M3, 98, and 90) which were all found to have increased EPS on α1-6 mannosidase pre-treated monolayers were further assessed, however, there were no differences in the eDNA and protein components between biofilms formed on untreated and exoglycosidase pre-treated monolayers. SEM imaging of biofilms formed on untreated and exoglycosidase pre-treated monolayers for all three M-types found GAS cocci chains arranged in aggregated three-dimensional structures. Two distinct varieties of EPS (web/thread-like and the globular form) were apparent, however, prevalence of each variety differed among the three M-types. In a study by Lembke et al. (2006), they described the thread-like EPS present only in M2 GAS biofilms, whereas the M18 GAS biofilm was completely absent of the thread-like EPS structures. Hence, it is likely that this EPS material may be produced at varying capacities in a strain dependent manner underscoring the subtle differences and variability among GAS strains. Future studies should consider additional CLSM imaging of these biofilms and their EPS matrix given some of the limitations presented by SEM. Particularly, the dehydration that occurs during SEM sample prep which impacts the EPS morphology as seen in the images presented here (crinkled/shrivelled structures),

especially given the otherwise highly hydrated nature of biofilms and their EPS (Williams and Bloebaum, 2010).

Although this study revealed that EPS production may be a contributing factor to the increased GAS biofilm biomass among some M-types, a notable limitation of this study was the use of a single EPS staining method. DMMB staining is used extensively for staining *S. aureus* biofilms which are relatively well characterised. The main constituent of *S. aureus* biofilm EPS has been identified as a poly-b-1,6-linked *N*-acetylglucosamine rich intracellular polysaccharide adhesin (PIA). DMMB detects S-GAGs which are structurally similar to PIAs, and hence this staining method is thought to confidently and directly ascertain the amount of EPS present in *S. aureus* biofilms (Pantanella et al., 2013). Unfortunately, GAS biofilm EPS remains poorly defined. Consequently, sole reliance on one EPS stain as a means to define total EPS may in fact underrepresent the amount of EPS detected among strains. Hence, future characterisation of GAS EPS should consider using a broader repertoire of stains/detection methods. For example, Concanavalin A coupled to a fluorophore which would enable the detection of a broader suite of polysaccharides, and may perhaps better capture total biofilm EPS (González-Machado et al., 2018).

In terms of categorising M-types by *emm* pattern to see if any trends or correlations were apparent, with the exception of pattern E GAS M-types (M9, 44, and 90), variances in biofilm formation in response to differentially exposed pharyngeal cell surface glycans were not *emm* pattern specific. As such, future studies should instead consider systematically exploring the various virulence factors that GAS possesses, and their role in mediating biofilm formation at the host-glycan interface. Firstly, the role of M protein and M family proteins (M-like and M-related protein) and their lectin like properties should be explored via knockouts of the M protein family genes; *emm* (encoding M protein), *mrp* (ecoding M-related protein), and *enn* (encoding M-like protein). This can

aid in further defining the functions of each of these distinct proteins in glycan dependent GAS biofilm formation. In addition to exploring M family proteins, the role of serum opacity factor (SOF) which is unique to pattern E M-types should be assessed. In this study, only pattern E GAS M-types were found to exhibit a pattern specific response, with significantly increased biofilm biomass in response to all three exoglycosidase pre-treated monolayers. Hence pattern E M-types should be examined in the context of SOF, an important surface exposed molecule of GAS (Courtney and Pownall, 2010). Since its discovery in 1938, SOF has been found to have several important roles, including involvement in GAS adhesion and subsequent colonisation of the tissues of the throat and skin giving them MSCRAMM (microbial surface component recognising adhesive matrix molecule) like properties (Courtney et al., 2002, Oehmcke et al., 2004, Courtney and Pownall, 2010). Moreover, SOF has previously been found to bind various host glycoproteins (fibronectin, fibrinogen, and fibulin-1) which are all important in bacterial adhesion (Oehmcke et al., 2004). As such, it is possible that SOF has enacted on the glycoproteins present on the Detroit 562 pharyngeal monolayer, potentiating biofilm formation among the pattern E M-types assessed. However, to date, the role SOF plays in GAS biofilm formation has not been investigated.

In addition to the above, other GAS virulence factors such as hyaluronic acid capsule should be investigated. Currently, the role of GAS capsule in biofilm formation remains to be thoroughly investigated, despite its importance as a virulence factor for GAS. It has been implicated as an important component in the adhesion and attachment of GAS to keratinocytes (Schrager et al., 1998). In terms of capsule involvement in biofilms, one study found that highly encapsulated GAS had a higher propensity to grow in an aggregated state (Cleary and Larkin, 1979). On the other hand, some studies have suggested that capsule impedes GAS adhesion/internalisation, with this inhibitory effect thought to arise from capsule masking GAS surface molecules required for interactions

with the host (Kawabata et al., 1999). As such, each of these strains should be assessed for the degree to which they are encapsulated via quantification of hyaluronic acid capsule biomass assays (Maamary et al., 2010). Encapsulation may be differentially mediating and facilitating biofilm formation between strains at each of the exoglycosidase pre-treated surfaces. This was particularly apparent for the M98 strain used in this study which is a *covS* mutant that is highly encapsulated (Maamary et al., 2010). It was the only pattern D GAS isolate exhibiting significant increases in biofilm biomass when grown on all three exoglycosidase pre-treated surfaces. Lastly, capsule is surface expressed, and composed of a polymer of glucuronic acid and *N*-acetylglucosamine (Stoolmiller and Dorfman, 1969), and perhaps there is some interplay between the interactions of these capsule-associated monosaccharides with those exposed on the pharyngeal cell surface upon exoglycosidase treatment. This is feasible given that GAS capsule can differentially bind to CD44, a transmembrane glycoprotein found on human keratinocytes, dependent on CD44 glycosylation profile (Skelton et al., 1998).

Other biofilm specific virulence mechanisms that trigger and prompt biofilm formation should also be assessed. One prominent avenue to explore is quorum sensing (QS). This cell-to-cell communication mechanism utilises signalling molecules to coordinate gene expression in response to a variety of stimuli/pressures/environmental conditions (Jimenez and Federle, 2014). As per other Gram-positive bacteria, GAS genomes contain several QS systems that mediate genetic exchange, competence, virulence factor secretion, and enhance biofilm formation (Jimenez and Federle, 2014, Aggarwal et al., 2015). Although some serotypes may possess only a subset of QS systems, regulator gene of glucosyltransferase 2/3 (Rgg2/3) QS system is ubiquitous among all GAS isolates (Gogos et al., 2018). One study by Chang et al. (2015) found that the Rgg2 coupled with neighbouring short hydrophobic peptide (SHP) genes (Rgg2-SHP QS system) are actively induced and dependent upon mannose when utilised as the carbon source by GAS. This

resulted in increased biofilm formation, which the authors suggested was necessary for successful colonisation and persistence within the host (Chang et al., 2015). This is plausible as transcriptomic studies have shown that gene expression needed for mannose uptake is triggered in GAS upon growth on various host soft tissues, saliva, and blood which are environments rich in mucins and glycoproteins containing mannose (Graham et al., 2005, Shelburne et al., 2005). Similarly, in the context of this work, liberation of terminal sialic acid or mannose upon exoglycosidase pre-treatment may reveal other mannose residues present on the glycoproteins that decorate the Detroit 562 pharyngeal cell surface. These in turn may be triggering this QS system resulting in increased biofilm biomass. Moreover, other non-glucose monosaccharides such as galactose which are present on glycans of the oropharynx (and on the Detroit 562 pharyngeal cells utilised in this study) have been noted to trigger QS systems among several streptococci (Gogos et al., 2018). Taken together, there is ample evidence to suggest that host glycans may directly impact GAS QS systems, which in turn shape and mediate GAS biofilm formation and should be the focus of further study.

Overall, the eight GAS *emm*-types assessed displayed increases in biofilm biomass in a strain- and glycan- dependent manner. These findings underscore the importance of the host glycomic landscape in mediating GAS biofilm formation. Further study is needed into characterising the GAS biofilms that form on the host surface. Such studies could lead to the development of novel therapeutic drugs and strategies that negate or hamper GAS biofilm formation in an attempt to improve antibiotic treatment success and patient outcomes.

Chapter 5: Conclusions and future directions

GAS is a human specific pathogen, and colonisation and subsequent biofilm formation is inextricably facilitated by distinct interactions with the human host and tissue surface. However, little is known about the role of GAS biofilms in pathogenesis. Although the contributions of previous *in vitro* plate-based studies have been valuable, most of these studies failed to mimic the host environment, with many studies utilising abiotic surfaces (plastic, glass, silicone etc). The GAS-pharyngeal cell model developed and optimised in this study supports and cultivates GAS biofilms of a variety of GAS M-types. Although M1 and M12 utilised in this study are heavily associated with GAS pharyngitis, utilising a broader variety of clinical GAS isolates derived directly from GAS pharyngitis/throat infections is encouraged.

The efficacious GAS-pharyngeal cell biofilm model developed herein supports long-term GAS biofilm formation, which more closely resemble those seen *in vivo* and is thus a far superior model. The development of this model has furthered, and will continue to, the field's understanding of GAS biofilm formation.

However, this model can be further built upon and optimised. Future studies should endeavor to better encapsulate the host environment. Specifically, the implementation of live epithelial substratum, as opposed to the fixed pharyngeal monolayers used here - as this is more physiologically relevant. There should also be consideration into the development of flow-based models with media supplemented with saliva given that the pharynx is a site of constant movement, with saliva flowing through the oropharynx (Sawair et al., 2009, Proctor et al., 2018). This is important because both flow/saliva can impact the physical/spatial structure (initial adherence and biofilm formation, arrangement, architecture) and the physiology and genetic expression of bacteria within these biofilms (Jin et al., 2004, Ahn et al., 2008, Inui et al., 2019). Thus, utilisation of a flow cell chamber model would be of significant benefit (Azeredo et al., 2017). Chamber

slides could be used to co-culture GAS biofilms atop pre-formed monolayers. On either side of the chamber slides there is inlet and outlet tubing which enables fresh media to flow through (e.g. THY supplemented with saliva) at distinct flow rates that mimic the salivary flow rate found at the pharynx.

GAS is a human specific pathogen which readily colonises the epithelia of the pharynx and skin (Bessen et al., 1996). Whilst this process is complex, dynamic, and multifaceted, glycans which are abundantly present on all host epithelial surfaces have recently gained attention as an important component mediating GAS pathogenesis (De Oliveira et al., 2017, De Oliveira et al., 2019). However, much remains to be understood of the glyco-interactions occurring at the host-GAS interface, with much of the prior research having only been conducted in the context of planktonic GAS.

The GAS-pharyngeal cell biofilm model developed here has further served to elucidate for the first time, the role of pharyngeal cell surface glycans in GAS biofilm formation among prominent GAS pharyngitis-associated M-types, as well as a diverse set of GAS M-types associated with a variety of GAS diseases. Removal of pharyngeal cell surface glycans increased biofilm biomass, independent of initial planktonic GAS adherence and the live cells of the biofilm determined upon culturing. With the findings indicating that EPS production was a likely contributor to the increased biofilm biomass, particularly for M12 GAS biofilms formed on pharyngeal monolayers removed of their terminal mannose and sialic acid residues.

However, much remains unknown of the GAS EPS, requiring further investigation. In the current study, the presence of eDNA and protein in the EPS was confirmed using selective staining. S-GAG polysaccharides of the EPS were also stained, however, overall polysaccharide content of the EPS of biofilms formed on untreated and exoglycosidase pre-treated monolayers is necessary. EPS-associated polysaccharide content should be especially considered given that polysaccharides are thought to make up a substantial

portion of a biofilms EPS (Flemming and Wingender, 2010, Karygianni et al., 2020). Assessment into EPS associated polysaccharide content can be done via staining with fluorescent stains such as concanavalin A conjugated to a fluorophore such as tetramethylrhodamine which will detect a broader variety of polysaccharides (González-Machado et al., 2018). Moreover, it would be interesting to profile and identify the secreted glycans present in the EPS of these GAS biofilms, given that high molecular weight polysaccharides have been thought to act as an important scaffold to which other EPS components (eDNA, protein, lipids etc) attach and interact with (Sutherland, 2001). One study found that the secreted monosaccharide composition of biofilm EPS of ESKAPE pathogens (*Enterococcus faecalis*, *S. aureus*, *Klebsiella pneumoniae*, *Acinetobacter baumannii*, *P. aeruginosa*, and *Enterobacter spp*.) were found to differ between species (Bales et al., 2013). The study found high total mannose content across all tested strains, with *P. aeruginosa* and *A. baumannii* total EPS secreted polysaccharide content comprised of 80-90% mannose. *E. coli* was found to have the least mannose (10%), and *K. pneumoniae* and *S. epidermidis* strains contained 40-50% mannose. Other sugars were also detected, with galactose and glucose present in all strains (Bales et al., 2013). Similarly, in the context of this thesis, the EPS secreted polysaccharide content of biofilms formed on untreated vs exoglycosidase pre-treated monolayers could be interrogated to survey for any commonalities and differences in polysaccharide content. This may reveal distinct abundances of monosaccharides being secreted into the EPS within each GAS M-type when grown on each of the exoglycosidase pre-treated surfaces. The mechanisms underpinning EPS production should also be evaluated to support our hypothesis that the witnessed biofilm biomass increases were indeed due to increased EPS production which was particularly evident in M12 GAS biofilms. This can be done by genomic sequencing of GAS strains to identify potential genes involved in EPS production. One study genomically screened a *P. aeruginosa* PAO1 strain, and found

three gene clusters (PA1381-1393, PA2231-2240, and PA3552-3558) were linked to EPS production (Matsukawa and Greenberg, 2004). Mutants were constructed with chromosomal insertions at PA1383, PA2231, and PA3552. PA2231 mutant showed a severe defect in biofilm formation as a direct result of reduced EPS production (Matsukawa and Greenberg, 2004). Similarly, identified GAS EPS genes can be knocked out, and EPS/consequent biofilm formation determined on untreated vs exoglycosidase pre-treated monolayers.

Finally, M12 GAS biofilms were assessed for penicillin tolerance. The GAS biofilms formed displayed significantly increased penicillin tolerance dependent on the host cell glycome. These findings describe the effect of host glycosylation on GAS biofilm formation, and GAS biofilm formation broadly as an important proponent in penicillin tolerance *in vitro*. Future studies should consider assessing the antibiotic tolerance profiles of these biofilms and the biofilms of the other M-types towards other antibiotics commonly prescribed for the treatment of GAS infection; ceftriaxone, cephalexin, clindamycin, erythromycin, and rifampin (Conley et al., 2003).

To explore the impact of host glycan modification on GAS biofilm formation more broadly, an additional eight GAS isolates were studied using similar methodology. To build upon this, GAS M-types were categorised by their *emm* patterns (pattern A-C, D, and E) to ascertain if there were any trends or correlation between GAS M-types belonging to distinct *emm* patterns and the biofilms formed in response to the de-glycosylated pharyngeal cell monolayers. Overall, the targeted removal of terminal mannose and sialic acid residues that predominate the surface of Detroit 562 pharyngeal cells resulted in increased biofilm biomass independent of initial adherence and biofilm CFU for all eight GAS M-types. This response was in a glycan- and strain-dependent manner and suggests that the influence the host glycome imparts on the GAS biofilm phenotype is not limited to a single strain or M-type. With the exception of pattern E GAS

M-types, variances in biofilm formation in response to differentially exposed pharyngeal cell surface glycans were not *emm* pattern specific. Future studies should generally consider looking at knockouts of M protein (and other M family proteins; M-related and M-like protein) and other virulence factors (e.g. serum opacity factor) to determine the precise role of these major surface expressed proteins in GAS biofilm formation at the pharyngeal cell glycan interface. Moreover, given the implication of other several important GAS virulence factors (e.g. capsule, pili, SpeB etc) in mediating GAS biofilm formation, these should also be assessed to see how these may also shape and drive GAS biofilms forming at the pharyngeal glycan interface.

In conclusion, an efficacious GAS-pharyngeal cell biofilm model that can support long-term biofilm formation has been developed, with biofilms formed resembling those seen *in vivo*. The model has been used to investigate for the first time, GAS biofilm formation upon the alteration of the Detroit 562 pharyngeal cell surface glycome. Here, it has been shown that modulation of the pharyngeal glycome has a direct impact on GAS biofilm formation, with increases in EPS likely to play an important role. Given the increasingly appreciated importance of glycans in the host-pathogen relationship and the abundance of glycosylated structures in the oropharynx, this work contributes to an improved understanding of the role of host glycans in the pathogenesis of GAS pharyngitis and antibiotic treatment failure and may contribute towards the development of novel therapeutics and antimicrobial treatment strategies.

References

ABBOT, E. L., SMITH, W. D., SIOU, G. P., CHIRIBOGA, C., SMITH, R. J., WILSON, J. A., HIRST, B. H. & KEHOE, M. A. 2007. Pili mediate specific adhesion of Streptococcus pyogenes to human tonsil and skin. *Cell Microbiol,* 9**,** 1822-33.

ABEE, T., KOVÁCS, Á. T., KUIPERS, O. P. & VAN DER VEEN, S. 2011. Biofilm formation and dispersal in Gram-positive bacteria. *Current Opinion in Biotechnology,* 22**,** 172-179.

AGGARWAL, C., JIMENEZ, J. C., LEE, H., CHLIPALA, G. E., RATIA, K. & FEDERLE, M. J. 2015. Identification of quorum-sensing inhibitors disrupting signaling between Rgg and short hydrophobic peptides in Streptococci. *MBio,* 6**,** e00393-15.

AGGARWAL, C., JIMENEZ, J. C., NANAVATI, D. & FEDERLE, M. J. 2014. Multiple Length Peptide-Pheromone Variants Produced by Streptococcus pyogenes Directly Bind Rgg Proteins to Confer Transcriptional Regulation. *The Journal of Biological Chemistry,* 289**,** 22427-22436.

AHN, S.-J., AHN, S.-J., WEN, Z. T., BRADY, L. J. & BURNE, R. A. 2008. Characteristics of Biofilm Formation by Streptococcus mutans in the Presence of Saliva. 76**,** 4259-4268.

AKIYAMA, H., MORIZANE, S., YAMASAKI, O., OONO, T. & IWATSUKI, K. 2003. Assessment of Streptococcus pyogenes microcolony formation in infected skin by confocal laser scanning microscopy. *Journal of Dermatological Science,* 32**,** 193-199.

AL-WRAFY, F., BRZOZOWSKA, E., GORSKA, S. & GAMIAN, A. 2017. Pathogenic factors of Pseudomonas aeruginosa - the role of biofilm in pathogenicity and as a target for phage therapy. *Postepy Hig Med Dosw (Online),* 71**,** 78-91.

APWEILER, R., HERMJAKOB, H. & SHARON, N. 1999. On the frequency of protein glycosylation, as deduced from analysis of the SWISS-PROT database11Dedicated to Prof. Akira Kobata and Prof. Harry Schachter on the occasion of their 65th birthdays. *Biochimica et Biophysica Acta (BBA) - General Subjects,* 1473**,** 4-8.

ASPHOLM, M., OLFAT, F. O., NORDÉN, J., SONDÉN, B., LUNDBERG, C., SJÖSTRÖM, R., ALTRAJA, S., ODENBREIT, S., HAAS, R., WADSTRÖM, T., ENGSTRAND, L., SEMINO-MORA, C., LIU, H., DUBOIS, A., TENEBERG, S., ARNQVIST, A. & BORÉN, T. 2006. SabA is the H. pylori hemagglutinin and is polymorphic in binding to sialylated glycans. *PLoS pathogens,* 2**,** e110-e110.

AZEREDO, J., AZEVEDO, N. F., BRIANDET, R., CERCA, N., COENYE, T., COSTA, A. R., DESVAUX, M., DI BONAVENTURA, G., HÉBRAUD, M., JAGLIC, Z., KAČÁNIOVÁ, M., KNØCHEL, S., LOURENÇO, A., MERGULHÃO, F., MEYER, R. L., NYCHAS, G., SIMÕES, M., TRESSE, O. & STERNBERG, C. 2017. Critical review on biofilm methods. *Critical Reviews in Microbiology,* 43**,** 313-351.

AZIZ, R. K., PABST, M. J., JENG, A., KANSAL, R., LOW, D. E., NIZET, V. & KOTB, M. 2004. Invasive M1T1 group A Streptococcus undergoes a phase-shift in vivo to prevent proteolytic degradation of multiple virulence factors by SpeB. *Mol Microbiol,* 51**,** 123-34.

BACHERT, B. A., CHOI, S. J., LASALA, P. R., HARPER, T. I., MCNITT, D. H., BOEHM, D. T., CASWELL, C. C., CIBOROWSKI, P., KEENE, D. R., FLORES, A. R., MUSSER, J. M., SQUEGLIA, F., MARASCO, D., BERISIO, R. & LUKOMSKI, S. 2016. Unique Footprint in the scl1.3 Locus Affects Adhesion and Biofilm Formation of the Invasive M3-Type Group A Streptococcus. *Front Cell Infect Microbiol,* 6**,** 90.

BALDASSARRI, L., CRETI, R., RECCHIA, S., IMPERI, M., FACINELLI, B., GIOVANETTI, E., PATARACCHIA, M., ALFARONE, G. & OREFICI, G. 2006. Therapeutic failures of antibiotics used to treat macrolide-susceptible Streptococcus pyogenes infections may be due to biofilm formation. *Journal of Clinical Microbiology,* 44**,** 2721-2727.

BALES, P. M., RENKE, E. M., MAY, S. L., SHEN, Y. & NELSON, D. C. 2013. Purification and Characterization of Biofilm-Associated EPS Exopolysaccharides from ESKAPE Organisms and Other Pathogens. *PLOS ONE,* 8**,** e67950.

BARRAUD, N., KARDAK, B. G., YEPURI, N. R., HOWLIN, R. P., WEBB, J. S., FAUST, S. N., KJELLEBERG, S., RICE, S. A. & KELSO, M. J. 2012. Cephalosporin-3′-diazeniumdiolates: Targeted NO-Donor Prodrugs for Dispersing Bacterial Biofilms. *Angewandte Chemie,* 124**,** 9191-9194.

BARTELT, M. A. & DUNCAN, J. L. 1978. Adherence of Group A Streptococci to Human Epithelial Cells. *Infect Immun,* 20**,** 200-208.

BARTHELSON, R., MOBASSERI, A., ZOPF, D. & SIMON, P. 1998. Adherence of Streptococcus pneumoniae to respiratory epithelial cells is inhibited by sialylated oligosaccharides. *Infection and immunity,* 66**,** 1439-1444.

BECHERELLI, M., MANETTI, A. G., BUCCATO, S., VICIANI, E., CIUCCHI, L., MOLLICA, G., GRANDI, G. & MARGARIT, I. 2012. The ancillary protein 1 of Streptococcus pyogenes FCT-1

pili mediates cell adhesion and biofilm formation through heterophilic as well as homophilic interactions. *Mol Microbiol,* 83**,** 1035-47.

BEEMA SHAFREEN, R. M., SELVARAJ, C., SINGH, S. K. & KARUTHA PANDIAN, S. 2014. In silico and in vitro studies of cinnamaldehyde and their derivatives against LuxS in Streptococcus pyogenes: effects on biofilm and virulence genes. *J Mol Recognit,* 27**,** 106-16.

BELICKÝ, Š., KATRLÍK, J. & TKÁČ, J. 2016. Glycan and lectin biosensors. *Essays in Biochemistry,* 60**,** 37-47.

BELOTSERKOVSKY, I., BARUCH, M., PEER, A., DOV, E., RAVINS, M., MISHALIAN, I., PERSKY, M., SMITH, Y. & HANSKI, E. 2009. Functional analysis of the quorum-sensing streptococcal invasion locus (sil). *PLoS Pathog,* 5**,** e1000651.

BERGEY, E. J. & STINSON, M. W. 1988. Heparin-inhibitable basement membrane-binding protein of Streptococcus pyogenes. *Infection and immunity,* 56**,** 1715-1721.

BESSEN, D., JONES, K. F. & FISCHETTI, V. A. 1989. Evidence for two distinct classes of streptococcal M protein and their relationship to rheumatic fever. *The Journal of experimental medicine,* 169**,** 269-283.

BESSEN, D. E. 2016. Tissue tropisms in group A Streptococcus: what virulence factors distinguish pharyngitis from impetigo strains? *Current opinion in infectious diseases,* 29**,** 295-303.

BESSEN, D. E. & LIZANO, S. 2010. Tissue tropisms in group A streptococcal infections. *Future microbiology,* 5**,** 623-638.

BESSEN, D. E., SOTIR, C. M., READDY, T. L. & HOLLINGSHEAD, S. K. 1996. Genetic correlates of throat and skin isolates of group A streptococci. *J Infect Dis,* 173**,** 896-900.

BJARNSHOLT, T., KIRKETERP-MØLLER, K., JENSEN, P. Ø., MADSEN, K. G., PHIPPS, R., KROGFELT, K., HØIBY, N. & GIVSKOV, M. 2008. Why chronic wounds will not heal: a novel hypothesis. *Wound Repair and Regeneration,* 16**,** 2-10.

BOUCHET, V., HOOD, D. W., LI, J., BRISSON, J.-R., RANDLE, G. A., MARTIN, A., LI, Z., GOLDSTEIN, R., SCHWEDA, E. K. & PELTON, S. I. J. P. O. T. N. A. O. S. 2003. Host-derived sialic acid is incorporated into Haemophilus influenzae lipopolysaccharide and is a major virulence factor in experimental otitis media. 100**,** 8898-8903.

BROUWER, S., BARNETT, T. C., RIVERA-HERNANDEZ, T., ROHDE, M. & WALKER, M. J. 2016. Streptococcus pyogenes adhesion and colonization. *FEBS Letters,* 590**,** 3739-3757.

BROWN, M. L., ALDRICH, H. C. & GAUTHIER, J. J. 1995. Relationship between glycocalyx and povidone-iodine resistance in Pseudomonas aeruginosa (ATCC 27853) biofilms. *Appl Environ Microbiol,* 61**,** 187-193.

BURMØLLE, M., WEBB, J. S., RAO, D., HANSEN, L. H., SØRENSEN, S. J. & KJELLEBERG, S. 2006. Enhanced biofilm formation and increased resistance to antimicrobial agents and bacterial invasion are caused by synergistic interactions in multispecies biofilms. *Applied and environmental microbiology,* 72**,** 3916-3923.

CAIAZZA, N. C., MERRITT, J. H., BROTHERS, K. M. & O'TOOLE, G. A. 2007. Inverse regulation of biofilm formation and swarming motility by Pseudomonas aeruginosa PA14. *J Bacteriol,* 189**,** 3603-3612.

CAPARON, M. G., STEPHENS, D. S., OLSÉN, A. & SCOTT, J. R. 1991. Role of M protein in adherence of group A streptococci. *Infect Immun,* 59**,** 1811-1817.

CARAPETIS, J. R., STEER, A. C., MULHOLLAND, E. K. & WEBER, M. 2005. The global burden of group A streptococcal diseases. *The Lancet infectious diseases,* 5**,** 685-694.

CERI, H., OLSON, M., STREMICK, C., READ, R., MORCK, D. & BURET, A. 1999. The Calgary Biofilm Device: new technology for rapid determination of antibiotic susceptibilities of bacterial biofilms. *Journal of clinical microbiology,* 37**,** 1771-1776.

CERONI, A., MAASS, K., GEYER, H., GEYER, R., DELL, A. & HASLAM, S. M. 2008. GlycoWorkbench: A Tool for the Computer-Assisted Annotation of Mass Spectra of Glycans. *Journal of Proteome Research,* 7**,** 1650-1659.

CHANG, J. C., JIMENEZ, J. C. & FEDERLE, M. J. 2015. Induction of a quorum sensing pathway by environmental signals enhances group A streptococcal resistance to lysozyme. 97**,** 1097-1113.

CHANG, J. C., LASARRE, B., JIMENEZ, J. C., AGGARWAL, C. & FEDERLE, M. J. 2011. Two group A streptococcal peptide pheromones act through opposing Rgg regulators to control biofilm development. *PLoS Pathog,* 7**,** e1002190.

CHO, K. H. & CAPARON, M. G. 2005. Patterns of virulence gene expression differ between biofilm and tissue communities of Streptococcus pyogenes. *Mol Microbiol,* 57**,** 1545-56.

CHRISTENSEN, G. D., SIMPSON, W., YOUNGER, J., BADDOUR, L., BARRETT, F., MELTON, D. & BEACHEY, E. 1985. Adherence of coagulase-negative staphylococci to plastic tissue culture plates: a quantitative model for the adherence of staphylococci to medical devices. *Journal of clinical microbiology,* 22**,** 996-1006.

CHRISTIANSEN, M. N., CHIK, J., LEE, L., ANUGRAHAM, M., ABRAHAMS, J. L. & PACKER, N. H. 2014. Cell surface protein glycosylation in cancer. 14**,** 525-546.

ÇIFTÇI, E., DOGRU, U., GURIZ, H., AYSEV, A. D. & İNCE, E. 2003. Antibiotic susceptibility of Streptococcus pyogenes strains isolated from throat cultures of children with tonsillopharyngitis. *J Ank Med School,* 25**,** 15-20.

CLEARY, P. P. & LARKIN, A. J. J. O. B. 1979. Hyaluronic acid capsule: strategy for oxygen resistance in group A streptococci. 140**,** 1090-1097.

COLLIN, M. & OLSÉN, A. 2001. EndoS, a novel secreted protein from Streptococcus pyogenes with endoglycosidase activity on human IgG. *The EMBO journal,* 20**,** 3046-3055.

CONLEY, J., OLSON, M. E., COOK, L. S., CERI, H., PHAN, V. & DELE DAVIES, H. 2003. Biofilm Formation by Group A Streptococci: Is There a Relationship with Treatment Failure? *Journal of Clinical Microbiology,* 41**,** 4043-4048.

COOK, L. C., LASARRE, B. & FEDERLE, M. J. 2013. Interspecies communication among commensal and pathogenic streptococci. *MBio,* 4.

COSTERTON, J., STEWART, P. & GREENBERG, E. 1999. Bacterial biofilms: a common cause of persistent infections. *Science,* 284**,** 1318 - 1322.

COSTERTON, J. W., LEWANDOWSKI, Z., CALDWELL, D. E., KORBER, D. R. & LAPPIN-SCOTT, H. M. 1995. Microbial biofilms. *Annual Reviews in Microbiology,* 49**,** 711-745.

COURTNEY, H. S., HASTY, D. L. & DALE, J. B. J. A. O. M. 2002. Molecular mechanisms of adhesion, colonization, and invasion of group A streptococci. 34**,** 77-87.

COURTNEY, H. S., OFEK, I., PENFOUND, T., NIZET, V., PENCE, M. A., KREIKEMEYER, B., PODBIELBSKI, A., HASTY, D. L. & DALE, J. B. 2009. Relationship between Expression of the Family of M Proteins and Lipoteichoic Acid to Hydrophobicity and Biofilm Formation in Streptococcus pyogenes. *PLoS ONE,* 4**,** e4166.

COURTNEY, H. S. & POWNALL, H. J. 2010. The Structure and Function of Serum Opacity Factor: A Unique Streptococcal Virulence Determinant That Targets High-Density Lipoproteins. *Journal of Biomedicine and Biotechnology,* 2010**,** 956071.

COWAN, T. 2010. Biofilms and their management: implications for the future of wound care. *J Wound Care,* 19**,** 117-120.

COWAN, T. 2011. Biofilms and their management: from concept to clinical reality. *Journal of Wound Care,* 20**,** 220.

CROSS, B. W. & RUHL, S. 2018. Glycan recognition at the saliva – oral microbiome interface. *Cellular Immunology,* 333**,** 19-33.

CROTTY ALEXANDER, L. E., MAISEY, H. C., TIMMER, A. M., ROOIJAKKERS, S. H., GALLO, R. L., KÖCKRITZ-BLICKWEDE, M. & NIZET, V. 2010. M1T1 group A streptococcal pili promote epithelial colonization but diminish systemic virulence through neutrophil extracellular entrapment. *J Mol Med,* 88.

CUNNINGHAM, M. W. 2000. Pathogenesis of Group A Streptococcal Infections. *Clinical Microbiology Reviews,* 13**,** 470-511.

CYWES, C., STAMENKOVIC, I. & WESSELS, M. R. 2000. CD44 as a receptor for colonization of the pharynx by group A Streptococcus. *J Clin Invest,* 106**,** 995-1002.

DANCHIN, M. H., ROGERS, S., KELPIE, L., SELVARAJ, G., CURTIS, N., CARLIN, J. B., NOLAN, T. M. & CARAPETIS, J. R. 2007. Burden of acute sore throat and group A streptococcal pharyngitis in school-aged children and their families in Australia. *Pediatrics,* 120**,** 950-7.

DAVIES, D. 2003. Understanding biofilm resistance to antibacterial agents. *Nat Rev Drug Discov,* 2**,** 114-22.

DE LA FUENTE-NÚÑEZ, C., REFFUVEILLE, F., FERNÁNDEZ, L. & HANCOCK, R. E. W. 2013. Bacterial biofilm development as a multicellular adaptation: antibiotic resistance and new therapeutic strategies. *Curr Opin Microbiol,* 16**,** 580-589.

DE OLIVEIRA, D. M., EVEREST-DASS, A., HARTLEY-TASSELL, L., DAY, C. J., INDRARATNA, A., BROUWER, S., CLEARY, A., KAUTTO, L., GORMAN, J., PACKER, N. H., JENNINGS, M. P., WALKER, M. J. & SANDERSON-SMITH, M. L. 2019. Human glycan expression patterns influence Group A streptococcal colonization of epithelial cells. 33**,** 10808-10818.

DE OLIVEIRA, D. M., HARTLEY-TASSELL, L., EVEREST-DASS, A., DAY, C. J., DABBS, R. A., VE, T., KOBE, B., NIZET, V., PACKER, N. H., WALKER, M. J., JENNINGS, M. P. & SANDERSON-SMITH, M. L. 2017. Blood Group Antigen Recognition via the Group A Streptococcal M Protein Mediates Host Colonization. *MBio,* 8.

DEWHIRST, F. E., CHEN, T., IZARD, J., PASTER, B. J., TANNER, A. C., YU, W. H., LAKSHMANAN, A. & WADE, W. G. 2010. The human oral microbiome. *J Bacteriol,* 192.

DOERN, C. D., HOLDER, R. C. & REID, S. D. 2008. Point mutations within the streptococcal regulator of virulence (Srv) alter protein–DNA interactions and Srv function. *Microbiol,* 154**,** 1998-2007.

DOERN, C. D., ROBERTS, A. L., HONG, W., NELSON, J., LUKOMSKI, S., SWORDS, W. E. & REID, S. D. 2009. Biofilm formation by group A Streptococcus: a role for the streptococcal regulator of virulence (Srv) and streptococcal cysteine protease (SpeB). *Microbiol,* 155.

DONLAN, R. & COSTERTON, J. 2002. Biofilms: survival mechanisms of clinically relevant microorganisms. *Clin Microbiol Rev,* 15**,** 167 - 193.

DONLAN, R. M. 2002. Biofilms: microbial life on surfaces. *Emerg Infect Dis,* 8.

EKELUND, K., DARENBERG, J., NORRBY-TEGLUND, A., HOFFMANN, S., BANG, D., SKINHØJ, P. & KONRADSEN, H. B. 2005. Variations in emm Type among Group A Streptococcal Isolates Causing Invasive or Noninvasive Infections in a Nationwide Study. 43**,** 3101-3109.

ELLEN, R. P. & GIBBONS, R. J. 1972. M protein-associated adherence of Streptococcus pyogenes to epithelial surfaces: prerequisite for virulence. *Infect Immun,* 5**,** 826-30.

EVEREST-DASS, A. V., ABRAHAMS, J. L., KOLARICH, D., PACKER, N. H. & CAMPBELL, M. P. 2013. Structural feature ions for distinguishing N- and O-linked glycan isomers by LC-ESI-IT MS/MS. *J Am Soc Mass Spectrom,* 24**,** 895-906.

EVEREST-DASS, A. V., JIN, D., THAYSEN-ANDERSEN, M., NEVALAINEN, H., KOLARICH, D. & PACKER, N. H. 2012. Comparative structural analysis of the glycosylation of salivary and buccal cell proteins: innate protection against infection by Candida albicans. *Glycobiology,* 22**,** 1465-1479.

EVEREST-DASS, A. V., KOLARICH, D., PASCOVICI, D. & PACKER, N. H. 2017. Blood group antigen expression is involved in C. albicans interaction with buccal epithelial cells. *Glycoconjugate Journal,* 34**,** 31-50.

FACINELLI, B., SPINACI, C., MAGI, G., GIOVANETTI, E. & VARALDO, P. E. 2001. Association between erythromycin resistance and ability to enter human respiratory cells in group A streptococci. *The Lancet,* 358**,** 30-33.

FALUGI, F., ZINGARETTI, C., PINTO, V., MARIANI, M., AMODEO, L., MANETTI, A. G. O., CAPO, S., MUSSER, J. M., OREFICI, G., MARGARIT, I., TELFORD, J. L., GRANDI, G. & MORA, M. 2008. Sequence Variation in Group A Streptococcus Pili and Association of Pilus Backbone Types with Lancefield T Serotypes. *J Infect Dis,* 198**,** 1834-1841.

FIEDLER, T., KÖLLER, T. & KREIKEMEYER, B. 2015. Streptococcus pyogenes biofilms—formation, biology, and clinical relevance. *Front Cell Infect Microbiol,* 5**,** 15.

FIEDLER, T., RIANI, C., KOCZAN, D., STANDAR, K., KREIKEMEYER, B. & PODBIELSKI, A. 2013. Protective Mechanisms of Respiratory Tract Streptococci against Streptococcus pyogenes Biofilm Formation and Epithelial Cell Infection. *J Appl Environ Microbiol,* 79**,** 1265-1276.

FLEMMING, H. C. & WINGENDER, J. 2010. The biofilm matrix. *Nat Rev Microbiol,* 8**,** 623-33.

FRICK, I. M., SCHMIDTCHEN, A. & SJOBRING, U. 2003. Interactions between M proteins of Streptococcus pyogenes and glycosaminoglycans promote bacterial adhesion to host cells. *Eur J Biochem,* 270**,** 2303-11.

GARBE, J., SJÖGREN, J., COSGRAVE, E. F. J., STRUWE, W. B., BOBER, M., OLIN, A. I., RUDD, P. M. & COLLIN, M. 2014. EndoE from Enterococcus faecalis Hydrolyzes the Glycans of the Biofilm Inhibiting Protein Lactoferrin and Mediates Growth. *PLOS ONE,* 9**,** e91035.

GJERMANSEN, M., RAGAS, P., STERNBERG, C., MOLIN, S. & TOLKER-NIELSEN, T. 2005. Characterization of starvation-induced dispersion in Pseudomonas putida biofilms. *Environmental Microbiology,* 7**,** 894-904.

GLOAG, E. S., TURNBULL, L., HUANG, A., VALLOTTON, P., WANG, H., NOLAN, L. M., MILILLI, L., HUNT, C., LU, J. & OSVATH, S. R. 2013. Self-organization of bacterial biofilms is facilitated by extracellular DNA. *Proc Natl Acad Sci,* 110**,** 11541-11546.

GOGOS, A., JIMENEZ, J. C., CHANG, J. C., WILKENING, R. V. & FEDERLE, M. J. 2018. A Quorum Sensing-Regulated Protein Binds Cell Wall Components and Enhances Lysozyme Resistance in Streptococcus pyogenes. *Journal of Bacteriology,* 200**,** e00701-17.

GONZÁLEZ-MACHADO, C., CAPITA, R., RIESCO-PELÁEZ, F. & ALONSO-CALLEJA, C. 2018. Visualization and quantification of the cellular and extracellular components of Salmonella Agona biofilms at different stages of development. *PLOS ONE,* 13**,** e0200011.

GRAHAM, M. R., VIRTANEVA, K., PORCELLA, S. F., BARRY, W. T., GOWEN, B. B., JOHNSON, C. R., WRIGHT, F. A. & MUSSER, J. M. J. T. A. J. O. P. 2005. Group A Streptococcus transcriptome dynamics during growth in human blood reveals bacterial adaptive and survival strategies. 166**,** 455-465.

GREWAL, P. K., UCHIYAMA, S., DITTO, D., VARKI, N., LE, D. T., NIZET, V. & MARTH, J. D. 2008. The Ashwell receptor mitigates the lethal coagulopathy of sepsis. *Nature medicine,* 14**,** 648-655.

HÅKANSSON, A., BENTLEY, C. C., SHAKHNOVIC, E. A. & WESSELS, M. R. 2005. Cytolysin-dependent evasion of lysosomal killing. *Proc Natl Acad Sci U S A* 102**,** 5192-5197.

HALL-STOODLEY, L., COSTERTON, J. W. & STOODLEY, P. 2004. Bacterial biofilms: from the natural environment to infectious diseases. *Nature Reviews Microbiology,* 2**,** 95-108.

HARVEY, D. J., ROYLE, L., RADCLIFFE, C. M., RUDD, P. M. & DWEK, R. A. 2008. Structural and quantitative analysis of N-linked glycans by matrix-assisted laser desorption ionization and negative ion nanospray mass spectrometry. *Anal Biochem,* 376**,** 44-60.

HELMERHORST, E. J. & OPPENHEIM, F. G. 2007. Saliva: a dynamic proteome. *J Dent Res,* 86**,** 680-93.

HENNINGHAM, A., YAMAGUCHI, M., AZIZ, R. K., KUIPERS, K., BUFFALO, C. Z., DAHESH, S., CHOUDHURY, B., VAN VLEET, J., YAMAGUCHI, Y., SEYMOUR, L. M., BEN ZAKOUR, N. L., HE, L., SMITH, H. V., GRIMWOOD, K., BEATSON, S. A., GHOSH, P., WALKER, M. J., NIZET, V. & COLE, J. N. 2014. Mutual Exclusivity of Hyaluronan and Hyaluronidase in Invasive Group A Streptococcus. *J Biol Chem,* 289**,** 32303-32315.

HØIBY, N., BJARNSHOLT, T., GIVSKOV, M., MOLIN, S. & CIOFU, O. 2010. Antibiotic resistance of bacterial biofilms. *International journal of antimicrobial agents,* 35**,** 322-332.

HOLLINGSHEAD, S. K., ARNOLD, J., READDY, T. L. & BESSEN, D. 1994. Molecular evolution of a multigene family in group A streptococci. *Molecular biology and evolution,* 11**,** 208-219.

HOLLINGSWORTH, M. A. & SWANSON, B. J. J. N. R. C. 2004. Mucins in cancer: protection and control of the cell surface. 4**,** 45-60.

INUI, T., PALMER, R. J., JR., SHAH, N., LI, W., CISAR, J. O. & WU, C. D. 2019. Effect of mechanically stimulated saliva on initial human dental biofilm formation. *Scientific reports,* 9**,** 11805-11805.

INUI, T., WALKER, L. C., DODDS, M. W. & HANLEY, A. B. 2015. Extracellular Glycoside Hydrolase Activities in the Human Oral Cavity. *Appl Environ Microbiol,* 81**,** 5471-6.

ISSA, S., MORAN, A. P., USTINOV, S. N., LIN, J. H.-H., LIGTENBERG, A. J. & KARLSSON, N. G. J. G. 2010. O-linked oligosaccharides from salivary agglutinin: Helicobacter pylori binding sialyl-Lewis x and Lewis b are terminating moieties on hyperfucosylated oligo-N-acetyllactosamine. 20**,** 1046-1057.

IYER, R. & CAMILLI, A. 2007. Sucrose metabolism contributes to in vivo fitness of Streptococcus pneumoniae. *Mol Microbiol,* 66**,** 1-13.

JENKINSON, H. F. & DEMUTH, D. R. 1997. Structure, function and immunogenicity of streptococcal antigen I/II polypeptides. *Mol Microbiol,* 23**,** 183-90.

JIMENEZ, J. C. & FEDERLE, M. J. 2014. Quorum sensing in group A Streptococcus. *Frontiers in Cellular and Infection Microbiology,* 4**,** 127.

JIN, Y., SAMARANAYAKE, L. P., SAMARANAYAKE, Y. & YIP, H. K. 2004. Biofilm formation of Candida albicans is variably affected by saliva and dietary sugars. *Archives of Oral Biology,* 49**,** 789-798.

JOHNSON, D. R., WOTTON, J. T., SHET, A. & KAPLAN, E. L. 2002. A Comparison of Group A Streptococci from Invasive and Uncomplicated Infections: Are Virulent Clones Responsible for Serious Streptococcal Infections? *The Journal of Infectious Diseases,* 185**,** 1586-1595.

KANIA, R. E., LAMERS, G. E., VONK, M. J., HUY, P. T., HIEMSTRA, P. S., BLOEMBERG, G. V. & GROTE, J. J. 2007. Demonstration of bacterial cells and glycocalyx in biofilms on human tonsils. *Arch Otolaryngol Head Neck Surg,* 133**,** 115-21.

KARYGIANNI, L., REN, Z., KOO, H. & THURNHEER, T. 2020. Biofilm Matrixome: Extracellular Components in Structured Microbial Communities. *Trends in Microbiology*.

KAWABATA, S., KUWATA, H., NAKAGAWA, I., MORIMATSU, S., SANO, K. & HAMADA, S. 1999. Capsular hyaluronic acid of group A streptococci hampers their invasion into human pharyngeal epithelial cells. *Microb Pathog,* 27**,** 71-80.

KIMURA, K. R., NAKATA, M., SUMITOMO, T., KREIKEMEYER, B., PODBIELSKI, A., TERAO, Y. & KAWABATA, S. 2012. Involvement of T6 pili in biofilm formation by serotype M6 Streptococcus pyogenes. *J Bacteriol,* 194**,** 804-812.

KING, S. J. 2010. Pneumococcal modification of host sugars: a major contributor to colonization of the human airway? 25**,** 15-24.

KÖLLER, T., MANETTI, A. G. O., KREIKEMEYER, B., LEMBKE, C., MARGARIT, I., GRANDI, G. & PODBIELSKI, A. 2010. Typing of the pilus-protein-encoding FCT region and biofilm formation as novel parameters in epidemiological investigations of Streptococcus pyogenes isolates from various infection sites. *J Med Microbiol,* 59**,** 442-452.

KOSTAKIOTI, M., HADJIFRANGISKOU, M. & HULTGREN, S. J. 2013. Bacterial biofilms: development, dispersal, and therapeutic strategies in the dawn of the postantibiotic era. *Cold Spring Harbor Perspectives in Medicine,* 3**,** a010306.

KRATOVAC, Z., MANOHARAN, A., LUO, F., LIZANO, S. & BESSEN, D. E. 2007. Population genetics and linkage analysis of loci within the FCT region of Streptococcus pyogenes. *J Bacteriol,* 189**,** 1299-1310.

KUHN, S. M., PREIKSAITIS, J., TYRRELL, G. J., JADAVJI, T., CHURCH, D. & DAVIES, H. D. 2001. Evaluation of Potential Factors Contributing to Microbiological Treatment Failure in Streptococcus Pyogenes Pharyngitis. *Canadian Journal of Infectious Diseases,* 12.

LEMBKE, C., PODBIELSKI, A., HIDALGO-GRASS, C., JONAS, L., HANSKI, E. & KREIKEMEYER, B. 2006. Characterization of biofilm formation by clinically relevant serotypes of group A streptococci. *Applied and environmental microbiology,* 72**,** 2864-2875.

LEWIS, A. L. & LEWIS, W. G. 2012. Host sialoglycans and bacterial sialidases: a mucosal perspective. *Cellular Microbiology,* 14**,** 1174-1182.

LEWIS, K. 2010. Persister cells. *Annual review of microbiology,* 64**,** 357-372.

LI, C., KURNIYATI, HU, B., BIAN, J., SUN, J., ZHANG, W., LIU, J., PAN, Y. & LI, C. 2012. Abrogation of neuraminidase reduces biofilm formation, capsule biosynthesis, and virulence of Porphyromonas gingivalis. *Infection and immunity,* 80**,** 3-13.

LUKOMSKI, S., NAKASHIMA, K., ABDI, I., CIPRIANO, V. J., IRELAND, R. M., REID, S. D., ADAMS, G. G. & MUSSER, J. M. 2000. Identification and characterization of the scl gene encoding a group A Streptococcus extracellular protein virulence factor with similarity to human collagen. *Infect Immun,* 68.

LYON, W. R., MADDEN, J. C., LEVIN, J. C., STEIN, J. L. & CAPARON, M. G. 2001. Mutation of luxS affects growth and virulence factor expression in Streptococcus pyogenes. *Mol Microbiol,* 42**,** 145-57.

MAAMARY, P. G., MAAMARY, P. G., SANDERSON-SMITH, M. L., AZIZ, R. K., HOLLANDS, A., COLE, J. N., MCKAY, F. C., MCARTHUR, J. D., KIRK, J. K., CORK, A. J., KEEFE, R. J., KANSAL, R. G., SUN, H., TAYLOR, W. L., CHHATWAL, G. S., GINSBURG, D., NIZET, V., KOTB, M. & WALKER, M. J. 2010. Parameters Governing Invasive Disease Propensity of Non-M1 Serotype Group A Streptococci. *Journal of Innate Immunity,* 2**,** 596-606.

MACLEAN, B., TOMAZELA, D. M., SHULMAN, N., CHAMBERS, M., FINNEY, G. L., FREWEN, B., KERN, R., TABB, D. L., LIEBLER, D. C. & MACCOSS, M. J. J. B. 2010. Skyline: an open source document editor for creating and analyzing targeted proteomics experiments. 26**,** 966-968.

MADDOCKS, S. E., WRIGHT, C. J., NOBBS, A. H., BRITTAN, J. L., FRANKLIN, L., STROMBERG, N., KADIOGLU, A., JEPSON, M. A. & JENKINSON, H. F. 2011. Streptococcus pyogenes antigen I/II-family polypeptide AspA shows differential ligand-binding properties and mediates biofilm formation. *Mol Microbiol,* 81.

MAGALHÃES, A. P., FRANÇA, Â., PEREIRA, M. O. & CERCA, N. 2019. RNA-based qPCR as a tool to quantify and to characterize dual-species biofilms. *Scientific Reports,* 9**,** 13639.

MANETTI, A. G., ZINGARETTI, C., FALUGI, F., CAPO, S., BOMBACI, M., BAGNOLI, F., GAMBELLINI, G., BENSI, G., MORA, M., EDWARDS, A. M., MUSSER, J. M., GRAVISS, E. A., TELFORD, J. L., GRANDI, G. & MARGARIT, I. 2007. Streptococcus pyogenes pili promote pharyngeal cell adhesion and biofilm formation. *Mol Microbiol,* 64**,** 968-83.

MANETTI, A. G. O., KÖLLER, T., BECHERELLI, M., BUCCATO, S., KREIKEMEYER, B., PODBIELSKI, A., GRANDI, G. & MARGARIT, I. 2010. Environmental Acidification Drives S. pyogenes Pilus Expression and Microcolony Formation on Epithelial Cells in a FCT-Dependent Manner. *PLOS ONE,* 5**,** e13864.

MARKS, L. R., MASHBURN-WARREN, L., FEDERLE, M. J. & HAKANSSON, A. P. 2014. Streptococcus pyogenes biofilm growth in vitro and in vivo and its role in colonization, virulence and genetic exchange. *Journal of Infectious Diseases***,** jiu058.

MARKS, L. R., PARAMESWARAN, G. I. & HAKANSSON, A. P. 2012. Pneumococcal interactions with epithelial cells are crucial for optimal biofilm formation and colonization in vitro and in vivo. *Infect Immun,* 80**,** 2744-60.

MAROUNI, M. J. & SELA, S. 2003. The luxS Gene of Streptococcus pyogenes Regulates Expression of Genes That Affect Internalization by Epithelial Cells. *Infection and Immunity,* 71**,** 5633-5639.

MATSUKAWA, M. & GREENBERG, E. P. 2004. Putative Exopolysaccharide Synthesis Genes Influence Pseudomonas aeruginosa Biofilm Development. 186**,** 4449-4456.

MATYSIK, A. & KLINE, K. A. 2019. Streptococcus pyogenes capsule promotes microcolony-independent biofilm formation. *Journal of Bacteriology***,** JB.00052-19.

MCDOUGALD, D., RICE, S. A., BARRAUD, N., STEINBERG, P. D. & KJELLEBERG, S. 2012. Should we stay or should we go: mechanisms and ecological consequences for biofilm dispersal. *Nat Rev Microbiol,* 10**,** 39-50.

MCGREGOR, K. F., SPRATT, B. G., KALIA, A., BENNETT, A., BILEK, N., BEALL, B. & BESSEN, D. E. J. J. O. B. 2004. Multilocus sequence typing of Streptococcus pyogenes representing most known emm types and distinctions among subpopulation genetic structures. 186**,** 4285-4294.

MCKAY, F. C., MCARTHUR, J. D., SANDERSON-SMITH, M. L., GARDAM, S., CURRIE, B. J., SRIPRAKASH, K. S., FAGAN, P. K., TOWERS, R. J., BATZLOFF, M. R., CHHATWAL, G. S., RANSON, M. & WALKER, M. J. 2004. Plasminogen binding by group A streptococcal isolates from a region of hyperendemicity for streptococcal skin infection and a high incidence of invasive infection. *Infection and immunity,* 72**,** 364-370.

MITCHELL, T. J. 2003. The pathogenesis of streptococcal infections: from Tooth decay to meningitis. *Nature Reviews Microbiology,* 1**,** 219-230.

NAKATA, M., KIMURA, K. R., SUMITOMO, T., WADA, S., SUGAUCHI, A., OIKI, E., HIGASHINO, M., KREIKEMEYER, B., PODBIELSKI, A., OKAHASHI, N., HAMADA, S., ISODA, R.,

TERAO, Y. & KAWABATA, S. 2011. Assembly mechanism of FCT region type 1 pili in serotype M6 Streptococcus pyogenes. *J Biol Chem,* 286**,** 37566-77.

NICKEL, J., RUSESKA, I., WRIGHT, J. & COSTERTON, J. 1985. Tobramycin resistance of Pseudomonas aeruginosa cells growing as a biofilm on urinary catheter material. *Antimicrob Agents Chemother,* 27**,** 619-624.

O'TOOLE, G. A. & KOLTER, R. 1998. Flagellar and twitching motility are necessary for Pseudomonas aeruginosa biofilm development. *Mol Microbiol,* 30**,** 295-304.

OEHMCKE, S., PODBIELSKI, A. & KREIKEMEYER, B. 2004. Function of the Fibronectin-Binding Serum Opacity Factor of Streptococcus pyogenes in Adherence to Epithelial Cells. *Infection and Immunity,* 72**,** 4302.

OGAWA, T., TERAO, Y., OKUNI, H., NINOMIYA, K., SAKATA, H., IKEBE, K., MAEDA, Y. & KAWABATA, S. 2011. Biofilm formation or internalization into epithelial cells enable Streptococcus pyogenes to evade antibiotic eradication in patients with pharyngitis. *Microbial Pathogenesis,* 51**,** 58-68.

OLIVA, B. & CHOPRA, I. 1992. Tet determinants provide poor protection against some tetracyclines: further evidence for division of tetracyclines into two classes. *Antimicrob Agents Chemother,* 36**,** 876-8.

OLIVER-KOZUP, H., MARTIN, K. H., SCHWEGLER-BERRY, D., GREEN, B. J., BETTS, C., SHINDE, A. V., VAN DE WATER, L. & LUKOMSKI, S. 2013. The group A streptococcal collagen-like protein-1, Scl1, mediates biofilm formation by targeting the extra domain A-containing variant of cellular fibronectin expressed in wounded tissue. *Mol Microbiol,* 87**,** 672-89.

OLIVER-KOZUP, H. A., ELLIOTT, M., BACHERT, B. A., MARTIN, K. H., REID, S. D., SCHWEGLER-BERRY, D. E., GREEN, B. J. & LUKOMSKI, S. 2011. The streptococcal collagen-like protein-1 (Scl1) is a significant determinant for biofilm formation by group A Streptococcus. *BMC Microbiol,* 11**,** 262.

OLSEN, I. 2020. Mucus is more than just a physical barrier for trapping oral microorganisms. Taylor & Francis.

ÖSTERLUND, A., POPA, R., NIKKILÄ, T., SCHEYNIUS, A. & ENGSTRAND, L. J. T. L. 1997. Intracellular reservoir of Streptococcus pyogenes in vivo: a possible explanation for recurrent pharyngotonsillitis. 107**,** 640-647.

PANKEY, G. & SABATH, L. 2004. Clinical relevance of bacteriostatic versus bactericidal mechanisms of action in the treatment of Gram-positive bacterial infections. *Clinical infectious diseases,* 38**,** 864-870.

PANTANELLA, F., VALENTI, P., NATALIZI, T., PASSERI, D. & BERLUTTI, F. 2013. Analytical techniques to study microbial biofilm on abiotic surfaces: pros and cons of the main techniques currently in use. *Ann Ig,* 25**,** 31-42.

PARKER, D., SOONG, G., PLANET, P., BROWER, J., RATNER, A. J. & PRINCE, A. 2009. The NanA neuraminidase of Streptococcus pneumoniae is involved in biofilm formation. *Infection and immunity,* 77**,** 3722-3730.

PEETERS, E., NELIS, H. J. & COENYE, T. 2008. Comparison of multiple methods for quantification of microbial biofilms grown in microtiter plates. *Journal of Microbiological Methods,* 72**,** 157-165.

PERCIVAL, S. L., HILL, K. E., WILLIAMS, D. W., HOOPER, S. J., THOMAS, D. W. & COSTERTON, J. W. 2012. A review of the scientific evidence for biofilms in wounds. *Wound Repair Regen,* 20**,** 647-657.

PICHICHERO, M. E. & CASEY, J. R. 2007. Systematic review of factors contributing to penicillin treatment failure in Streptococcus pyogenes pharyngitis. *Otolaryngol Head Neck Surg,* 137**,** 851-857.

PODBIELSKI, A., FLOSDORFF, A. & WEBER-HEYNEMANN, J. 1995. The group A streptococcal virR49 gene controls expression of four structural vir regulon genes. *Infect Immun,* 63**,** 9-20.

POOLE, J., DAY, C. J., VON ITZSTEIN, M., PATON, J. C. & JENNINGS, M. P. 2018. Glycointeractions in bacterial pathogenesis. *Nat Rev Microbiol,* 16**,** 440-452.

PROCTOR, D. M., FUKUYAMA, J. A., LOOMER, P. M., ARMITAGE, G. C., LEE, S. A., DAVIS, N. M., RYDER, M. I., HOLMES, S. P. & RELMAN, D. A. 2018. A spatial gradient of bacterial diversity in the human oral cavity shaped by salivary flow. *Nature Communications,* 9**,** 681.

PROSSER, B., TAYLOR, D., DIX, B. A. & CLEELAND, R. 1987. Method of evaluating effects of antibiotics on bacterial biofilm. *Antimicrob Agents Chemother,* 31**,** 1502-1506.

REID, S. D., CHAUSSEE, M. S., DOERN, C. D., CHAUSSEE, M. A., MONTGOMERY, A. G., STURDEVANT, D. E. & MUSSER, J. M. 2006. Inactivation of the group A Streptococcus regulator srv results in chromosome wide reduction of transcript levels, and changes in extracellular levels of Sic and SpeB. *FEMS Immunol Med Microbiol,* 48**,** 283-292.

ROBERTS, A. L., CONNOLLY, K. L., KIRSE, D. J., EVANS, A. K., POEHLING, K. A., PETERS, T. R. & REID, S. D. 2012. Detection of group A Streptococcus in tonsils from pediatric patients reveals high rate of asymptomatic streptococcal carriage. *BMC Pediatrics,* 12**,** 3-3.

ROBERTSON, J., MCGOVERIN, C., VANHOLSBEECK, F. & SWIFT, S. 2019. Optimisation of the Protocol for the LIVE/DEAD® BacLightTM Bacterial Viability Kit for Rapid Determination of Bacterial Load. 10.

ROLLET, C., GAL, L. & GUZZO, J. 2009. Biofilm-detached cells, a transition from a sessile to a planktonic phenotype: a comparative study of adhesion and physiological characteristics in Pseudomonas aeruginosa. *FEMS Microbiol Lett,* 290**,** 135-42.

ROSENBERG, M., AZEVEDO, N. F. & IVASK, A. 2019. Propidium iodide staining underestimates viability of adherent bacterial cells. *Scientific Reports,* 9**,** 6483.

ROY, S., HONMA, K., DOUGLAS, C. I., SHARMA, A. & STAFFORD, G. P. J. M. 2011. Role of sialidase in glycoprotein utilization by Tannerella forsythia. 157**,** 3195.

RUTHERFORD, S. T. & BASSLER, B. L. 2012. Bacterial quorum sensing: its role in virulence and possibilities for its control. *Cold Spring Harb Perspect Med,* 2**,** a012427.

RYAN, P. A. & JUNCOSA, B. 2016. Group A streptococcal adherence.

RYAN, P. A., PANCHOLI, V. & FISCHETTI, V. A. 2001. Group A streptococci bind to mucin and human pharyngeal cells through sialic acid-containing receptors. *Infect Immun,* 69**,** 7402-12.

SAKATA, H. 2013. Susceptibility and emm type of Streptococcus pyogenes isolated from children with severe infection. *Journal of infection and chemotherapy : official journal of the Japan Society of Chemotherapy,* 19**,** 1042-1046.

SANDERSON-SMITH, M., DE OLIVEIRA, D. M. P., GUGLIELMINI, J., MCMILLAN, D. J., VU, T., HOLIEN, J. K., HENNINGHAM, A., STEER, A. C., BESSEN, D. E., DALE, J. B., CURTIS, N., BEALL, B. W., WALKER, M. J., PARKER, M. W., CARAPETIS, J. R., VAN MELDEREN, L., SRIPRAKASH, K. S. & SMEESTERS, P. R. 2014. A Systematic and Functional Classification of Streptococcus pyogenes That Serves as a New Tool for Molecular Typing and Vaccine Development. *The Journal of Infectious Diseases,* 210**,** 1325-1338.

SAWAIR, F. A., RYALAT, S., SHAYYAB, M. & SAKU, T. 2009. The Unstimulated Salivary Flow Rate in a Jordanian Healthy Adult Population. *Journal of Clinical Medicine Research,* 1**,** 219-225.

SCHRAGER, H. M., ALBERTÍ, S., CYWES, C., DOUGHERTY, G. J. & WESSELS, M. R. 1998. Hyaluronic acid capsule modulates M protein-mediated adherence and acts as a ligand for attachment of group A Streptococcus to CD44 on human keratinocytes. *The Journal of clinical investigation,* 101**,** 1708-1716.

SHAFREEN, R. M., SRINIVASAN, S., MANISANKAR, P. & PANDIAN, S. K. 2011. Biofilm formation by Streptococcus pyogenes: modulation of exopolysaccharide by fluoroquinolone derivatives. *J Biosci Bioeng,* 112**,** 345-50.

SHEA, P. R., EWBANK, A. L., GONZALEZ-LUGO, J. H., MARTAGON-ROSADO, A. J., MARTINEZ-GUTIERREZ, J. C., REHMAN, H. A., SERRANO-GONZALEZ, M., FITTIPALDI, N., BERES, S. B., FLORES, A. R., LOW, D. E., WILLEY, B. M. & MUSSER, J. M. 2011. Group A Streptococcus emm gene types in pharyngeal isolates, Ontario, Canada, 2002-2010. *Emerging infectious diseases,* 17**,** 2010-2017.

SHELBURNE, S. A., SUMBY, P., SITKIEWICZ, I., GRANVILLE, C., DELEO, F. R. & MUSSER, J. M. J. P. O. T. N. A. O. S. 2005. Central role of a bacterial two-component gene regulatory system of previously unknown function in pathogen persistence in human saliva. 102**,** 16037-16042.

SHUNMUGAPERUMAL, T. 2010. *Biofilm Eradication and Prevention: A Pharmaceutical Approach to Medical Device Infections*, John Wiley & Sons.

SIEMENS, N., CHAKRAKODI, B., SHAMBAT, S. M., MORGAN, M., BERGSTEN, H., HYLDEGAARD, O., SKREDE, S., ARNELL, P., MADSEN, M. B., JOHANSSON, L., GROUP, I. S., JUAREZ, J., BOSNJAK, L., MÖRGELIN, M., SVENSSON, M. & NORRBY-TEGLUND, A. 2016. Biofilm in group A streptococcal necrotizing soft tissue infections. *JCI Insight,* 1**,** e87882.

SILLER, M., JANAPATLA, R. P., PIRZADA, Z. A., HASSLER, C., ZINKL, D. & CHARPENTIER, E. 2008. Functional analysis of the group A streptococcal luxS/AI-2 system in metabolism, adaptation to stress and interaction with host cells. *BMC Microbiol,* 8**,** 188-188.

SKELTON, T. P., ZENG, C., NOCKS, A. & STAMENKOVIC, I. 1998. Glycosylation provides both stimulatory and inhibitory effects on cell surface and soluble CD44 binding to hyaluronan. *J Cell Biol,* 140**,** 431-46.

SMEESTERS, P. R., MCMILLAN, D. J. & SRIPRAKASH, K. S. 2010. The streptococcal M protein: a highly versatile molecule. *Trends in microbiology,* 18**,** 275-282.

SMITH, W. D., POINTON, J. A., ABBOT, E., KANG, H. J., BAKER, E. N., HIRST, B. H., WILSON, J. A., BANFIELD, M. J. & KEHOE, M. A. 2010. Roles of minor pilin subunits Spy0125 and Spy0130 in the serotype M1 Streptococcus pyogenes strain SF370. *J Bacteriol,* 192**,** 4651-4659.

STEER, A. C., LAW, I., MATATOLU, L., BEALL, B. W. & CARAPETIS, J. R. 2009. Global emm type distribution of group A streptococci: systematic review and implications for vaccine development. *The Lancet infectious diseases,* 9**,** 611-616.

STEWART, P. S. & WILLIAM COSTERTON, J. 2001. Antibiotic resistance of bacteria in biofilms. *The Lancet,* 358**,** 135-138.

STIEFEL, P., SCHMIDT-EMRICH, S., MANIURA-WEBER, K. & REN, Q. 2015. Critical aspects of using bacterial cell viability assays with the fluorophores SYTO9 and propidium iodide. *BMC microbiology,* 15**,** 36-36.

STOOLMILLER, A. C. & DORFMAN, A. 1969. The biosynthesis of hyaluronic acid by Streptococcus. *J Biol Chem,* 244**,** 236-46.

SUGAREVA, V., ARLT, R., FIEDLER, T., RIANI, C., PODBIELSKI, A. & KREIKEMEYER, B. 2010. Serotype- and strain- dependent contribution of the sensor kinase CovS of the CovRS two-component system to Streptococcus pyogenes pathogenesis. *BMC Microbiology,* 10**,** 34.

SUITS, M. D., ZHU, Y., TAYLOR, E. J., WALTON, J., ZECHEL, D. L., GILBERT, H. J. & DAVIES, G. J. 2010. Structure and kinetic investigation of Streptococcus pyogenes family GH38 alpha-mannosidase. *PLoS One,* 5**,** e9006.

SUTHERLAND, I. 2001. Biofilm exopolysaccharides: a strong and sticky framework. *Microbiology (Reading),* 147**,** 3-9.

THENMOZHI, R., BALAJI, K., KUMAR, R., RAO, T. S. & PANDIAN, S. K. 2011. Characterization of biofilms in different clinical M serotypes of Streptococcus pyogenes. *J Basic Microbiol,* 51**,** 196-204.

TRAPPETTI, C., KADIOGLU, A., CARTER, M., HAYRE, J., IANNELLI, F., POZZI, G., ANDREW, P. W. & OGGIONI, M. R. J. T. J. O. I. D. 2009. Sialic acid: a preventable signal for pneumococcal biofilm formation, colonization, and invasion of the host. 199**,** 1497-1505.

TYLEWSKA, S. K., FISCHETTI, V. A. & GIBBONS, R. J. 1988. Binding selectivity ofStreptococcus pyogenes and M-protein to epithelial cells differs from that of lipoteichoic acid. *Curr Microbiol,* 16**,** 209-216.

VARKI, A. 2016. Biological roles of glycans. *Glycobiology,* 27**,** 3-49.

VARKI, A., CUMMINGS, R. D., AEBI, M., PACKER, N. H., SEEBERGER, P. H., ESKO, J. D., STANLEY, P., HART, G., DARVILL, A., KINOSHITA, T., PRESTEGARD, J. J., SCHNAAR, R. L., FREEZE, H. H., MARTH, J. D., BERTOZZI, C. R., ETZLER, M. E., FRANK, M., VLIEGENTHART, J. F., LÜTTEKE, T., PEREZ, S., BOLTON, E., RUDD, P., PAULSON, J., KANEHISA, M., TOUKACH, P., AOKI-KINOSHITA, K. F., DELL, A., NARIMATSU, H., YORK, W., TANIGUCHI, N. & KORNFELD, S. 2015. Symbol Nomenclature for Graphical Representations of Glycans. *Glycobiology,* 25**,** 1323-4.

VICKERY, K., HU, H., JACOMBS, A. S., BRADSHAW, D. A. & DEVA, A. K. 2013. A review of bacterial biofilms and their role in device-associated infection. *Healthcare Infection,* 18**,** 61-66.

VYAS, H. K. N., INDRARATNA, A. D., EVEREST-DASS, A., PACKER, N. H., DE OLIVEIRA, D. M. P., RANSON, M., MCARTHUR, J. D. & SANDERSON-SMITH, M. L. 2020. Assessing the Role of Pharyngeal Cell Surface Glycans in Group A Streptococcus Biofilm Formation. *Antibiotics,* 9**,** 775.

VYAS, H. K. N., PROCTOR, E.-J., MCARTHUR, J., GORMAN, J. & SANDERSON-SMITH, M. 2019. Current Understanding of Group A Streptococcal Biofilms. *Current Drug Targets,* 20**,** 982-993.

WADSTROM, T. & LJUNGH, Å. 1999. Glycosaminoglycan-binding microbial proteins in tissue adhesion and invasion: key events in microbial pathogenicity. 48**,** 223-233.

WALKER, M. J., BARNETT, T. C., MCARTHUR, J. D., COLE, J. N., GILLEN, C. M., HENNINGHAM, A., SRIPRAKASH, K. S., SANDERSON-SMITH, M. L. & NIZET, V. 2014. Disease Manifestations and Pathogenic Mechanisms of Group A Streptococcus. *Clinical Microbiology Reviews,* 27**,** 264-301.

WALZ, A., ODENBREIT, S., MAHDAVI, J., BORÉN, T. & RUHL, S. J. G. 2005. Identification and characterization of binding properties of Helicobacter pylori by glycoconjugate arrays. 15**,** 700-708.

WANG, J. R. & STINSON, M. W. 1994. Streptococcal M6 protein binds to fucose-containing glycoproteins on cultured human epithelial cells. *Infection and Immunity,* 62**,** 1268-1274.

WANNAMAKER, L. W. 1970. Differences between streptococcal infections of the throat and of the skin. I. *N Engl J Med,* 282**,** 23-31.

WESSELS, M. R. 2016. Pharyngitis and scarlet fever. *Streptococcus pyogenes: Basic Biology to Clinical Manifestations [Internet].* University of Oklahoma Health Sciences Center.

WHEELER, K. M., CÁRCAMO-OYARCE, G., TURNER, B. S., DELLOS-NOLAN, S., CO, J. Y., LEHOUX, S., CUMMINGS, R. D., WOZNIAK, D. J. & RIBBECK, K. 2019. Mucin glycans attenuate the virulence of Pseudomonas aeruginosa in infection. *Nature Microbiology*.

WILLIAMS, D. L. & BLOEBAUM, R. D. 2010. Observing the biofilm matrix of Staphylococcus epidermidis ATCC 35984 grown using the CDC biofilm reactor. *Microscopy and Microanalysis,* 16**,** 143-152.

WILSON, C., LUKOWICZ, R., MERCHANT, S., VALQUIER-FLYNN, H., CABALLERO, J., SANDOVAL, J., OKUOM, M., HUBER, C., BROOKS, T. D., WILSON, E., CLEMENT, B.,

WENTWORTH, C. D. & HOLMES, A. E. 2017. Quantitative and Qualitative Assessment Methods for Biofilm Growth: A Mini-review. *Research & reviews. Journal of engineering and technology,* 6**,** http://www.rroij.com/open-access/quantitative-and-qualitative-assessment-methods-for-biofilm-growth-a-minireview-.pdf.

WOLCOTT, R. D., RHOADS, D. D. & DOWD, S. E. 2008. Biofilms and chronic wound inflammation. *J Wound Care,* 17**,** 333-341.

WONG, A., GRAU, M. A., SINGH, A. K., WOODIGA, S. A., KING, S. J. J. I. & IMMUNITY 2018. Role of neuraminidase-producing bacteria in exposing cryptic carbohydrate receptors for Streptococcus gordonii adherence. 86**,** e00068-18.

XU, Y., KEENE, D. R., BUJNICKI, J. M., HÖÖK, M. & LUKOMSKI, S. 2002. Streptococcal Scl1 and Scl2 proteins form collagen-like triple helices. *J Biol Chem,* 277.

YOUNG, C., HOLDER, R. C., DUBOIS, L. & REID, S. D. 2016. Streptococcus pyogenes Biofilm.

ZALEWSKA-PIATEK, B. M., WILKANOWICZ, S. I., PIATEK, R. J. & KUR, J. W. 2009. Biofilm formation as a virulence determinant of uropathogenic Escherichia coli Dr+ strains. *Pol J Microbiol,* 58**,** 223-9.

ZOBELL, C. E. 1943. The Effect of Solid Surfaces upon Bacterial Activity. *J Bacteriol,* 46**,** 39-56.

Appendices

Appendix A: Media and general buffer composition

Unless stated otherwise, all media and buffers were made up to volume with distilled H_2O

Media composition

Todd-Hewitt broth (THY)

Todd-Hewitt 30 g/L

Yeast extract 10 g/L

THY agar (THYA)

THY

Agar 15g/L

Dulbecco's Modified Eagle Medium (DMEM) F12

DMEM F12 powder

$NaHCO_3$ 29 mM

Supplemented with L-glutamine (2mM) and 10% (v/v) foetal bovine serum

Buffer composition

1 × Phosphate buffer saline (PBS)

NaCl 8 g/L

KCl 0.2 g/L

Na_2HPO_4 1.44 g/L

KH_2PO_4 0.24 g/L

Make up to 800 mL volume with dH_2O, adjust to pH 7.4 and expand to 1L with dH_2O.

Appendix B: Planktonic overnight GAS cultures enumerated

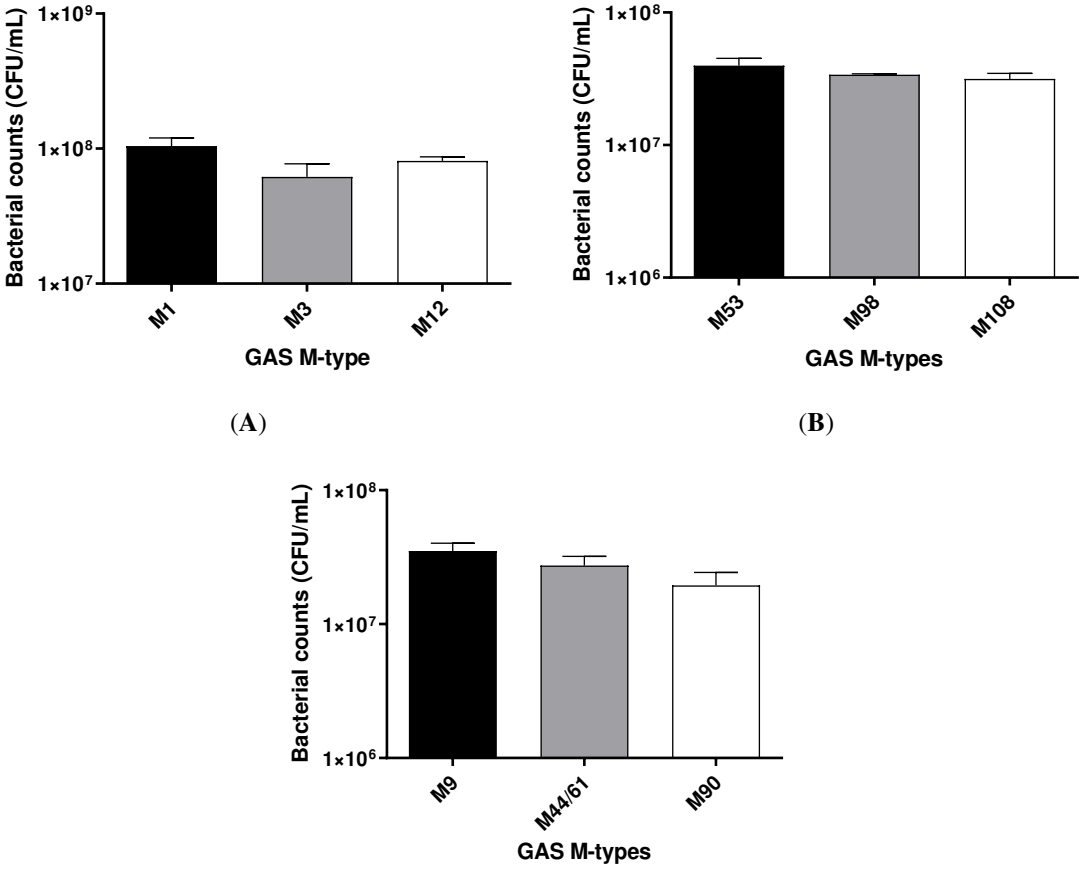

Figure B. Graphs of planktonic overnight GAS cultures enumerated for their bacterial counts (CFU/mL). GAS M types have been categorized into *Emm* patterns; A-C (M1, M3, and M12), D (M53, M98, and M108), and E (M9, M44/61, and M90). Data represents mean ± SEM, with statistical analysis performed using a one-way ANOVA with Tukey's multiple comparisons test, no significant differences noted among GAS M types belonging to their respective *Emm* pattern; n = 3 biological replicates, with 3 technical replicates each.

Appendix C: Proposed *N*-glycans structures identified on the Detroit 562 pharyngeal cell surface

Table C. Proposed *N*-glycan structures identified by PGC-LC-ESI-MS/MS following PNGase F treatment of membrane proteins extracted from Detroit-562 pharyngeal cells. Structures are assigned based on precursor m/z, retention time and MS^2 fragmentation spectra (Ceroni et al., 2008, Harvey et al., 2008, Everest-Dass et al., 2012, Everest-Dass et al., 2013). Relative abundances were calculated based on integration of peak area of extracted ion chromatograms and reported as mean ± SEM across three biological replicates. Abundances of structural isomers sharing the same m/z, monosaccharide composition and terminal monosaccharide presentation have been combined for clarity. Glycans are represented using conventional graphical nomenclature as per (Varki et al., 2015). Red triangle = fucose (dHex), yellow circle = galactose (GalNAc), blue square = *N*-acetylglucosamine (GlcNAc), green circle = mannose (Man), purple diamond = sialic acid (NeuAc).

#	m/z $[M-H]^{-2}$	m/z $[M-H]^{-1}$	Composition	Terminal mono-saccharide	Proposed structure	Structural isomers	Relative abundance (%)
1)	617.2	1235.4	$(Man)_5$ $(GlcNAc)_2$	Mannose	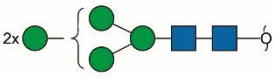	4	1.90 ± 0.04
2)	698.2		$(Man)_6$ $(GlcNAc)_2$	Mannose	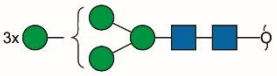	3	17.43 ± 0.36
3)	771.3		$(Man)_6$ $(GlcNAc)_2$ $(dHex)_1$	Mannose	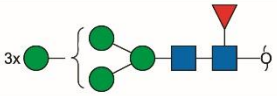	2	1.07 ± 0.12
4)	779.3		$(Man)_7$ $(GlcNAc)_2$	Mannose	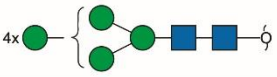	3	25.36 ± 1.24
5)	820.3		$(Man)_3$ $(GlcNAc)_4$ $(Gal)_2$	Galactose	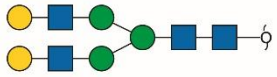	2	0.66 ± 0.06
6)	860.3		$(Man)_8$ $(GlcNAc)_2$	Mannose	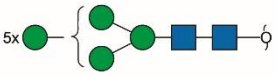	2	26.05 ± 0.54
7)	893.3		$(Man)_3$ $(GlcNAc)_4$ $(Gal)_2$ $(dHex)_1$	Galactose	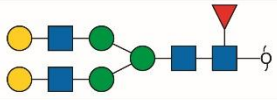	2	1.24 ± 0.07
8)		895.3	$(Man)_2$ $(GlcNAc)_2$ $(dHex)_1$	Mannose	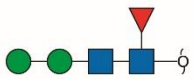	2	1.53 ± 0.04
9)	937.7		$(Man)_4$ $(NeuAc)_1$ $(GlcNAc)_3$ $(Gal)_1$ $(dHex)_1$	Mannose Sialic acid	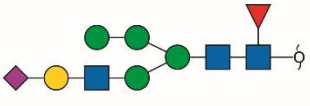	3	1.50 ± 0.09
10)	941.3		$(Man)_9$ $(GlcNAc)_2$	Mannose	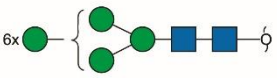	3	7.77 ± 0.91
11)	945.3		$(Man)_5$ $(NeuAc)_1$ $(GlcNAc)_3$ $(Gal)_1$	Mannose Sialic acid	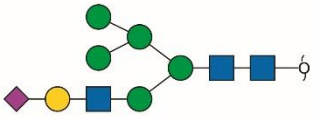	2	2.50 ± 0.51

12)	957.8		$(Man)_3$ $(NeuAc)_1$ $(GlcNAc)_4$ $(Gal)_1$ $(dHex)_1$	GlcNAc Sialic acid	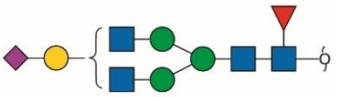	3	0.55 ± 0.14
13)	965.8		$(Man)_3$ $(NeuAc)_1$ $(GlcNAc)_4$ $(Gal)_2$	Galactose Sialic acid	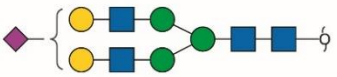	3	2.31 ± 0.41
14)	1018.4		$(Man)_5$ $(NeuAc)_1$ $(GlcNAc)_3$ $(Gal)_1$ $(dHex)_1$	Mannose Sialic acid	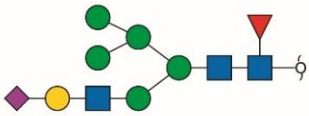	2	1.24 ± 0.24
15)	1038.9		$(Man)_3$ $(NeuAc)_1$ $(GlcNAc)_4$ $(Gal)_2$ $(dHex)_1$	Galactose Sialic acid	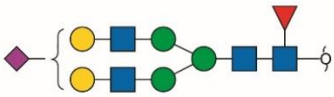	4	5.63 ± 0.86
16)	536.15	1073.3	$(Man)_4$ $(GlcNAc)_2$	Mannose	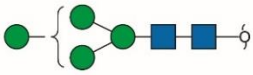	3	0.99 ± 0.33
17)	1111.4		$(Man)_3$ $(NeuAc)_2$ $(GlcNAc)_4$ $(Gal)_2$	Sialic acid	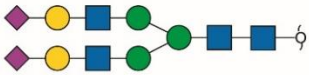	2	0.63 ± 0.27
18)	1111.9		$(Man)_3$ $(NeuAc)_1$ $(GlcNAc)_4$ $(Gal)_2$ $(dHex)_2$	Galactose Sialic acid Fucose	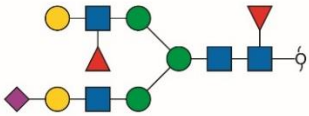	2	0.56 ± 0.06
19)	1184.3		$(Man)_3$ $(NeuAc)_2$ $(GlcNAc)_4$ $(Gal)_2$ $(dHex)_1$	Sialic acid	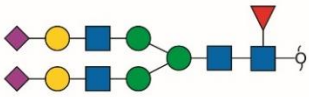	3	1.22 ± 0.06

Appendix D: Confirming removal of *N*-linked glycan structures via PNGase F treatment of Detroit 562 pharyngeal cell monolayers

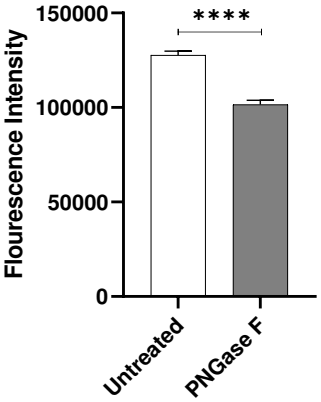

Figure D. Lectin binding assay confirming removal of *N*-linked glycans via PNGase F treatment of Detroit 562 pharyngeal cell monolayers. *N*-linked glycan removal was confirmed via Concanavalin A Alexa Fluor 647 lectin binding to untreated and PNGase F pre-treated pharyngeal cell monolayers. Bound Concanavalin A Alexa Fluor 647 was detected spectrofluorometrically at excitation 625-30 nm/emission 680-30 nm. Data represents mean ± SEM, with statistical analysis performed, **** ($P \leq 0.0001$); n = 3 biological replicates, with 2 technical replicates each.

Appendix E: Confirming removal of mannose and sialic acid via exoglycosidase treatment of Detroit 562 pharyngeal cell monolayers

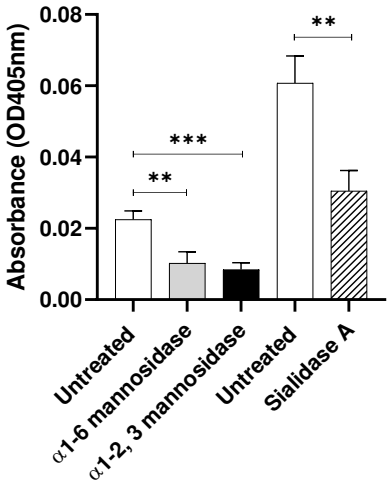

Figure E. Lectin binding assay confirming removal of terminal mannose and sialic acid residues via exoglycosidase treatment of Detroit 562 pharyngeal cell monolayers. Glycan removal was confirmed via lectin binding assay with α1-6 mannosidase and α1-2,3 mannosidase pre-treated pharyngeal cell monolayers incubated with biotinylated *Hippeastrum Hybrid* lectin (binding mannose residues), and Sialidase A pre-treated pharyngeal cell monolayers incubated with biotinylated *Sambucus negra* lectin (binding sialic acid residues). Untreated pharyngeal cell monolayer controls were incubated with respective lectins. Data represents mean ± SEM, with statistical analysis performed, ** ($P \leq 0.01$) and *** ($P \leq 0.001$); n = 5 biological replicates, with 3 technical replicates each.

Appendix F: Minimum inhibitory concentration (MIC) Assay

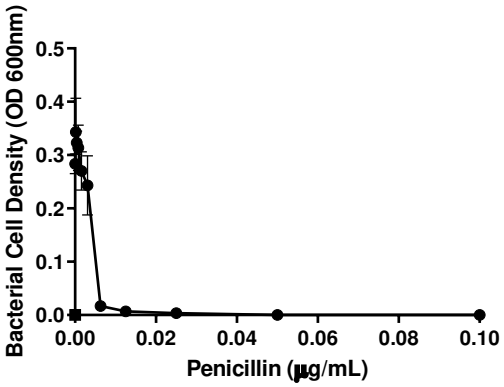

(**A**)

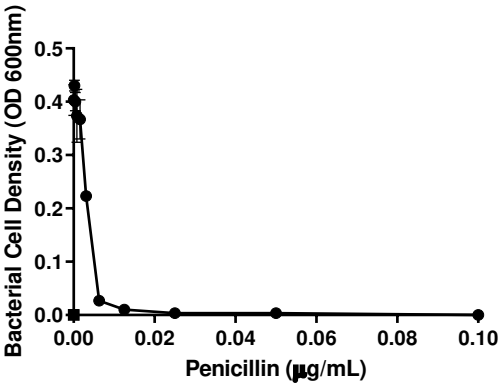

(**B**)

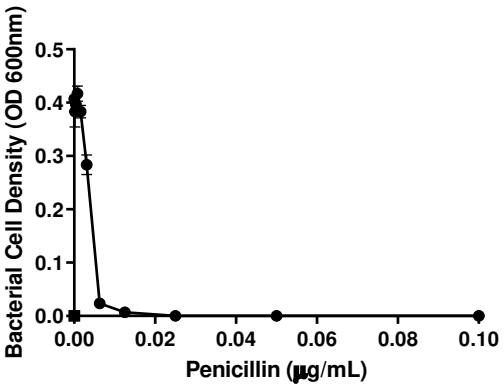

(**C**)

Figure F. Minimum inhibitory concentration (MIC) determined for planktonic M12 GAS after 24 h challenge with penicillin. Data displays MIC graphs generated for 3 biological replicates (**A**-**C**)**.** Data represents mean ± SEM; n = 3 biological replicates, with 3 technical replicates each.